0008-7114

Caryologia

International Journal of Cytology, Cytosystematics and Cytogenetics

2019
Vol. 72 - n. 2

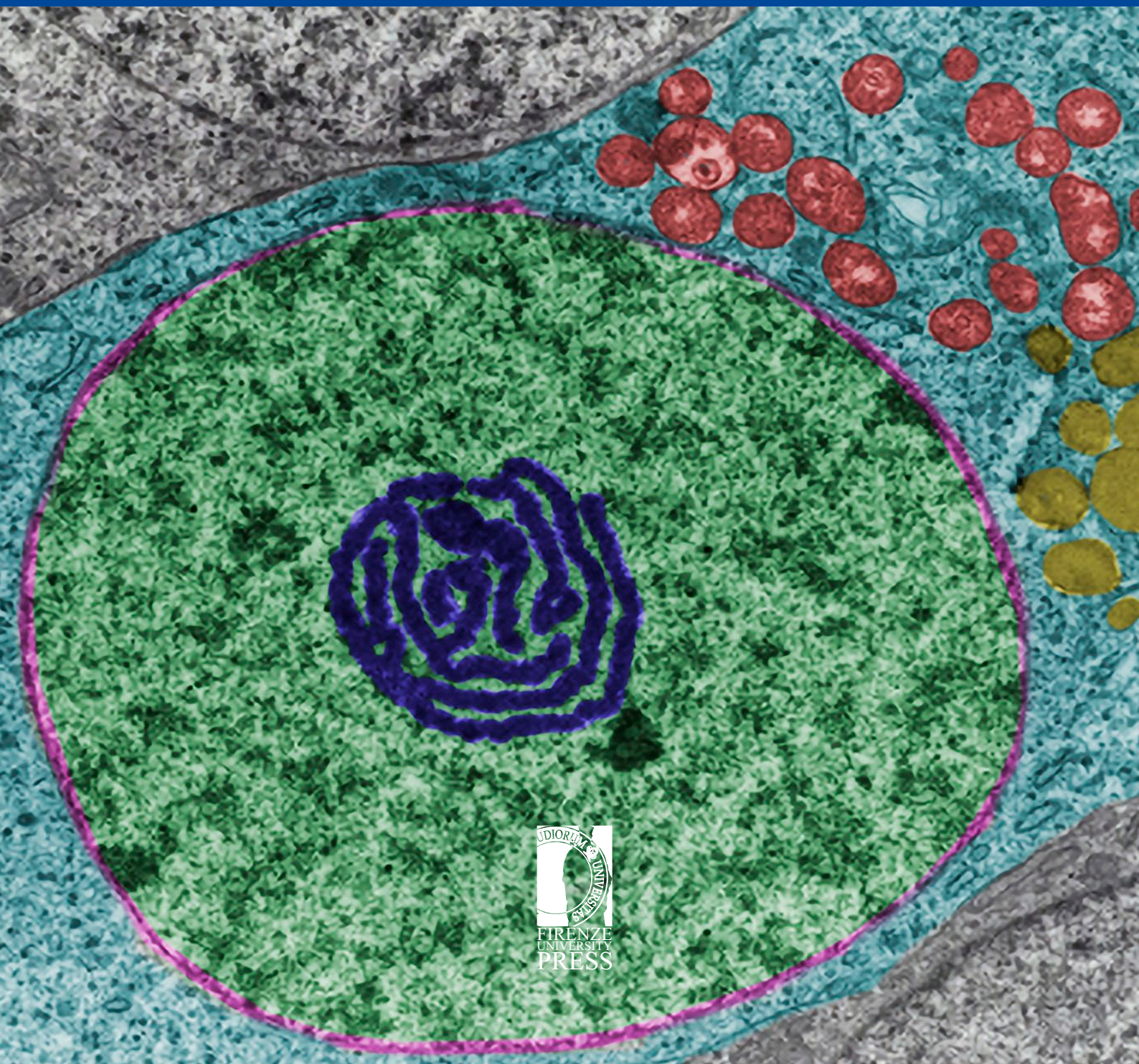

FIRENZE UNIVERSITY PRESS

Caryologia. International Journal of Cytology, Cytosystematics and Cytogenetics

Caryologia is devoted to the publication of original papers, and occasionally of reviews, about plant, animal and human karyological, cytological, cytogenetic, embryological and ultrastructural studies. Articles about the structure, the organization and the biological events relating to DNA and chromatin organization in eukaryotic cells are considered. *Caryologia* has a strong tradition in plant and animal cytosystematics and in cytotoxicology. Bioinformatics articles may be considered, but only if they have an emphasis on the relationship between the nucleus and cytoplasm and/or the structural organization of the eukaryotic cell.

Caryologia

International Journal of Cytology, Cytosystematics and Cytogenetics

Volume 72, Issue 2 - 2019

Firenze University Press

***Caryologia*. International Journal of Cytology, Cytosystematics and Cytogenetics**

Published by
Firenze University Press – University of Florence, Italy
Via Cittadella, 7 - 50144 Florence - Italy
http://www.fupress.com/caryologia

Caryologia
International Journal of Cytology, Cytosystematics and Cytogenetics

Firenze University Press
www.fupress.com/caryologia

OPEN ACCESS

Citation: J.-X. Wang, Y.-J. Cao, Y.-C. Han, S.-. Zhou, K. Liu (2019) Karyotype analysis of a natural *Lycoris* double-flowered hybrid. *Caryologia* 72(2): 3-7. doi: 10.13128/caryologia-720

Published: December 5, 2019

Data Availability Statement: All relevant data are within the paper and its Supporting Information files.

Competing Interests: The Author(s) declare(s) no conflict of interest.

Karyotype analysis of a natural *Lycoris* double-flowered hybrid

Jin-Xia Wang[1], Yuan-Jin Cao[1], Yu-Chun Han[1], Shou-Biao Zhou[1,2], Kun Liu[1,*]

[1] *Anhui Provincial Key Laboratory of the Conservation and Exploitation of Biological Resources, College of Life Sciences, Anhui Normal University, Wuhu, Anhui, China*
[2] *Anhui Provincial Engineering Laboratory of Water and Soil Pollution Control and Remediation, College of Environmental Science and Engineering, Anhui Normal University, Wuhu, Anhui, China*
* Corresponding author: hudixiao@126.com

Abstract. A putative natural double-flowered hybrid in *Lycoris* Herb. was found on Mt. Zhangjiajie in Hunan, China. The putative natural hybrid had a chromosome number of 2n = 18 and was karyotypically formulated as $2n$ = 4m + 6st + 5t + 3T. The karyotype of the putative natural hybrid was classified as 2B type according to the degree of asymmetry and Stebbins' criteria. According to the gross morphology, phenology and karyotype of the putative natural hybrid, it was suggested that this taxon was probably from the natural hybridization between *L. aurea* and *L. radiata*.

Keywords. Karyotype, *Lycoris* Herb., natural hybrid.

INTRODUCTION

The genus *Lycoris* Herb., a small group of the family Amaryllidaceae, comprises approximately 20 species, distributed in warm temperate and subtropical zones of East Asia, with a few extending to northern Indochina and Nepal (Liu and Hsu 1989; Hsu et al. 1994; Shi et al. 2006). The *Lycoris* species are very popular bulb flowers characterized by their plentiful colors and beautiful and varied shapes (Hsu et al. 1994; Zhou et al. 2007). The hybridization frequently happens in the genus *Lycoris* and causes a number of the presently established hybrid taxa, such as *L. houdyshelii* Traub, *L. straminea* Lindl., *L. squamigera* Maxim., *L. incarnata* Comes ex C. Sprenger and *L.* × *hubeiensis* K. Liu (Kurita 1987; Hsu et al. 1994; Shi et al. 2006; Meng et al. 2018). During our field investigations of the wild populations of *Lycoris* in Hunan Province, China, a mixed population of three taxa, namely *L. aurea* (L'Her.) Herb., *L. radiata* (L'Her.) Herb., and a putative natural hybrid was found. The putative natural double-flowered hybrids attracted our more attention, which were discovered for the first time in *Lycoris* in the wild. To illustrate the origin of the natural double-flowered hybrids, some bulbs were successfully transplanted and cultivated in the experimental garden, together

with their putative parents. The karyotypes of the three *Lycoris* taxa were analyzed in this study, indicating that the double-flowered taxon might be from the hybridization between *L. aurea* and *L. radiata*.

MATERIALS AND METHODS

The plants were collected from Mt. Zhangjiajie, Hunan, China (110°17'E, 29°19'N), and then transplanted to the experimental garden of Anhui Normal University, Wuhu, China. The flowers of each taxon were shown in Fig. 1. For chromosome observation, actively growing root tips were pretreated in p-Dichlorobenzene solution at 4 °C for 5 h before they were fixed in Carnoy I (glacial acetic acid : absolute ethanol = 1:3) at 4 °C for 20 h. Then they were macerated in 1 mol L^{-1} hydrochloric acid at 60 °C for 3 minutes, stained in Phenol-Fuchsin for 20 h, and squashed in 45% acetic acid.

The karyotype formula was based on the measurements of metaphase chromosomes taken from photographs. For each taxon, measurements were taken from at least five well-spread metaphase cells in no fewer than three different individuals. For the description of karyotypes, the symbols had been adapted according to Levan et al. (1964): m for median-centromeric chromosome with arm ratio of 1.01-1.70; st for subterminal-centromeric chromosome with arm ratio of 3.01-7.00; t for terminal-centromeric chromosome with arm ratio of over 7.00; T for terminal-centromeric chromosome with no short arm. Karyotypes were classified on the basis of their degrees of asymmetry according to Stebbins (1971) and Li and Chen (1985). The intrachromosomal asymmetry index (A_1) and interchromosomal asymmetry index (A_2) were calculated using Romero Zarco' equations (1986).

RESULTS

1. The putative natural *Lycoris* double-flowered hybrid (Table 1, 2; Figure 2A, 2D) – The chromosomes were counted to be $2n = 18$, consisting of 4 large median-centromeric (m), 6 subterminal-centromeric (st), 5 terminal-centromeric (t) and 3 Terminal-centromeric (T). The karyotype was formulated as $2n = 4m + 6st + 5t + 3T$. The average length of chromosome complement was 122.3 μm. The ratio of the length of the largest chromosome to that of the smallest was 3.39, and the proportion of chromosomes with arm ratio >2:1 was 77.8%. The karyotype was therefore of 2B type according to the degree of asymmetry and the chromosomes ranged from

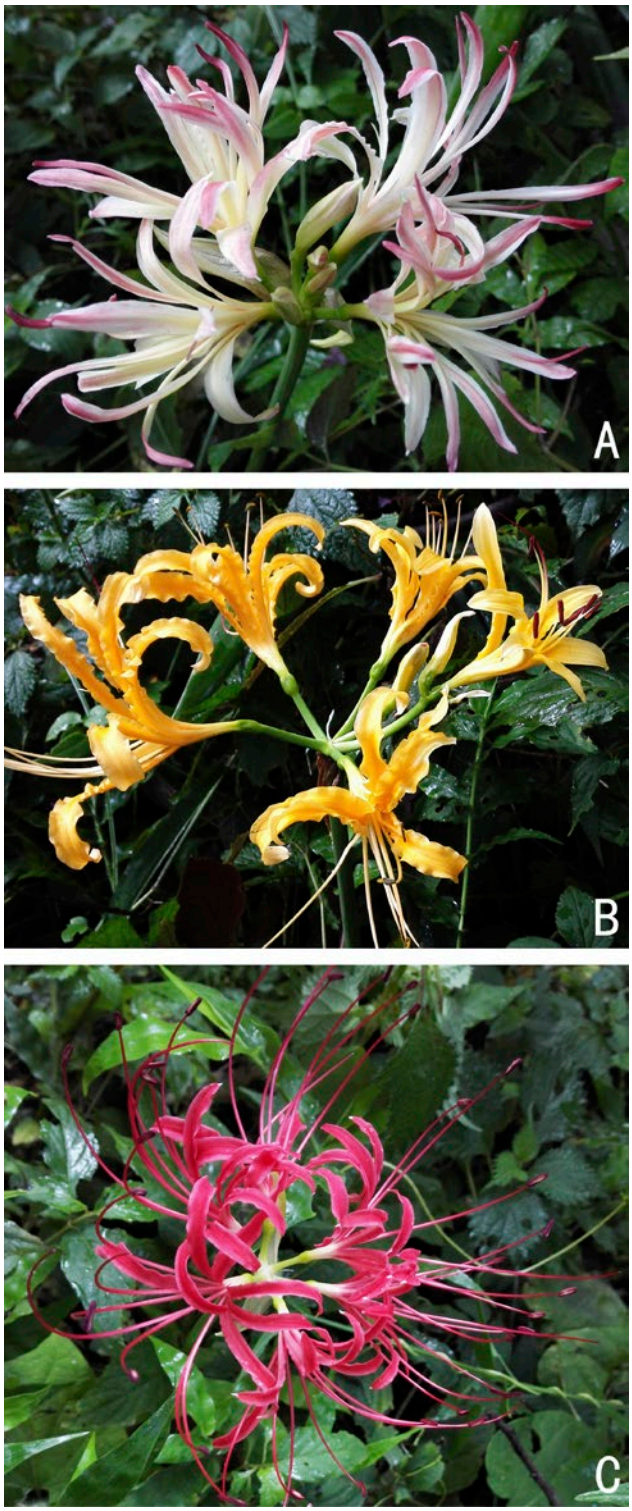

Fig 1. The flowers of the three taxa. A: the putative natural hybrid; B: *L. aurea*; C: *L. radiata*.

Table 1. Karyotype characteristics of the studied *Lycoris* taxa.

Species	Karyotypic formula	Stebbins' type	A_1	A_2	TCL (μm)
Hybrid	$2n$ = 4m + 6st + 5t + 3T	2B	0.72	0.50	122.3
L. aurea	$2n$ = 8m + 6T	2B	0.47	0.44	138.6
L. radiata	$2n$ = 12st + 10t	4A	0.86	0.10	111.2

A_1: intrachromosomal asymmetry index, A_2: interchromosomal asymmetry index, TCL: average length of total chromosome complement.

Table 2. Measurements of somatic chromosomes of the putative natural hybrid**.**

No.	Relative length			Arm ratio	Type
	LL	SL	TL		
1	5.71	5.67	11.38	1.01	m
2	5.81	5.38	11.19	1.08	m
3	6.11	4.65	10.76	1.31	m
4	4.39	4.09	8.48	1.07	m
5	4.63	0.37	5.00	12.51	t
6	4.63	0.33	4.96	14.03	t
7	3.97	0.65	4.62	6.11	st
8	4.53	0.00	4.53	∞	T
9	4.49	0.00	4.49	∞	T
10	3.90	0.46	4.36	8.48	t
11	4.34	0.00	4.34	∞	T
12	3.47	0.54	4.01	6.43	st
13	3.61	0.31	3.92	11.65	t
14	3.39	0.49	3.88	6.92	st
15	3.22	0.46	3.68	7.00	st
16	2.99	0.60	3.59	4.98	st
17	2.99	0.46	3.45	6.50	st
18	3.03	0.33	3.36	9.18	t

Note: LL, relative length of long arm; SL, relative length of short arm; TL, total relative length; LL + SL = TL. The same is below.

3.36~11.38 in relative length. The values of A_1 and A_2 were 0.72 and 0.50, respectively.

2. *Lycoris aurea* (Table 1, 3; Figure 2B, 2E) – The chromosome number was $2n$ = 14, consisting of 8 large median-centromeric (m) and 6 Terminal-centromeric (T). The karyotype formula was $2n$ = 8m + 6T. The average length of chromosome complement was 138.6 μm. The ratio of the length of the largest chromosome to that of the smallest was 3.32, and the proportion of chromosomes with arm ratio >2:1 was 42.9%. The karyotype type was 2B. The relative lengths of all chromosomes ranged from 3.49 to 11.59. The values of A_1 and A_2 were 0.47 and 0.44, respectively.

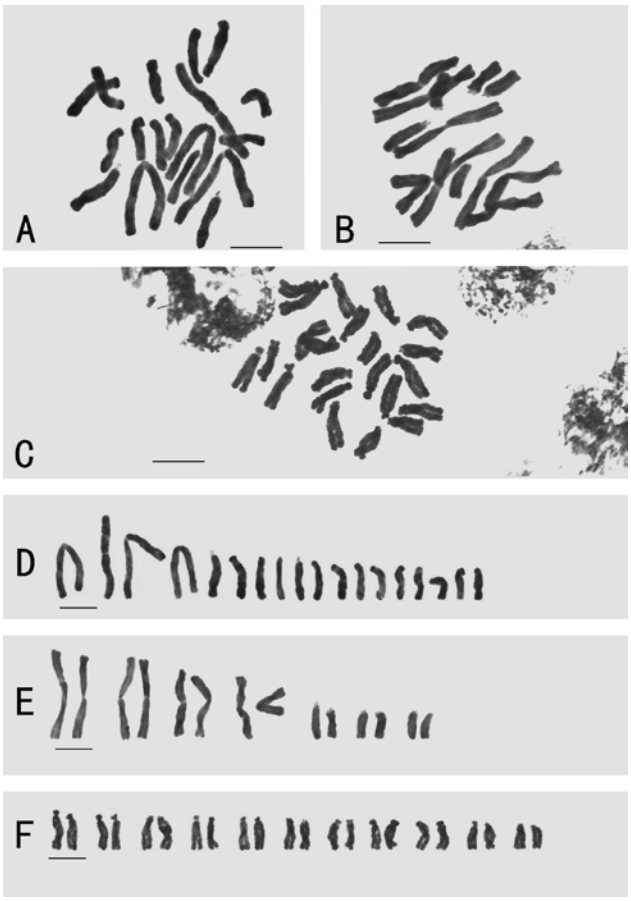

Fig 2. The metaphase chromosome morphology and karyotypes of the putative natural hybrid, *Lycoris aurea* and *L. radiata*. A, D: the putative natural hybrid; B, E: *L. aurea*; C, F: *L. radiata*. Scale bar = 10 μm.

Table 3. Measurements of somatic chromosomes of *L. aurea***.**

No.	Relative length			Arm ratio	Type
	LL	SL	TL		
1	5.81	5.76	11.57	1.01	m
2	5.56	5.38	10.94	1.03	m
3	5.52	5.34	10.86	1.03	m
4	5.47	4.93	10.40	1.11	m
5	4.75	4.13	8.88	1.15	m
6	4.39	4.26	8.65	1.03	m
7	4.13	3.90	8.03	1.06	m
8	3.99	3.41	7.40	1.17	m
9	4.93	0.00	4.93	∞	T
10	3.81	0.00	3.81	∞	T
11	3.77	0.00	3.77	∞	T
12	3.68	0.00	3.68	∞	T
13	3.59	0.00	3.59	∞	T
14	3.49	0.00	3.49	∞	T

Table 4. Measurements of somatic chromosomes of *L. radiata*.

No.	Relative length			Arm ratio	Type
	LL	SL	TL		
1	4.60	0.75	5.35	6.13	st
2	4.43	0.67	5.10	6.61	st
3	4.38	0.70	5.08	6.26	st
4	4.25	0.70	4.95	6.07	st
5	4.63	0.27	4.90	17.15	t
6	4.23	0.62	4.85	6.82	st
7	4.25	0.57	4.82	7.46	t
8	4.05	0.67	4.72	6.05	st
9	4.18	0.52	4.70	8.04	t
10	3.81	0.85	4.66	4.48	st
11	4.08	0.55	4.63	7.42	t
12	4.01	0.60	4.61	6.68	st
13	4.08	0.51	4.59	8.00	t
14	3.91	0.67	4.58	5.84	st
15	4.11	0.38	4.49	10.81	t
16	3.73	0.55	4.28	6.78	st
17	3.81	0.45	4.26	8.47	t
18	3.86	0.30	4.16	12.87	t
19	3.38	0.55	3.93	6.15	st
20	3.41	0.52	3.93	6.56	st
21	3.38	0.47	3.85	7.19	t
22	3.21	0.35	3.56	9.17	t

3. *Lycoris radiata* (Table 1, 4; Figure 2C, 2F) – The chromosome number of this species was $2n = 22$. It consisted of 12 subterminal-centromeric (st) and 10 terminal-centromeric (t). The karyotype was formulated as $2n = 12st + 10t$. The average length of chromosome complement was 111.2 μm. The ratio of the length of the largest chromosome to that of the smallest was 1.43, and the proportion of chromosomes with arm ratio >2:1 was 100%. The karyotype type was 4A. The relative lengths of all chromosomes ranged from 3.56 to 5.10. The values of A_1 and A_2 were 0.86 and 0.10, respectively.

DISCUSSION

The karyotype of the putative natural double-flowered hybrid is formulated as $2n = 18 = 4m + 6st + 5t + 3T$. *Lycoris aurea* in this study has a chromosome number of $2n = 14$, in agreement with other reports (Liu and Hsu 1989; Hsu et al. 1994). *L. radiata* has a chromosome number of $2n = 22$, similar to some previous studies (Shao et al. 1994; Zhou et al. 2007; Liu et al. 2016). Based on the values of the two indices, A_1 and A_2, *L. radiata* had the largest intrachromosomal asymmetry and the smallest interchromosomal asymmetry among the three taxa. Considering the sympatric distribution of *L. aurea* and *L. radiata*, it was supposed that this putative natural hybrid might be a diploid between *L. aurea*, which produced the gamete having 4m + 3T, and *L. radiata* with a- reduced gamete having 6st + 5t. According to our observation, the leaf of this putative natural hybrid emerged in September, the same as the putative parents. The sizes of leaf blade and bulb of this putative natural hybrid were intermediate between its two putative parents. So far, some *Lycoris* species were confirmed to be hybrids by karyotype or molecular sequence analysis, such as *L. houdyshelii*, *L. straminea*, and *L. incarnata* (Hsu et al. 1994; Shi et al. 2006; Liu et al. 2011), and these hybrids had the similar flower characteristics with their putative parents. Here, a putative natural double-flowered hybrid with no pistil and stamen was discovered and its karyotype was described for the first time. Based on the karyotype analysis, further molecular study was needed to uncover the origin of this natural hybrid and distinguish the paternal donor from the maternal donor.

Judging from the absence of seed, pistil and stamen, the putative natural hybrid could be sexually sterile. The *Lycoris* species all had considerable ornamental value. Compared with the normal *Lycoris* species, the double-flowered hybrid had more ornamental value. Because of the lack of seed, it was needed to propagate the double-flowered hybrid for the large application in landscaping in future by tissue culture and quick propagation technology.

ACKNOWLEDGMENTS

We thank the anonymous reviewers for helpful comments that improved the paper.

FUNDING

This work was financially funded by the National Natural Science Foundation of China (31400291) and Collaborative Innovation Center of Recovery and Reconstruction of Degraded Ecosystem in Wanjiang City Belt, Anhui Province; College of Life Sciences, Anhui Normal University.

REFERENCES

Hsu BS, Kurita S, Yu ZZ, Lin JZ. 1994. Synopsis of the genus *Lycoris* (Amaryllidaceae). SIDA. 16:301–331.

Kurita S. 1987. Variation and evolution on the karyotype of *Lycoris*, Amaryllidaceae II. Karyotype analysis of ten taxa among which seven are native to China. Cytologia. 52: 19–40.

Levan L, Fredga K, Sandberg AA. 1964. Nomenclature for centromeric position on chromosomes. Hereditas. 52: 201–220.

Li MX, Chen RY. 1985. A suggestion on the standardization of karyotype analysis in plants. J Wuhan Bot Res. 3 (4): 297–302.

Liu K, Zhou SB, Wang Y, Zhang D. 2011. A karyomorphological study on two newly recorded taxa of *Lycoris* (Amaryllidaceae) in Anhui province, China. Caryologia. 64 (2): 158–163.

Liu Y, Hsu BS. 1989. A study on karyotypes of the genus *Lycoris*. Acta Phyto Sin. 27 (4): 257–264.

Liu YX, Zheng YH, Xia T, Zhou J. 2016. Karyotype studies on *Lycoris radiata* populations from China. Genet Mol Res. 15 (1): 15017357.

Meng WQ, Zheng L, Shao JW, Zhou SB, Liu K. 2018. A new natural allotriploid, *Lycoris* × *hubeiensis* hybr. nov. (Amaryllidaceae), identified by morphological, karyological and molecular data. Nord J Bot. 36 (6): e01780.

Romero Zarco C. 1986. A new method for estimating karyotype asymmetry. Taxon 35 (3): 526–530.

Shao JZ, Yang JG, Zhang DC, Nie LW. 1994. The discovery of diploid *Lycoris radiata* Herb. from Anhui. Acta Phyto Sin. 32 (6): 549–552.

Shi SD, Qiu YX, Li EX, Wu L, Fu CX. 2006. Phylogenetic relationships and possible hybrid origin of *Lycoris* species (Amaryllidaceae) revealed by ITS sequences. Biochem Genet. 44: 198–206.

Stebbins GL. 1971. Chromosomal evolution in higher plants. London: Edward Arnold Ltd.

Zhou SB, Yu BQ, Luo Q, Hu JR, Bi D. 2007. Karyotypes of six populations of *Lycoris radiata* and discovery of the tetraploid. Acta Phyto Sin. 45 (4): 513–522.

Caryologia
International Journal of Cytology, Cytosystematics and Cytogenetics

Firenze University Press
www.fupress.com/caryologia

OPEN ACCESS

Citation: J.G. Nzweundji, M.F.S. Ngo Ngwe, S. Siljak-Yakovlev (2019) Insights on cytogenetic of the only strict African representative of genus *Prunus* (*P. africana*): first genome size assessment, heterochromatin and rDNA chromosome pattern. *Caryologia* 72(2): 9-19. doi: 10.13128/cayologia-253

Published: December 5, 2019

Data Availability Statement: All relevant data are within the paper and its Supporting Information files.

Competing Interests: The Author(s) declare(s) no conflict of interest.

Insights on cytogenetic of the only strict African representative of genus *Prunus* (*P. africana*): first genome size assessment, heterochromatin and rDNA chromosome pattern

Justine Germo Nzweundji[1], Marie Florence Sandrine Ngo Ngwe[2], Sonja Siljak-Yakovlev[3,*]

[1] *Medicinal Plants and Traditional Medicine Research Centre, Institute of Medical Research and Medicinal Plants Studies (IMPM), P. O. Box 6163 Yaoundé, Cameroon*
[2] *National Herbarium of Cameroon-Institute of Agricultural Research For Development, BP 1601 Yaoundé-Cameroon*
[3] *Ecologie, Systématique et Evolution, Univ. Paris-Sud, CNRS, AgroParisTech, Université Paris-Saclay, Bât 360, 91405 Orsay, France*
*Corresponding author: sonia.yakovlev@u-psud.fr

Abstract. *Prunus africana* is a multipurpose evergreen species endemic to Africa and an endangered species because of overexploitation. The great importance of this species resides particularly in the use of its bark against benign prostatic hyperplasia. As for most tropical trees and generally woody species, cytogenetic studies are scarce. Standard and molecular cytogenetic approaches have been implemented for the first time to study *P. africana* from Cameroon. This is the tetraploid species with a chromosome number of 2n=4x=32. Genome size estimated by flow cytometry was 2C=1.44 pg. Five loci (ten signals) of 35S rRNA genes were observed after fluorescence *in situ* hybridization. Ten G-C rich DNA regions were detected by chromomycin A3 fluorochrome banding. All chromomycin positive bands were co-localized with 35 S rDNA signals. *Prunus africana*, the only strict African representative of genus *Prunus,* is in need of the conservation strategy and *in situ* management that we are also discussing in this work.

Keywords. Chromomycin fluorochrome banding, chromosome number and 2C DNA value, fluorescent in situ hybridization (FISH), heterochromatin and rRNA gene patterns.

INTRODUCTION

The genus *Prunus s. l.* comprise from 200 to 430 species according different authors: over 200 (Rehder 1940), approximately 250 (Wen et al. 2008), 400 (Maghuly et al. 2010), and 430 (according Wielgorskaya 1995 and Niklas 1997).

Prunus africana (Hook. f.) Kalkman, (Syn. *Pygeum africanum* Hook.f.) belonging to the Rosaceae family (subfamily Amygdaloideae), known as African Cherry (Kalkman 1965), is the only species of the genus *Prunus* endemic

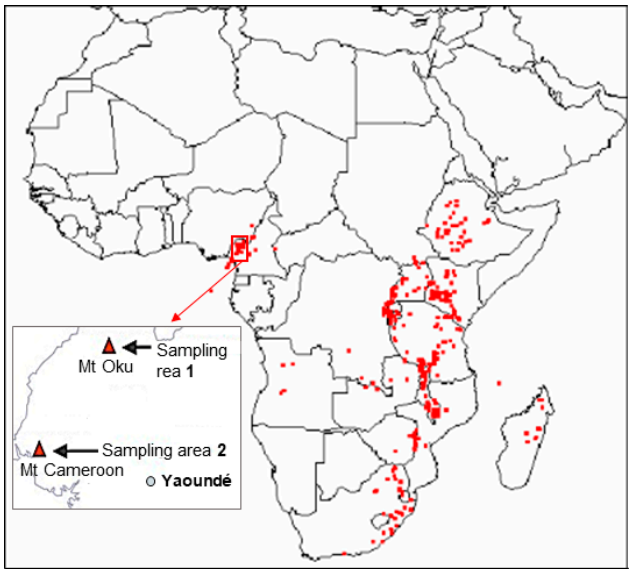

Fig. 1. Global distribution of *P. africana* according Hall et al. (2000) with geographic position of collection sites in Cameroon (box).

to Africa (Fig. 1). It belongs to subgenus *Laurocerasus* which comprises all evergreen species of the genus *Prunus* (Kalkman 1965; Bodeker et al. 2014). This species of the Afromontane flora is present along the central and southern part of Africa, as well as Madagascar and on the islands of Bioko, São-Tomé, and Grande Comore (Kalkman 1965; Cunningham et al. 1997; White 1983; Hall et al. 2000). The main habitats of this species are fallow land, primary and secondary forests. It grows in montane and sub montane forest at a relatively high altitude, from 600 m to 3000 m in the Tropical Africa according to Kalkman (1965) and Stewart (2003a, b). The eastern limit of the distribution of the species is in Cameroon, where *Prunus africana* is found on mountain ranges called "volcanic line of Cameroon" which includes the regions of Southwest, Northwest, West and Adamaoua, and in some sites of the Central region (Melle et al. 2016). This species has several vernacular names in Cameroon (Cunningham and Mbenkum 1993) but it is commonly called African pygeum which is the name attributed to this plant during its first description by Hooker (1864) as *Pygeum africanum* Hook.f. and later was moved to the genus *Prunus* subg. *Laurocerasus* by Kalkman (1965).

Prunus africana attains a height of 30 to 40 m (Stewart 2003; Kadu et al. 2012). Its mature bark resembles the skin of the crocodile and its wood is brown and red. However, the morphology of the species varies according to its habitat, especially concerning the diameter and the height of the trees. The flowers of *Prunus africana* are hermaphrodite (Hall et al. 2000) and the flowering period coincides with low seasonal rainfall and the lowest temperatures, including November to February. Its fruiting is irregular, two to three months intervening between flowering and fruit maturity, and occurs every 2 to 3 years (Geldenhuys 1981). The first flowering takes place when the tree is between 15 and 20 years old, when it is not exploited (Simons et al. 1998). Seeds are recalcitrant (Schaefer, 1990) and lose their germinative power after three weeks (Ondigui 2001). Both self-pollination and insect cross-pollination (Were et al. 2001) occur in *Prunus africana*; however, cross-pollination is the preferential reproductive system of this species (Tonye et al. 2000).

Prunus africana is used for multiple purposes, including artisanal and medicinal uses (Cunningham et al. 2002). The great importance given to this tree resides particularly in the use of its bark against benign prostatic hyperplasia, first discovered and patented by Debat (1966) and since studied by several authors (Njamnshi and Ekati 2008; Kadu et al. 2012). The *Prunus* leaves and roots are also used in the traditional pharmacopoeia as febrifuge for the treatment of upset stomach, pulmonary infection (chest pain), malaria, fever, sexually transmitted diseases and injuries (Carter 1992; Cunnigham and Mbenkum 1993). Apart from this medicinal use, its wood is used locally as firewood and for construction, especially the construction of wagons (Stewart 2003a and b). This plant gives important economic opportunities to rural communities, and over the past decades interest for *P. africana* has changed from traditional to international commercial use. Since 1972, Cameroon has been the major source of bark trade (Cunningham and Mbenkum 1993). Despite the multiplicity of its uses, the declining of *P. africana* populations has been observed in many areas due to the overexploitation of its bark, which threatens a gradual disappearance of the species mainly by commercial harvesting (Cameroon, Equatorial Guinea, Kenya, DRC, Uganda, Madagascar) and by habitat degradation and fragmentation accompanied by invasive alien species which is the case in the southern Africa (Jimu et al. 2011). This overexploitation led the World Alliance for Nature to classify *P. africana* as a vulnerable species which was listed in Appendix II of the Convention on International Trade in Endangered Species of Fauna and Flora (CITES) in 1994, becoming effective in 1995 (Sunderland and Tako 1999). To ensure sustainable utilization and management of *P. africana* in many African countries where it grows, exportation requires a permission.

Before other considerations, the conservation and *in situ* management of *P. africana* requires a good knowledge

of the genetic structure of this species with low potential of colonization. For *Prunus africana*, many studies have been carried out on genetic diversity (Barker et al. 1994; Dawson 1999; Avana et al. 2004; Muchugi et al. 2006; Atnafu 2007; Clair and Howe 2011; Kadu et al. 2013; Mihretie et al. 2015, Nantongo et al. 2016), biochemical property (Tchouakionie 2014; Nzweundji 2015) but cytogenetic studies are still lacking, hence the present study.

The karyological studies in the genus *Prunus* were principally limited on chromosome count. If we consider, as Wen et al. (2008), that the genus *Prunus* comprises about 250 species, the chromosome number is available for more than 76 percent of species (191/250 according to available chromosome databases). The genus presents the basic chromosome number of x=8 (Darlington 1927, 1928) and at least three ploidy levels, diploid, tetraploid and hexaploid (Oginuma 1987; Bennett and Leitch 1995; Iwatsubo et al. 2002; Maghuly et al. 2010). However, some species have been studied by molecular cytogenetics as *P. amygdalus* Stokes (Corredor et al. 2004), *P. persica* (L.) Batsch Peach (Yamamoto et al. 1999; Yamamoto 2012) and *P. subhirtella* Hook. (Maghuly et al. 2010).

Genome size is a fundamental parameter in many genetic and molecular biological studies. Knowledge of the genome size or the 2C value is important for basic and applied studies involving genome organization, species relationships, phylogeny and even taxonomy and biodiversity (Bennett 1984; Bennett and Leitch 2005). At present, flow cytometry is the main method for evaluation of nuclear DNA content because it is both rapid and precise, and reveals even the small differences in DNA content (Marie and Brown 1993; Doležel and Bartoš 2005). However, till today, and according to available databases the genome size of about only 25 species of *Prunus* has been estimated (Arumuganathan and Earle 1991; Dickson et al. 1992; Baird et al. 1994; Bennett and Leitch 1995; Loureiro et al. 2007; Siljak-Yakovlevet al. 2010; Gainza-Cortés 2014; Žabka et al. 2018), which presents 10% for the genus.

Despite the importance of genome size, to the best of our knowledge there is no report on the DNA amount of *Prunus africana,* which is the only species of *Prunus* originating from Africa. It is the same case for cytogenetical characterization of this species, despite the fact that for other species of this genus the banding techniques and Fluorescent *In Situ* Hybridization (FISH) has been developed in order to detect respectively the difference between morphologically similar chromosomes and localization of useful genes (Soodan et al. 1988; Corredor et al. 2004; Maghuly et al. 2010; Yamamoto 2012).

Therefore, we consider that it was necessary to characterize the genome of *P. africana:* 1) by assessment of DNA content using the flow cytometry technique; 2) chromosome counting for determination of ploidy level using the standard cytogenetic method; 3) distribution patterns of GC-rich heterochromatin using the fluorochrome banding; 4) chromosome localization of 18S-5.8S-26S (35S) rRNA genes using a fluorescent *in situ* hybridization. The results will be compared and discussed with those available for other species of the genus *Prunus*.

MATERIALS AND METHODS

Origin and conditioning of plant material

The seed samples (50 seeds from two populations) of *Prunus africana* were collected in Mont Oku at 2400 m and Mont Cameroon at 2500 m of altitude in Cameroon (Fig. 1, box). The hard endocarps of seeds were removed and seeds of uniform size (about 0.7 cm) were used for germination. They were germinated directly in glass dishes containing watered filter paper (Fig. 2C). Cultures were visually checked daily and irrigated with tap water when necessary under laboratory conditions at about 24°C. After 6 weeks, the root meristems of germinated seeds were used for cytogenetic studies. Germinated seeds were transferred to pots and after 4 weeks the leaves were collected for flow cytometry (Fig. 2D).

Genome size assessment by flow cytometry

The total nuclear DNA content was determined by flow cytometry according to Marie and Brown (1993). *Solanum lycopersicum*, 2C= 1.99 pg (Lepers-Andrzewski et al. 2011) was used as internal standard. Leaf tissue of *Prunus africana* and *Solanum lycopersicum* was placed in a plastic Petri dish and chopped together with a razor blade in 600 µL of cold Gif Nuclear Buffer which is slightly modified Galbraith's buffer (Galbraith et al. 1983): 45 mM $MgCl_2$, 30 mM sodium citrate, 60 mM 4-morpholinepropane sulfonate pH 7, 0.1 % (w/v) Triton X-100, 1% polyvinylpyrrolidone (~10,000M_r, Sigma P6755), 5 mM sodium metabisulfite and 10 µg/ml RNase (Sigma Aldrich, Saint Quentin, France). Nuclear suspensions were filtered through nylon mesh (pore size 50 mm, Cell Trics, Partec) and stained with 50 mg ml^{-1}propidiumiodide (PI: Sigma-Aldrich, France). After 5 min incubation on ice, nuclear suspensions were analyzed. Five individuals per accessions were analyzed in order to obtain the mean DNA content. At least 5000 to 10, 000 nuclei were analyzed for each sample using a Cyflow SL3, Partec, 532-nm laser cytometer (Munster, Ger-

Fig. 2. *Prunus africana:* A) 6-years-old tree; B) fruit - two-lobed drupe, with a seed in each lobe; C) germination of seeds in Petri dishes; D) seedlings.

many). Nuclear DNA content was estimated using the linear relationship between the fluorescent signals from stained nuclei of *P. africana* specimens and the internal standard (*S. lycopersicum*) according to the following equation:

2C DNA content/nucleus = [Sample 2C peak mean × Standard 2C DNA] (pg)

Standard 2C peak mean

The symbol C corresponds to the holoploid nuclear genome size (the whole chromosome complement with chromosome number *n*), 1C and 2C being, respectively, the DNA contents of the haploid (*n*) and diploid (2*n*) sets of chromosomes, irrespective of ploidy level (Greilhuber et al. 2005). The conversion from picograms (pg) to base

pairs (bp) was done as follows: 1 pg DNA = 978 Mbp (Doležel et al. 2003).

Determination of chromosome number

Root tips, obtained from potted plants were pretreated with 0.002 M 8-hydroxyquinoline at 16°C for 3h. Fixation was performed in freshly prepared 3:1(v/v) ethanol-acetic acid for at least 24h. Fixed root tips were stored for a few days in the first fixative, or several months in 70% ethanol at 4°C. For chromosome counting the root tips were hydrolyzed in 1N HCl for 10 min at 60°C and stained in Schiff reagent following the standard Feulgen method, or in an enzymatic mixture for 45 min at 37°C. The squash was performed in a drop of acetic carmine. The chromosome number was also verified on slides prepared for fluorochrome banding by chromomycin A_3 or for FISH for which they were counterstained with DAPI (4', 6-diamidini-2-phenylindole). Chromosome plates were observed under a Zeiss Axiophot microscope. The chromosome number was determined for at least 10 individuals, from several well-spread metaphases per root tip.

Preparation of protoplasts for fluorochrome banding and fluorescence in situ hybridization (FISH)

Fixed root tips were washed in 0.01 M citrate buffer pH 4.6 for 15 min, then incubated in an enzymatic mixture for 45 min at 37°C. This enzymatic mixture was composed of 4% cellulase R10 (Onozuka Yakult Honsha Co.), 1% pectolyase Y23 (Seishin Pharmaceutical, Co., Tokyo, Japan), and 4% hemicellulase (Sigma Chemical Co.) in 0.01M citrate buffer at pH 4.6.

These digested meristems were squashed onto a drop of freshly prepared 45% acetic acid and the preparations were observed at a phase contrast microscope. The best slides were frozen at -80° C over night and then the cover slips were removed and the slides were rinsed with absolute ethanol and air-dried.

Fluorochrome banding

For detection of GC-rich DNA regions, the chromosomes were stained with chromomycin A_3 (CMA_3) fluorochrome using Schweizer's (1976) method, with slight modifications, from Siljak-Yakovlev et al. (2002) concerning the concentration of chromomycin (0.2 mg/ml) and time of staining (60 min). After chromosome observation, the best slides were distained in 3 :1 ethanol-acetic acid, dehydrated in a graded ethanol series (70%, 90%,100%), air-dried for at least 12h at room temperature, and then used for FISH experiment.

Florescence in situ *hybridization*

FISH was performed for the detection of 35S rDNA loci. The 35S rDNA probe was a clone of 4-kb from *Eco*RI fragment, including 18S-5.8S-26S rDNA sequences from *Arabidopsis thaliana* (L.) Heynh. labelled with the direct Cy3 fluorochrome (Amersham, Courtaboeuf, France) by nick translation, according to the manufacturer's protocol. *In situ* hybridization was carried out following Heslop-Harrison et al. (1991) with some minor modifications. Slides were counter-stained and mounted in Vectashied medium (Vector Laboratories, Peterborough, UK) with DAPI. Chromosome plates were observed using an epifluorescence Zeiss Axiophot microscope with different combinations of excitation and emission filter sets (01, 07, 15 and triple filter set 25). Hybridization signals were analyzed and the best metaphase plates were photographed using a highly sensitive CCD camera (RETIGA 200R, Princeton Instruments, Every, France) and image analyzer (Metavue, Every, France).

RESULTS

Nuclear DNA content and chromosome number

In this study both the genome size and chromosome number of *Prunus africana* were determined for the first time. Nuclear DNA content of *P. africana* was 2C=1.44 pg or 1408 Mbp (1pg DNA = 978 Mbp according to Doležel et al. 2003), ranking the taxon in the category of very small genomes (2C ≤ 2.8 pg, according to Leitch et al. 1998). The chromosome number showed that *P. africana* is a tetraploid species with 2n=4x=32 small (~ 1 to 2 μm) chromosomes (Fig. 3) and basic chromosome number x=8. This number, which showed a high stability, has been verified with all used techniques: squash in acetic acid after staining in carmine acetic (Fig. 3A); protoplast technique with chromosome speeded in acetic acid without staining (Fig. 3B – phase contrast picture), after fluorochrome bandings with DAPI staining (Fig. 3C) and CMA_3 (Fig. 3D), and after FISH experiment (Fig. 3F).

rRNA genes and heterochromatin pattern

Fluorochrome banding revealed ten G-C rich heterochromatin regions (CMA^+ bands), which were always

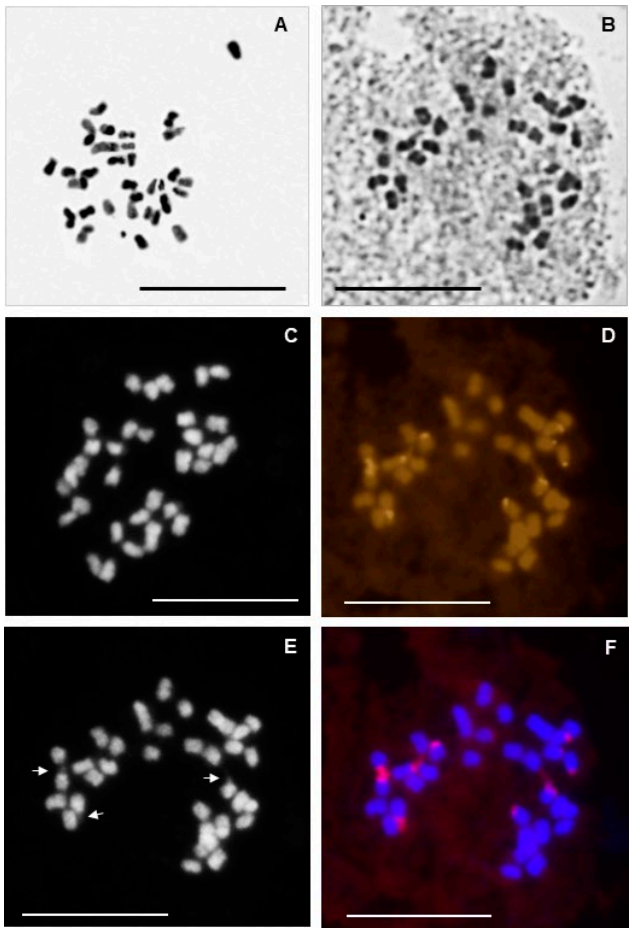

Fig. 3. A) Schiff stained metaphase plate showing 2n=32 chromosomes. B) Non-colored metaphase chromosome plate obtained after enzymatic hydrolysis photographed under microscope with phase-contrast. C) DAPI stained chromosomes without visible bands. D) The same metaphase plate (D, E and F) after the fluorochrome banding with chromomycin A_3. The CMA^+ bands corresponded to DNA regions rich in G-C bases. E) DAPI stained chromosome after FISH experiment showing DAPI negative bands (arrows) corresponding to A-T low DNA regions. F) FISH experiment revealed ten 35 rDNA (red) signals which corresponded to ten CMA^+ bands (see Fig. C). Bar scale = 10 μm.

associated with rDNA loci (Fig. 3D). The karyotype of *P. africana* is characterized by five loci of 35S rDNA (visible as ten red hybridization signals), which were located in terminal or subtelomeric positions. These strong red signals appeared as weakly stained regions after DAPI counterstaining which indicated their richness in G-C bases (Fig. 3E, arrows). The number and the position of 35S rDNA loci are presented in Fig. 3F. Some centromeric 35S signals were of weaker fluorescent intensity than terminal signals and do not appear in all observed metaphase plates. DAPI stained chromosomes did not display any visible bands (Fig. 3C).

DISCUSSION

Phylogenetic context

The subfamily Amygdaloideae comprises nine tribes and for several of them the relationships were uncertain in previous phylogenetic study (Potter et al. 2007). In recent work of Xiang et al. (2016) the tribe *Neillieae* is supported as the basal lineage of Amygdaloideae, followed by the tribe *Spiraeeae*. The only species of *Lyonothamneae*, previously placed as the basal lineage, becomes the sister to *Amygdaleae*. This phylogenetic context is also very well supported by the basic chromosome number. The two basal clades have x = 9, which is also the ancestral basic number of Rosaceae (Vilanova et al. 2008), and two tribes *Lyonothamneae* and *Amygdaleae,* formed the only clade with x = 8 in subfamily Amygdaloideae. It is, at the same time, the only events of decreasing dysploidy in this subfamily while in the subfamily Rosoideae this phenomenon occurred several times because x = 7 is the most frequent base number. The closest genera of *Prunus*, *Maddenia* and *Pygeum* also have x = 8.

In the phylogenetic frame *Prunus africana* is always in the same clade especially with the Asian tropical species of the genus *Pygeum* which shows that they are very close (Wel et al. 2008).

Chromosome number and nuclear DNA content

To verify the genome size and chromosome number data for the genus *Prunus* and to attribute the status of novelty for investigated species, we used updated databases: Kew plant DNA C-values database (http://data.kew.org/cvalues), FLOWer, a plant DNA flow cytometry database (http://botany.natur.cuni.cz/flower/index.php), Index to Plant Chromosome Numbers (IPCN) - Tropicos (http://www.tropicos.org/Project/IPCN) and The *Chromosome Counts Database* (*CCDB),* (http://ccdb.tau.ac.il/search/).

In the genus *Prunus*, which has been highly studied from many viewpoints, the number of species with available genome size information is very low, only about 25 (10 %) species have genome size records to date, whereas chromosome numbers have been reported for at least 76 % of the taxa. It is a very good report knowing that chromosome number has been determined to date for about only 25% of angiosperms taxa (Stuessy 2009) or for only 20% according to Rice (2015).

The basic chromosome number of *Prunus* genus is x=8 (Darlington 1927, 1928) and their ploidy level ranges from diploid ($2n$=$2x$=16) to tetraploid ($2n$=$4x$=32)

Table 1. *Prunus* species for which some molecular cytogenetic data are available. Comparison with our results of *P. africana*.

Species	2n (ploidy level)	2C DNA in pg	35S rDNA signals number (position)	$CMA^+/DAPI^-$ bands number	References
P. africana (Hook. f.) Kalkman	32 (4*x*)	1.44	10 (terminal, satellite)	10	Present work
P. amygdalus Stokes	16 (2*x*)	0.66	6 (terminal satellite)	-	Corredor et al. 2004
P. armeniaca L.	16 (2*x*)	0.60	-	6	Yamamoto 2012; Arumuganathan and Earle 1991
P. incisa x *serrula*	32 (4*x*)	1.22	12 (terminal satellite)	-	Maghuly et al. 2010
P. mume (Siebold) Siebold & Zucc	16 (2*x*), 32 (4*x*)	-	-	5 to 8	Yamamoto 2012
P. persica (L.) Batsch Peach	16 (2*x*)	0.55	6 (terminal, satellite, proximal)	6	Yamamoto et al. 1999, Yamamoto 2012
P. salicina Lindl.	16 (2*x*)	-	-	6	Yamamoto 2012
P. subhirtella Hook.	probably 16 (2*x*)	0.61	6 (terminal)	-	Corredor et al. (2004); Maghuly et al. 2010

and hexaploid (2*n*=6*x*=48) (Bennett and Leitch 1995; Maghuly et al. 2010; Siljak-Yakovlev et al. 2010). *Prunus africana* is a tetraploid species (2*n*=32) with genome size 2C=1.44 pg. Based on available bibliographic data genome size for diploid *Prunus* species ranges from 0.55 to 1.00 pg (Dickson et al. 1992) and for tetraploids from 1.14 to 1.30 (Arumuganathan and Earle 1991; Siljak-Yakovlev et al., 2010). The 2C values of *P. africana* (1.44 pg) was slightly bigger that in other tetraploids. The only hexaploid species measured until now is *P. domestica* L. (Darlington and Wylie 1955) with 2C=1.85 pg (Arumuganathan and Earle 1991; Bennett and Leitch 1995). Horjales et al. (2003) reported 2C=2.35 pg for *P. padus* L. and Zonneveld et al. (2005) 7.30 pg for *P. laurocerasus* L. which indicated the existence of higher ploidy levels that 6*x* in this genus.

Heterochromatin and 35S rDNA pattern recorded

In this study the data concerning heterochromatin and rRNA genes patterns for *Prunus africana* were reported for the first time. In Table 1 we presente available molecular cytogenetics data for some species of the genus *Prunus* and compare with the results obtained in this work. We observed 10 G-C rich DNA regions in all the samples used for this experiment. Previous studies performed for *Prunus persica* (Yamamoto et al. 1999; Yamamoto 2012), *P. salicina* Lindl. (Yamamoto 2012) and *P. armeniaca* L. (Yamamoto 2012; Arumuganathan and Earle 1991) revealed six and in *P. mume* five to eight G-C rich DNA regions (Yamamoto 2012). The GC-rich heterochromatin was always co-localized with 35S rDNA loci. The same observation has been reported by Yamamoto et al. (1999) and Yamamoto (2012) for *Prunus persica*. The co-localization of GC-rich heterochromatin and ribosomal genes has been frequently reported; e.g. in *Retama* (Benmiloud-Mahieddine et al. 2011); *Fraxinus* (Siljak-Yakovlev et al. 2014); *Tanacetum* L. (Olanj et al. 2015); *Eucalyptus* (Riberio et al. 2016); *Sclerocaria* (Bationo-Kando et al. 2016). Other rDNA patterns have been described in several *Prunus* species. This is the case of 5S and 18S-5.8S-25S ribosomal RNA genes which have been located in *Prunus persica* (Yamamoto et al. 1999), in *P. amygdalus* Batsch (Corredor et al. 2004) and in two others species of Cherry rootstock; *P. subhirtella* Miq. (Corredor et al. (2004); Maghuly et al. 2010) and *P. incisa* x *serrula* (Maghuly et al. 2010). In these last studies the diploid *P. subhirtella* presented six 35S rDNA signals as in the majority of diploid *Prunus* species (Yamamoto 2012), while the recent tetraploid hybrid *P. incisa* x *serrula* presented namely the double (12 signals). The diploid ancestor of *P. africana* probably had three loci of 35S rDNA whose numbers decrease from six to five loci during the chromosomal restructuring after polyploidisation.

CONCLUSION

The present paper has focused on the cytogenetic characterization of *Prunus africana*, contributing to the better knowledge of this useful African tree. How-

ever, future studies from populations collected in other regions would provide more information for the sustainable management of this endangered species. Currently, *P. africana* is on the IUCN Red List and has been classified as a priority for conservation by FAO. In Cameroon and at the international level, provisions have been made and laws have been drawn up to ensure the rational exploitation of this species. These investigations will make possible to identify the priority areas for the conservation of this species but also to establish a best management plans for the sustainability of genetic resources of *Prunus africana*.

ACKNOWLEDGEMENTS

We would like to thank Michael Bourge for his expertise of the Flow Cytometry of I2BC (www.i2bc.paris-saclay.fr), Gif-sur-Yvette, France. Samuel Pyke is acknowledged for critical reading of the manuscript and English text revision. This work was partially supported by grants from The International Union of Biochemistry and Molecular Biology (grant MFS Ngo Ngwe).

REFERENCES

Arumuganathan K, Earle E. 1991. Nuclear DNA content of some important plant species. Plant Molecular Biology Reporter 9: 208-218.

Atnafu H. 2007. Genetic variation in some natural population of *Prunus africana* from Ethiopia as revealed by randomly amplified polymorphic DNA (RAPD). [Dissertation]. Addis Ababa University.

Avana ML, Tchoundjeu Z, Bell MJ Vaillant A, Chevalier MH. 2004. Diversité génétique de *Prunus africana* (Hook.f.) Kalkman au Cameroun. Bois et Forêts des tropiques 282: 41-49.

Baird VW, Estager AS, Wells JK. 1994. Estimating nuclear DNA content in peach and related diploid species using laser flow cytometry and DNA hybridization. Journal of the American Society of Horticultural Science 119(6): 1312-1316.

Barker NP, Cunningham AB, Morrow C, Harley EH. 1994. A preliminary investigation into the use of RAPD to assess the genetic diversity of a threatened African tree species: *Prunus africana*. Strelitzia 1: 221-230.

Bationo-kando, Zongo PJ, Siljak-Yakovlev S. 2016. First genome size assessment, heterochromatin and rDNA chromosome mapping in the genus *Sclerocarya* (Anacardiaceae): insight into the new basic chromosome number. Botany Letters 163 (1):11-17.

Benmiloud-Mahieddine R, Abirached-Darmency M, Brown SC, Kaid-Harche M, Siljak-Yakovlev S. 2011. Genome size and cytogenetic characterization of three Algerian *Retama* species. Tree Genetics and Genomes 7: 987-998.

Bennett MD, Leitch IJ. 2005. Nuclear DNA amounts in angiosperms: progress, problems, prospects. Annals of Botany 95: 45–90.

Bennett MD, Leith I.J. 1995. Nuclear DNA Amounts in Angiosperms. Annals of botany 76:113-176.

Bennett MD. 1984. The genome, the natural karyotype and biosystematics. In: Grant WF Grant, editor. Plant systematics from in plants and its ecological implication. New Phytologist 106:177-200.

Bodeker G, Van'T Klooster C, Weisbord E. 2014. *Prunus africana* (Hook.f.) Kalkman: the overexploitation of a medicinal plant species and its legal context. Journal of Alternative and Complementary Medicine. 20(11): 810–822.

Carter E. 1992. Limbe Botanical Garden and Rainforest Genetic Conservation project: socioeconomic and institutional study. Final report to Overseas Development Agency. London. 52p.

Clair SJB, Howe GT. 2011. Strategies for conserving forest genetic resources in the face of climate change. Turkish Journal of Botany 35: 403–409.

Corredor E, Román M, García E, Perera E, Arús P, Naranjo T. 2004. Physical mapping of rDNA genes establishes the karyotype of almond. Annals of Applied Biology 144: 219–222.

Cunnigham AB, Mbenkum FT. 1993. Sustainability of Harvesting *Prunus africana* Bark in Cameroon: medicinal plant in international trade. People and plants working paper 2. UNESCO, Paris, p.1-28.

Cunningham M, Cunningham AB, Schippmann U. 1997. Trade in *Prunus africana* and the implementation of CITES. Bonn, Germany: German Federal Agency for Nature Conservation. 52 p.

Cunninghan AB, Ayuk E, Franzel S, Duguma B, Asanga AC. 2002. An economic evaluation of medicinal tree cultivation *Prunus africana* in Cameroon. People and Plants Working Paper .10, 35 p.

Darlington C D. 1927. The behaviour of polyploids. Nature, 119: 390-392.

Darlington CD, Wylie AP. 1955. Chromosome atlas of flowering plants. London: George Allen & Unwin.

Darlington CD. 1928. Studies in *Prunus* I, II. Journal Genetic 19: 213-256.

Dawson IK, Powell W. 1999. Genetic variation in the Afromontane tree *Prunus africana*, an endangered medicinal species. Molecular Ecology 8: 151-156.

Debat, J. 1966. Br. App., 25.893/66, June, 10.

Dickson EE, Arumuganathan K, Kresovich S, Doyle JJ. 1992. Nuclear DNA content variation within the Rosaceae. American Journal of Botany 79: 1081-1086.

Doležel J, Barto J, Voglmayr H., Greilbuber J. 2003. Nuclear DNA content and genome size of trout and humain. Cytometry A. 51(2): 127-128.

Doležel J, Barto J. 2005. Plant DNA flow cytometry and estimation of nuclear genome size. Annals of Botany 95: 99-110.

Gainza-Cortés F, Angeles M, Reig G, Fabiane KC, Almaba R, Ortiz M, Gogorcena Y, Vallés MP, Castillo AM. 2014. Ploidy determination by flow cytometry in *Prunus* species used as Rootstocks. Poster session presented at: IX Reunión de Biología Vegetal REBIVE; IX Reunión de Biología Vegetal REBIVE; Serena, Chile.

Galbraith DW, Harkins KR, Maddox JM, Ayres NM, Sharma DP, Firoozabady E. 1983. Rapid flow cytometric analysis of the cell cycle in intact plant tissues. Science 220: 1049–1051.

Geldenhuys CJ. 1981. *Prunus africana* in the Bloukrans River Gorge, Southern Cape. South African Forestry Journal 118: 61–66.

Greilhuber J, Doležel J, Lysák M, Bennet MD. 2005. The origin, evolution, and proposed stabilization of the terms 'genome size' and 'C-value' to describe nuclear DNA contents. Annals of Botany 95: 255–260.

Hall JB, O'Brien EM, Sinclair FL. 2000. *Prunus africana*: a monograph. School of Agricultural and Forest Sciences Publication Number 18, University of Wales, Bangor. 104 p.

Heslop-Harrison JS, Schwarzacher T, Anamthawat-Jonsson K, Leitch IJ. 1991. *In situ* hybridization with automated chromosome denaturation; Techniques: a Journal of Methods in Cell and Molecular Biology 3: 109-116.

Hooker JD. 1864. On the plants of the temperate regions of the Cameroons mountains and islands in the Bight of Benin; collected by Mr. Gustav Mann, Government Botanist. Botanical Journal of the Linnean Society 7: 191–192.

Horjales M, Redondo N, Blanco A, Rodríguez MA. 2003. Cantidades de DNA nuclear en árboles y arbustos [Quantities of nuclear DNA in trees and shrubs]. Nova Acta Cient Compost (Biol). 13: 23–33.

Iwatsubo Y, Kawasaki T, Naruhashi N. 2002. Chromosome numbers of 193 cultivated taxa of *Prunus*. J. Phytogeogr. Taxon. 50: 21–34.

Jimu L, Ngoroyemoto N, Mujuru L 2011. Structural diversity and regeneration of the endangered *Prunus africana* (Rosaceae) in Zimbabwe. African Journal of Ecology 51 (1): 102-110.

Kadu CA, Parich A, Schueler S, Konrad H, Muluvi GM, Eyog-Matig O, Muchugi A, Williams VL, Ramamonjisoa L, Kapinga C, et al. 2012. Bioactive constituents in *Prunus africana*: geographical variation throughout Africa and associations with environmental and genetic parameters. Phytochemistry 83:70–78.

Kadu CAC, Konrad H, Schueler S, Muluvi GM, Eyog-Matig O, MuchugiA, Williams VL, Ramamonjisoa L, Kapinga C, Foahom B. et al. 2013. Divergent pattern of nuclear genetic diversity across the range of the Afromontane *Prunus africana* mirrors variable Pleistocene cli-mate of African highlands. Ann Bot. 111:47–6.

Kalkman C. 1965. The Old-World species of *Prunus* subg. Laurocerasus including those formerly referred to *Pygeum*. Blumea 13: 1–174.

Leitch IJ, Chase MW, Bennett MD. 1998. Phylogenetic analysis of DNA C-values provides evidence for a small ancestral genome size in flowering plants. Annals of Botany 82: 85-94.

Lepers-Andrzejewski S, Siljak-Yakovlev S, Brown SC, Wong M, Dron M. 2011. Diversity and dynamics of plant genome size: an example of polysomaty from a cytogenetic study of *Tahitian vanilla* (Vanilla x tahitensis, Orchidaceae). American Journal of Botany 98: 986–997.

Loureiro J, Rodriguez E, Doležel J, Santos. C. 2007. Two new nuclear isolation buffers for plant DNA flow cytometry: a test with 37 species. Annals of Botany 100(4): 875-888.

Maghuly F, Schmoeller B, Temsch EM, Laimer M. 2010. Genome size, karyotyping and FISH physical mapping of 45S and 5S genes in two cherry rootstocks: *Prunus subhirtella* and *Prunus incisaxserrula*. Journal of Biotechnology 149(1-2): 88-94.

Marie D, Brown SC. 1993**.** *A cytometric exercise in plant DNA histograms, with 2C values for 70 species.* Biology of the Cell 78*:* 41–51.

Melle EM, Nkwatoh AF, Nsadzetsen RA. 2016. The Ecological Distribution of Wild *Prunus africana* in Mount Cameroon National Park, Cameroon. Int. J. Curr. Res. Biosci. Plant Biol. 3(7): 73-80.

Mihretie Z, Schueter S, Honrad H, Bekele E, Geburek T. 2015. Partterns of genetic diversity of *Prunus africana* in Ethiopia: Hotspot but not point of origin for range-wide diversity. Tree Genetics Genome 11:118.

Muchugi A, Lengkeek AG, Kadu CAC, Muluvi GM, Njagi ENM, GM, Dawson IK. 2006. Genetic variation in the threatened medicinal tree *Prunus africana* in Cameroon and Kenya: implications for current management and evolutionary history. South African

Journal of Botany 72: 498-506.

Nantongo JS, Eilu G, Geburek T, Schueler S, Konrad H. 2016. Detection of self incompatibility genotypes in *Prunus africana*: Characterization, evolution and spatial analysis. PLoS ONE 11(6): e0155638. doi:10.1371/journal.pone.0155638

Niklas J, Karl, 1997. The evolutionary biology of plants. Chicago: University of Chicago Press.

Njamnshi B, Ekati J. 2008. Le cas du *Prunus africana* [*Prunus africana* case]. Troisième atelier panafricain de renforcement de capacités en matière d'accès aux ressources génétiques et de partage des avantages. Antsiranana, Madagascar. 21 p.

Nzweundji JG, Niemenak N, Oumar, Tsafack J.J., Konan K, Nyochembeng L, Noumi C, Donfagsiteli TN, Omokolo ND. 2015. Biochemical profile of cuttings used for in vitro organogenesis of *Prunus africana*: An endangered species in Cameroon. African Journal of Biotechnology 14(33): 2568-2575.

Oginuma, K. 1987. Karyomorphological studies on *Prunus* in Japan. J. Sci. Hiroshima Univ., Ser. B, Div. 2, Bot. 21: 1–66.

Olanj N, Garnatje T, Sonboli A, Vallès J, Garcia S. 2015. The striking and unexpected cytogenetic diversity of genus *Tanacetum* L. (Asteraceae): a cytometric and fluorescent *in situ* hybridization study of Iranian taxa. BMC Plant Biology **15**: 174.

Ondigui B. 2001. Gestion de *Prunus africana*: situation et perspectives au Cameroun et ailleurs [Management of *Prunus africana*: situation and prospects in Cameroon and abroad]. Rapport GTZ. 85 p.

Potter D, Eriksson T, Evans RC, Oh S, Smedmark JEE, Morgan DR, Kerr M, Robertson KR, Arsenault M, Dickinson TA, Campbell CS. 2007. Phylogeny and classification of Rosaceae. Plant Systematics and Evolution 266:5–43.

Rehder A. 1940. Manual of cultivated trees and shrubs hardy in North America. 2nd edn. New York: The Macmillan Company.

Rice A, Glick L, Abadi S, Einhorn M, Kopelman NM, Salman-Minkov A, Mayzel J, Chay O, Mayrose I. 2015. The Chromosome Counts Database (CCDB): A community resource of plant chromosome numbers. New Phytologist 206: 19–26.

Schaefer, C. 1990. Processing, storage and germination of *Prunus africana* seeds. Technical Note No. 10. Kenya Forestry Research Institute.

Schweizer D. 1976. Reverse fluorescent chromosome banding with chromomycin and DAPI. Chromosoma 58:307-324.

Siljak-Yakovlev S, Cerbah M, Coulaud J, Stoian V, Brown SC, Zoldos V, Jelenic S, Papes D. 2002. Nuclear DNA content, base composition, heterochromatin and rDNA in *Picea omorika* and *Picea abies*. Theoretical and Applied Genetics 104:505-512.

Siljak-Yakovlev S, Pustahija F, Šolić EM, Bogunić F, Muratović E, Bašić N, Catrice O, Brown C.S. 2010. Towards a genome size and chromosome number database of Balkan flora: C-values in 343 taxa with novel values for 242. Advanced Science Letters 3: 190–213.

Siljak-Yakovlev S, Temunović M, Robin O, Raquin C, Frascaria-Lacoste N. 2014. Molecular–cytogenetic studies of ribosomal RNA genes and heterochromatin in three European *Fraxinus* species. Tree Genetics & Genomes 10(2): 231–239.

Simons AJ, Dawson IK, Duguma B, Tchoundjeu Z. 1998. Passing problems: prostate and *Prunus*. Herbal Gram 43, 49–53.

Soodan AS, Koul AK, Wafai BA. 1988. Assessment of the Germplasm of Rosaceous Fruits under Cultivation in Kashmir Valley II. Meiotic system and pollen production in almond (*Prunus amygdalus* L. Batsch), peach (*Prunus persica* L. Batsch) and their hybrid. Cytologia 53: 665-670.

Stewart KM. 2003a. The African cherry (*Prunus africana*): can lessons be learned from an over-exploited medicinal tree? Journal of Ethnopharmacology 89: 3-13

Stewart KM. 2003b. The African cherry (*Prunus africana*): From hoe-handles to the international herb market. Economic Botany 57(4): 559-569.

Stuessy TF. 2009. Plant taxonomy. The systematic evaluation of comparative data. New York: Columbia University Press.

Sunderland TCH, Tako CT. 1999. The exploitation of *Prunus africana* on the island of Bioko, Equatorial Guinea. A report for the People and plants initiative, WWF-Germany and the IUCN/SSC Medicinal Plant Specialist Group.

Tchouakionie M, Youmbi E, Nkeng MN, Kouam SF, Lamshöft M, Spiteller M. 2014. Effect of some abiotic factors on the concentration of β- sitosterol of *Prunus africana* (Hook.f.) Kalkman in the tropical forests of Cameroon. International Journal of Agricultural Research 4 (2): 1-11.

Tonye M, Stella A, Ndam N, Blackmore P. 2000. State of knowledge of *Prunus africana* (Hook. f.) Kalkman. Report established for Central Africa region at program for the Enviroment (CARPE). Washington DC. 82 p.

Vilanova S, Daniel J Sargent DJ, Arús P, Monfort A. 2008. Synteny conservation between two distantly-related Rosaceae genomes: *Prunus* (the stone fruits) and *Fragaria* the strawberry). BMC Plant Biology 8:67.

Wen J, Berggren ST, Lee C-H, Ickert-Bond S, Yi T-S, Yoo K-O, Xie L, Shaw J, Potter D. 2008. Phylogenetic inferences in *Prunus* (Rosaceae) using chloroplast*ndhF* and ribosomal ITS sequences. *Journal of Systematics and Evolution* 46:322–332.

Were JM, Munjuga M, Simon AJ, Dawson I, Ruigu S. 2001. Reproductive Biology of the endangered medicinal Prunus africana tree in central Kenya. ICRAF, Nairobi, Nairobi. East African Forestry Journal, 67(1): 47-54.

White F. 1983. The vegetation of Africa: a descriptive memoir to accompany the UNESCO/AETFAT/UNSO vegetation map of Africa by F. White. UNESCO, Paris.

Wielgorskaya T. 1995. Dictionary of Generic Names of Seed Plants. Bishen Singh Mahendra Pal Singh, Dehra Dun (India).

Xiang Y, Huang CH, Hu Y, Wen J, Li S, Yi T,5 Chen H, Xiang J, Ma H. 2016. Phylogeny in the context of geological times and genome duplication. Molecular Biology and Evolution. 34(2):262–281 doi:10.1093/molbev/msw242

Yamamoto M, Haji T, Yamaguchi M, Yaegaki M, Sanada T, Kudo K Mase N. 1999. Fluorescent banding pattern of peach (*Prunus persica* (L.) Batsch) chromosomes. Journal of Japanese Society for Horticultural Science 68: 471–475.

Yamamoto M. 2012. Recent progress on studies of chromosome observation in deciduous fruit trees. Journal of Japanese Society for Horticultural Science 81 (4): 305–313.

Žabka M, Ďurišová L, Eliáš Jr P, Baranec T, 2018. Genome size and ploidy level among wild and cultivated *Prunus* taxa in Slovakia. Biologia 73(2) : 121–128.

Zonneveld BJM, Leitch IJ, Bennett MD. 2005. First Nuclear DNA Amounts in more than 300 Angiosperms. Ann Bot. 96(2): 229–244.

Caryologia
International Journal of Cytology, Cytosystematics and Cytogenetics

Firenze University Press
www.fupress.com/caryologia

Citation: A. Özkara (2019) Assessment of cytotoxicity and mutagenicity of insecticide Demond EC25 in *Allium cepa* and Ames Test. *Caryologia* 72(2): 21-27. doi: 10.13128/caryologia-698

Published: December 5, 2019

Data Availability Statement: All relevant data are within the paper and its Supporting Information files.

Competing Interests: The Author(s) declare(s) no conflict of interest.

Assessment of cytotoxicity and mutagenicity of insecticide Demond EC25 in *Allium cepa* and Ames Test

Arzu Özkara

Department of Molecular Biology and Genetic, Faculty of Arts and Sciences, Afyon Kocatepe University, Afyonkarahisar/Turkey
E-mail: ozkara@gmail.com

Abstract. The mutagenicity and cytotoxicity of Demond EC25, a synthetic pyrethroid insecticide, was assessed using two standard genotoxicity assays of the *Salmonella typhimurium* mutagenicity assay (Ames test) and *Allium cepa* test. Cytogenetic effects of Demond EC25 were evaluated in the root meristem cells of *Allium cepa*. The test concentrations of compounds were selected by determining EC_{50} of the *Allium* root growth and onion seeds were exposed to Demond EC25 (50, 100, and 200 ppm) for 24, 48, and 72 hours. The concentrations Demond EC25 was compared with the value for the negative control using Dunnet-t test, 2 sided. The results indicated that mitotic index was clearly decreased with increasing the concentration of Demond EC25 in each treatment group as compared to the controls. Demond EC25 was tested for mutagenicity in bacterial reversion assay systems with two strains (TA98 and TA100) of *Salmonella typhimurium* absence and presence of S9 fraction. The doses of Demond EC25 were 50, 100, 200, 400, 800 µg/plate and test materials were dissolved in DMSO. Our results show that Demond EC25 was found to be mutagenic in 800 and 400 µg/plate doses of TA98 in the without S9 mix and 800 µg/plate in the with S9 mix. In TA100, Demond EC25 was found to be mutagenic only 800 µg/plate doses without S9 mix. The other doses of this insecticide was not found to be mutagenic in both test strains.

Keywords. Allium test, Ames test, cytotoxicity, Demond EC25, mutagenicity, pesticide.

INDRODUCTION

Pyrethroids are among the most commonly used insecticides in agriculture; they are also widely used indoors in pet shampoo, lice treatment, and even insect repellent (Saillenfait et al. 2015). They are therefore frequently present in food, air and dust of dwellings and thus can lead to both dietary and non-dietary exposure (Morgan 2012). Pyrethroids are botanical insecticides which are synthetic derivatives of pyrethrins and have been used for many years. However, most of pyrethroids are defined as moderately hazardous (Class II) by the World Health Organization (WHO 2009) (Jensen et al. 2011). The residues of pyrethroids have been detected in fruits, vegetables,

tea, pasteurized milk and porcine muscle (Nakamuraet al. 1993). Wider use of pyrethroids posed a serious risk to environment and human. Therefore, it may be an urgent need to evaluate the possible adverse effects of their use (Miao et al. 2017)

Pyrethroid pesticides disrupt the nervous system of insects and, to a lesser degree, of mammals, and thus raise human health concerns. (Oulhote and Bouchard 2013; Viel et al. 2015). Pyrethroid residual insecticides exert their toxic effects by targeting the nervous system of insects. Pyrethroids interfere with sodium channels in nerve fiber membrane and organophosphates bind to inhibit the activity of AChE found in the synaptic junction. Both actions result in continued nerve signaling and over-stimulation of nerve cells. Poisoned insect exhibits tremors and convulsions, eventually leading to death (ATSDR 2003; Valles and Koehler 2003). It is essential to carefully study and analyze the hazards of pyrethroids on human health including their genotoxic and cytotoxic properties. Hereby, it can be take adequate measures to prevent humans from potential mutagenic and carcinogenic effects. (Nagy et al. 2014).

Deltamethrin is a synthetic pyrethroid insecticide, sold by Safa Tarım Limited with trade names Demond EC 25 in local market. To our knowledge, there is no study mutagenicity of Demond EC 25 except in the present paper. The aim of this experiment was to evaluate both the mutagenic and cytotoxic effects of different doses of Demond EC 25 by the bacterial reverse mutation assay in *S. typhimurium* TA98 and TA100 strains with or without S9 mix and *Allium cepa* test, respectively.

MATERIAL METHOD

Chemicals

The test substance Demond EC25 was purchased from a local market in Afyonkarahisar/Turkey and dissolved in sterille distilled water. *Allium cepa* onion bulbs, 25–30 mm diameter, were obtained from a local market without any treatments. The other chemicals were obtained from Merck and Riedel.

Test strains

The LT-2 TA98 and TA100 histidine demanding auxotrophs of *S. typhimurium* were kindly obtained from Prof. B.N. Ames (University of California, Berkeley). These strains were incubated for 16h in liquid nutrient broth and kept at -80°C. Their genetic markers and other properties, such as the numbers of spontaneous revertants and responses to positive controls, were controlled as described by Maron and Ames (1983).

Allium Test

EC_{50} determination and mitotic index analysis

The procedure of the root inhibition test as described by Fiskesjo (1985) was followed with some modifications. The *Allium* root inhibition test was carried out to determine suitable concentrations for the genotoxicity assay. The outer scales of the bulbs and the dry bottom plate were removed without destroying the root primordia. The onions were grown in freshly distilled water for the first 24h and afterwards exposed for 96h to the Demond EC25 solutions (12.5, 25, 50, 100, and 200 ppm, respectively). In order to determine the EC_{50} values, the roots from each bundle were cut off on the fifth day and the length of each root was measured from both the Demond EC25 exposed bulbs and the control group. The EC_{50} value was considered as the concentration which retards the growth of the root 50% less when compared to the control group.

The EC_{50} value for Demond EC25 was approximately 100 ppm. In order to demonstrate possible concentration-dependent effects of this pesticide, the root tips were treated with 50 ppm (EC_{50}/2), 100 ppm (EC_{50}), 200 ppm (EC_{50}x2) concentrations of Demond EC25, and all application groups were tested 24, 48, and 72h treatment periods. Additionally we also used positive control group by using methyl methanesulfonate (MMS). After the treatment, the roots were washed in distilled water and fixed in 3:1 ethanol: glacial acetic acid for 24h and then the roots were transferred into 70% alcohol and stored at +4°C. The root tip cells were stained with Feulgen and five slides were prepared for each test group.

Ames *Salmonella*/Microsome Assay

The mutagenicity of the Demond EC25 was determined using the standard plate incorporation assay. *Salmonella typhimurium* strains TA98 and TA100 were used with or without S9 mix in this test (Ames et al. 1975; Maron and Ames 1983). The tester strains were tested for the presence of the strain-specific markers as described by Maron and Ames (1983). The cytotoxic doses of the Demond EC25 (800, 400, 200, 100, 50 µg/plate) were determined by the method of Dean et al. (1985). The stock solutions of the test materials were dissolved in sterile distilled water and stored at 4°C. The *S. typhimurium* strains were incubated in nutrient broth at 37°C for 16h with shaking. The positive controls were

4-nitro-o-phenylenediamine (NPD) for the TA 98 and sodium azide (SA) for the TA100, used without metabolic activation, and 2-aminofluorene (AF) for TA 98 and 2-aminoanthracene (2AA) for the TA 100 used with metabolic activation.

The test plates for the assays without the S9 mix were prepared by adding 0.1 ml of the test suspension for each concentration, 0.1 ml bacterial suspension from an overnight culture, and 0.5 ml phosphate buffer to 2 ml top agar (kept in 45°C water bath). The mixture was shaken for 3 s using a vortex mixer and then poured into the minimal agar. The test plates with the S9 mix were prepared by adding 0.5 ml of S9 mix instead of the phosphate buffer. All the test plates were incubated for 72h at 37°C, and then the revertant colonies on each plate were counted. The experiments were run in triplicate for each concentration and all the results from the two independent parallel experiments were used for the statistical analysis.

Statistical analysis

The data obtained for the root length, MI, and mitotic phases were expressed as percentages. The levels of difference in the treatment groups were analyzed statistically by using the SPSS 15.0 version for Windows. In the analyses, the Dunnett-t test (2 sided) was performed on both the *Allium* and Ames tests.

Table 1. Allium root growth inhibition test.

Test Substance	Concentrations (ppm)	Mean of root length±SD
Negative Control	-	3.57±0.24
Positive Control	-	1.03±0.15*
Demond EC25	12.5	3.12±0.42*
	25	2.02±0.15*
	50	1.68±0.41*
	100	1.45±0.23*
	200	1.12±0.22*

*Significantly different from negative control (p<0.05 Dunnet-t test, 2-sided), SD: Standart deviation.

RESULTS

Allium root growth test results are summarized in Table 1 and Table 2 gives the effect of Demond EC25 on MI and mitotic phase in the root meristematic cells of *A. cepa* treated for 24, 48 and 72h. The effective concentration (EC_{50}) was determined as 100 ppm in *Allium* test. At all concentrations treated in the incubations of root decreased MI compared to negative control at all exposure time. The reduced of MI results (p<0.05) were found statistically significant with all concentrations and all treatment time. All doses of Demond EC25 applied in the experiment caused changes in the percentage of particular phases' distribution in comparison to the control.

Table 2. The effects of Demond EC25 on MI and mitotic phases in the root cells of *A. cepa.*

Concentration (ppm)	Treatment Time	Counted Cell Number	Mitotic Index ± SD	Mitotic Phases (%) ± SD			
				Prophase	Metaphase	Anaphase	Telophase
Negative control	24 hour	4965	82.45±6.71	79.12±9.42	1.80±0.32	1.12±0.32	0.92±0.57
Positive control		5001	68.78±5.46*	34.24±4.62*	0.48±0.70*	0.49±0.54*	0.52±0.81
50		4889	51.48±4.09*	34.05±2.17*	1.00±0.72*	0.79±0.21*	1.10±0.62
100		4963	46.25±4.74*	32.54±4.20*	0.94±0.42*	0.68±0.34*	1.03±0.42
200		5013	45.21±2.69*	30.21±2.54*	0.82±0.40*	0.52±0.21*	0.59±0.74
Negative control	48 hour	5007	67.28±3.47	70.11±6.74	1.62±0.21	1.27±0.24	1.21±0.26
Positive control		4997	63.11±3.14*	31.75±3.45*	0.45±0.31*	0.52±0.16*	0.65±0.13
50		5101	52.25±3.45*	30.26±3.35*	0.71±0.92*	0.62±0.21*	1.19±0.21
100		5051	42.42±3.65*	28.45±2.70*	0.68±0.40*	0.54±0.02*	1.06±0.32
200		5113	36.20±1.25*	24.45±2.92*	0.52±0.32*	0.45±0.18*	0.89±0.14
Negative control	72 hour	5142	38.21±2.65*	57.52±3.41	1.43±0.41	1.21±0.21	1.09+±0.52
Positive control		5123	26.36±3.02*	29.04±2.28*	0.31±0.43*	0.60±0.42*	0.68±0.32
50		5263	19.23±1.75*	25.45±3.85*	0.58±0.23*	0.52±0.45*	0.49±0.41
100		5047	14.12±2.42*	21.42±2.56*	0.49±0.41*	0.46±0.71*	0.50±0.72
200		4985	13.21±2.21*	16.47±2.31*	0.34±0.42*	0.39±0.43*	0.56±0.61

* Significantly different from negative control (p< 0.05 Dunnet-t test. 2-sided) SD: Standart deviation.

Table 3.The mutagenicity assay results of Demond EC25 for *S. tyhimurium* TA98 and TA100 strains

Test Substance	Concentration (µg/plate)	No of His+ revertants/plate, mean±SD			
		TA98		TA100	
		- S9	+ S9	- S9	+ S9
Demond EC25	800	95.32±5.41*	116.42±5.52*	206.45±9.44*	215.52±12.85
	400	88.04±4.13*	102.21±3.96	178.42±7.45	203.12±10.25
	200	68.12±4.63	92.54±4.25	142.45±6.74	184.32±9.54
	100	52.09±3.86	78.09±4.52	121.22±6.61	168.35±8.65
	50	47.31±3.38	56.24±4.45	102.10±5.08	123.09±6.85
Neg. Control	100	36.07±3.36	49.14±3.70	90.10±13.42	114.23±7.38
SA	10			2965.56±56.35*	
2AA	5				2628.42±60.41*
2AF	200		1002.40±16.65*		
NPD	200	1575.50±24.56*			

*Mean statistically significant at p<0.05 (Dunnett t-test), SA:Sodium azide, NPD: 4-nitro-o-phenylendiamine, 2AF: 2-aminofluorene, 2AA: 2-aminoanthracene, SD: Standard deviation, Negative control: distilled water.

The results of the Ames test are shown in Table 3. In this experiment, first, the cytotoxic doses of Demond EC25 were determined. As seen in Table 3, spontaneous revertants were within the normal values in all the strains examined. All of the doses with and without S9 mix in TA98 and TA100 slightly increased when compared to the negative control. On the other hand, the plates containing positive control mutagens displayed very significant increases in the spontaneous mutation rate in two strains tested. Most of the results, whether increasing or decreasing relative to the negative control group, were not statistically significant at P<0.05 (Dunnett-t test, 2 sided) in the examined strains, except for in the 800 and 400 µg/plate doses of the Demond EC25 in the TA98 without S9 mix and 800 µg/plate doses with S9 mix. Additionally it was obtained mutagenic in the TA100 without S9 mix 800 µg/plate doses.

DISCUSSION

Pyrethroid insecticides are commonly used in agriculture, veterinary medicine, and to control insect pests in human dwellings because of their high selective toxicity for insects and relatively low acute toxicity to mammals (Casida and Quistad 1998). These insecticides are favored because of their effective role and have replaced organophosphorus pesticides in many areas of applications (Ministry of the Environment in Japanese 2011).

Because of their advantages, pyrethroid insecticides including Demond EC25 are becoming widespread and, therefore, studies on the biological effects of these pesticides are of immediate concern. Numerous studies on their toxicity, both in insects and mammals, have been reported in the literature. Although pyrethroid insecticides have consistently shown negative results in microbial genotoxicity tests, the outcome of other assays has been variable and it has not been possible to draw definite conclusions about the genotoxicity of this group of pesticides (Grossman 2007; Surralles et al. 1995).

In determining mutagenicity of chemicals, the Ames test has shown a variety of chemicals to be either mutagenic or anti-mutagenic, and has been shown to be over 90% accurate in predicting genotoxicity (Weisburger 2001). In the Ames test, *S. typhimurium* strains that have a mutation in the *his*-operon are used to detect the mutagenicity of chemicals (Maron and Ames 1983). In the present study, Demond EC25 was studied for its mutagenic activity with the Ames test and results can be concluded that Demond EC25 induced mutations in the 800 and 400 µg/plate doses of the TA98 without S9 mix and 800 µg/plate doses with S9 mix and in the TA100 without S9 mix.

Under our experimental conditions, Demond EC25 showed to produce point mutations in the Ames test, both in the absence and presence of the S9 metabolic activation system in high concentrations of both test strains. In order to characterize the possible mechanism of mutagenicity, the important bacterial strains, sensitive to different mutational events due to their specific genotypes, were used.

Particularly, *S. typhimurium* TA98 is characterized by the -1 frameshift deletion hisD3052, which affects the reading frame of a nearby repetitive –C–G– sequence

and can be reverted by frameshift mutagens. TA100 contains the marker hisG46, which results from a base-pair substitution of a leucine (GAG/CTC) by a proline (GGG/CCC): this mutation is reverted by mutagens causing base substitutions at G-C base pairs (Di Sotto et al. 2008). Taking into account these bacterial features, our results highlighted that the Demond EC25 mutagenicity, in the absence and presence of S9 in TA98, was likely due to frameshift mutations, and in the absence S9 in TA100 due to base-change mechanisms.

The data reported on the genotoxicity of synthetic pyrethroids are rather controversial, depending on the genetic system used (Akintonwa et al. 2008; Saleem et al. 2014). Studies have shown an important relationship between a substance's chemical structure and its biological activity (Oztas¸ 2005) chlor. Several factors, including rings, the functional groups, and the positions of binding locations in the chemical structure may affect a chemical's binding ability.

Mitotic index proved to be a useful parameter that allows one to detect the frequency of the cellular division (Marcano et al. 2004). The estimation of the potential cytotoxicity of the compounds is generally related to the inhibition of the mitotic activities (Smaka-Kincl et al. 1996). In this study, the used concentrations of Demond EC25 also caused significant inhibition of the mitotic index. The significant decline in the mitotic index could be due to the inhibition of the DNA synthesis or the blocking of the G1 suppressing the DNA synthesis or effecting the test compound at the G2 phase of the cell cycle (Sudhakar et al. 2001; Majewska et al. 2003). When a pesticide penetrates the cells and reaches a critical concentration, it could be in an active form, causing lesions during several following cellular cycles (Marcano et al. 2004). The decrease of the mitotic index in our study can be related to this.

In this study, all the concentrations of Demond EC25 caused the changes in the percentage of the particular phases' distribution when compared to the control group. Pesticides accumulate in the cell due to this substance not being able to emerge out of the cell easily after once penetrating the cell and it may be highly toxic in the cell (Antunes-Madeira and Madeira 1979).

Deltamethrin, the active ingredient in Demond EC25 has immunosuppressive (Lukowicz and Krechniak, 1992), reproductive effects on sperm cells (Bhunya and Pati 1990; Carrera et al. 1996) and developmental toxicity (Martin 1990). Deltamethrin is reported to cause chromosomal damage in *Allium cepa* (Chauhan et al. 1986), chromosomal aberrations and micronucleus formation in bone marrow cells of mice exposed *in vivo* (Chauhan et al. 1997; Gandhi et al. 1995). Saxena et al. (2009) evaluated of cytogenetic effects of deltamethrin in root meristem cells of *Allium sativum* and *Allium cepa* and cells analyzed immediately after the exposure showed a significant, concentration-dependent inhibition of mitotic index (MI) and induction of mitotic and chromosomal aberrations in both the test systems. Additionally, i*n vitro* exposure of Deltamethrin is reported to cause DNA damage in Comet assay in human peripheral blood leukocytes (Villarini et al. 1998). In the present study with *Allium cepa* root tip meristem cells however, the three concentrations of Demond EC25 tested induced genotoxicity thus corroborating the findings of these studies.

In contrast to our results, no genotoxic response of Deltamethrin was observed in *Salmonella typhimurium* and V79 Chinese hamster ovary cells (Pluijmen et al. 1984). Data on the genotoxicity and carcinogenicity of Deltamethrin are rather controversial, depending on the genetic system or the assay used (Shukla and Taneja, 2000).

The safety evaluation of a fragrance material includes a broad range of toxicological information, both for the compound itself and for structurally related chemicals belonging to the same chemical group (Bickers et al., 2003). Among toxicological information, genotoxicity is a systemic consideration, as it can be related to carcinogenicity (Di Sotto et al. 2008). Normally, to evaluate a potential genotoxic risk due to a chemical exposition, *in vitro* assays for detecting point mutations (Ames test) and extended treatment (e.g., micronucleus assay, *Allium* test, single cell gel electrophoresis assay or comet assay) are used in the first instance (EMEA 2008; Di Sotto et al. 2013). If the results of these studies are positive, *in vivo* studies, for example a mammalian cytogenetic study, are performed (EFSA 2014).

The tested substances with different test systems can be genotoxic or not genotoxic depending on a number of factors such as chemical structure and biological activity, having rings in the structure and the positions of the binding location (Kutlu et al. 2011). In addition to these, it might be related to differences in test conditions, such as exposure time, cell types, concentrations of substances, the dispersal of the materials and physicochemical characteristics of the compounds (Ema et al. 2012).Therefore, it could be explained why some studies find an increase of genetic damage while in others result as negative.

In conclusion, Demond EC25 was found to be cytotoxic due to decreasing of MI in Allium test and showed mutagenic activity at some doses in the Ames test. Demond EC25 had clear cytotoxic effects and may pose a genotoxic risk for humans. For this reason, further

investigations are needed to determine the toxicity of this compound using other *in vivo and in vitro* biological test systems. A single test system is not enough to determinate a compound whether it is toxic or non-toxic. In this study we performed two different test methods. Further investigations are needed to determine the toxicity of this compound using multiple test systems.

REFERENCES

Agency for Toxic Substances and Disease Registry (ATSDR). 2003. Toxicological profile for pyrethrins and pyrethroids. Atlanta, GA: Department of Health and Human Services, Public Health Service, Toxicology.

Akintonwa A, Awodele O, Olayemi SO, Oreagba IA, Olaniyi OM. 2008. The mutagenic testing of different brands of commonly used insecticides. African J Biotech. 7: 2134–2136.

Ames BN, McCann J, Yamasaki E. 1975. Methods for detecting carcinogens and mutagens with the Salmonella/mammalian-microsome mutagenicity test. Mutat Res. 31: 347–364.

Antunes-Madeira MC, Madeira VMC. 1979. Interaction of insecticides with lipidmembranes. Biocihim Biophys Acta. 550: 384–392.

Bhunya SP, Pati PC. 1990. Effect of deltamethrin, a synthetic pyrethroid, on the induction of chromosome aberrations, micronuclei and sperm abnormalities in mice. Mutagenesis 5: 229–232.

Bickers DR, Calow P, Greim HA, Hanifin JM, Rogers AE, Saurat JH, Sipes IG, Smith RL, Tagamii H. 2003. The safety assessment of fragrance materials. Regul Toxicol Pharmacol. 37: 218-273.

Carrera A, Moos J, Ning XP, Gerton GL, Tesarik J, Kopf GS, Moss SB.1996. Regulation of protein tyrosine phosphorylation in human sperm by a calciumrcalmodulin dependent mechanism: identification of A kinase anchor proteins as major substrates for tyrosine phosphorylation. Dev Biol. 180: 284–296.

Casida J, Quistad G. 1998. Golden age of insecticide research: past, present, or future? Annu Rev Entomol. 43: 1–16.

Chauhan LKS, Agarwal DK, Sundaraman V. 1997. In vivo induction of sister chromatid exchange in mouse bone marrow following oral exposure to commercial formulations of alpha-cyano pyrethroids. Toxicol Lett. 93: 153–157.

Chauhan LKS, Dikshith TSS, Sundaraman V. 1986. Effect of deltamethrin on plant cells I cytological effects on the root meristem of *Allium cepa*. Mutat Res. 171: 25–30.

Di Sotto A, Evandri MG, Mazzanti G. 2008. Antimutagenic and mutagenic activities of some terpenes in the bacterial reverse mutation assay. Mutat Res. 653: 130-133

Di Sotto A, Maffei F, Hrelia P, Castelli F, Sarpietro MG, Mazzanti G. 2013. Genotoxicity assessment of b-caryophyllene oxide. Regul Toxicol Pharmacol. 66: 264-268.

Ema M, Imamura T, Suzuki H. 2012. Evaluation of genotoxicity of multi-walled carbon nanotubes in a battery of in vitro and in vivo assays. Regul Toxicol Pharmacol. 63: 188–195.

EMEA, 2008. Committee on Herbal Medicinal Products (HMPC), Guideline on the Assessment of Genotoxicity of Herbal Substances/Preparations. EMEA/HMPC/ 107079/2007.

European Food Safety Authority CEF Panel (EFSA Panel on Food Contact Materials, Enzymes, Flavourings and Processing Aids). 2014. Scientific opinion on flavouring group evaluation 213, revision 1 (FGE.213Rev1): consideration of genotoxic potential for a,b-unsaturated alicyclic ketones and precursors from chemical subgroup 2.7 of FGE.19. EFSA J. 12: 3661-3707.

Fiskesjo G. 1985. The Allium test as a standart in environmental monitoring. Hereditas. 102: 99–112.

Gandhi G, Chowdhury JB, Sareen PK, Dhillon VP.1995. Genotoxic effects of deltamethrin in the mouse bone marrow micronucleus assay. Mutat Res. 346: 203–206.

Grossman N. 2007. Influence of pyrethroids and piperonyl butoxide on histamine release from isolated rat mast cells. Inflamm Res. 56: 473–478.

Jensen HK, Konradsen F, Dalsgaard A. 2011. Pesticide use and self-reported symptoms of acute pesticide poisoning among aquatic farmers in Phnom Penh, Cambodia. Int J Toxicol. 1687-8191.

Kutlu M, Öztaş E, Aydoğan G. 2011. An investigation of mutagenic activities of some 9-substitued phenanthrene derivatives with Ames/Salmonella/microsome test. Anadolu University J Sci Tech. 1: 83–94.

Lukowicz RJ, Krechniak J. 1992. Effects of deltamethrin on the immune system in mice. Environ Res. 59: 467–475.

Majewska AE, Wolska E, Sliwinska M, Furmanowa N, Urbanska A, Pietrosiuk A, Zobel A, Kuran M. 2003. Antimitotic effect, G2/M accumulation, chromosomal and ultrastructure changes in meristematic cells of *Allium cepa* L. root tips treated with the extract from *Rhadiola rosea* roots. Caryologia. 56: 337–351.

Marcano L, Carruyo I, Del Campo A, Montiel X. 2004. Cytotoxicity and mode of action of maleic hydrazide

in root tips of *Allium cepa* L. Environ Res. 94: 221-226.

Maron DM, Ames BN. 1983. Revised methods for the *Salmonella* mutagenicity test. Mutat Res. 113: 173–215.

Martin PA.1990. Effects of carbofuran, chlorpyrifos and deltamethrin on hatchability, deformity, chick size and incu- bation time of Japanese quail *Coturnix japonica*. eggs, Environ Toxicol Chem. 9: 529–534.

Miao J, Wang D, Yan J, Wang Y, Teng M, Zhou Z, Zhu W. 2017. Comparison of subacute effects of two types of pyrethroid insecticides using metabolomics methods. Pest Biochem Physiol. 143: 161–167

Ministry of the Environment. 2011. Compilation of pollutant release and transfer register data Ministry of the Environment; in Japanese. Available from: http://www.env.go.jp/chemi/prtr/result/todokedegaiH22/suikei/sanko3.pdf.

Morgan MK. 2012. Children's exposures to pyrethroid insecticides at home: a review of data collected in published exposure measurement studies conducted in the United States. Int J Environ Res Public Health. 9: 2964–2985.

Nagy K, Racz G, Matsumoto T, Adany R, Adam B. 2014. Evaluation of the genotoxicity of the pyrethroid insecticide phenothrin. Mutat Res Genet Toxicol Environ Mutagen. 770: 1–5.

Nakamura Y, Tonogai Y, Tsumura Y, Ito Y. 1993. Determination of pyrethroid residues in vegetables, fruits, grains, beans, and green tea leaves: applications to pyrethroid residue monitoring studies. J AOAC Int. 76: 1348–1361.

Oulhote Y, Bouchard MF. 2013. Urinary metabolites of organophosphate and pyrethroid pesticides and behavioral problems in Canadian children. Environ Health Perspect. 121: 1378–1384.

Oztas E. 2005. Bazı 9-substitiue fenantren turevlerinin mutajenik aktivitelerinin Ames/Salmonella/mikrozom testi ile araştırılması. Eskisehir, Yuksek Lisans Tezi, Anadolu Universitesi, Fen Bilimleri Enstitusu.

Pluijmen M, Drevon C, Montesano R, Malaveille C, Hautefeuille A, Bartsch H. 1984. Lack of mutagenicity of synthetic pyrethroids in *Salmonella typhimurium* strains and in V79, Chinese hamster ovary cells. Mutat Res. 137: 7–15.

Saleem U, Ejaz S, Ashraf M, Omer MO, Altaf I, Batool Z, Fatima R, Afzal M. 2014. Mutagenic and cytotoxic potential of Endosulfan and Lambda-cyhalothrin – in vitro study describing individual and combined effects of pesticides. J Environ Sci. 26: 1471–1479.

Saxena PN, Chavalı M, Gupta SK. 2009. Evaluation of cytogenetic effects of deltamethrin in root meristem cells of Allium sativum and Allium cepa: A possible mechanism of chromosome damage.Toxicol Environ Chem. 91(3): 577-594.

Shukla Y, Taneja P. 2000. Mutagenic evaluation of deltamethrin using rodent dominant lethal assay. Mutat Res. 467: 119–127.

Smaka-Kincl V, Stegnar P, Lovka M, Toman MJ. 1996. The evaluation of waste, surface and ground water quality using the *Allium* test procedure. Mutat Res. 368: 171-179.

Sudhakar R, Gowda N, Venu G. 2001. Mitotic abnormalities induced by silk dyeing industry effluents in the cells of *Allium cepa*. Cytologia. 66: 235–239.

Surralles J, Xamena N, Creus A, Catalan J, Norppa H,Marcos R.1995. Induction of micronuclei by five pyrethroid insecticides in whole-blood and isolated human lymphocyte cultures. Mutat Res. 341: 169–184.

Valles SM, Koehler PG. 2003. Insecticides used in the urban environment: mode of action (ENY282). Gainesville, FL: Department of Entomology and Nematology University of Florida.

Viel JF, Warembourg C, Le Maner-Idrissi G, Lacroix A, Limon G, Rouget F, Monfort C, Durand G, Cordier S, Chevrier C. 2015. Pyrethroid insecticide exposure and cognitive developmental disabilities in children: the PELAGIE motherchild cohort. Environ Int. 82: 69–75.

Villarini M, Moretti M, Pasquini R, Scassellati-Sforzolini G, Fatigoni C, Marcarelli M, Monarca S, Rodroguez AV.1998. In vitro genotoxic effects of the insecticide deltamethrin in human peripheral blood leucocytes: DNA damage 'comet' assay in relation to the induction of sister- chromatid exchanges and micronuclei. Toxicol. 130: 129–139.

Caryologia
International Journal of Cytology, Cytosystematics and Cytogenetics

Firenze University Press
www.fupress.com/caryologia

OPEN ACCESS

Citation: Ö.S. Aslantürk (2019) Cytogenetic effects of Fulvic acid on *Allium cepa* L. root tip meristem cells. *Caryologia* 72(2): 29-35. doi: 10.13128/cayologia-257

Published: December 5, 2019

Data Availability Statement: All relevant data are within the paper and its Supporting Information files.

Competing Interests: The Author(s) declare(s) no conflict of interest.

Cytogenetic effects of Fulvic acid on *Allium cepa* L. root tip meristem cells

Özlem Sultan Aslantürk

Adnan Menderes University, Faculty of Art and Science, Department of Biology, 09010 Aydın, Turkey
E-mail: osaslanturk@adu.edu.tr

Abstract. Fulvic acid is a class of compounds of humic substances and is found in a significant proportion of the substances in the environment. It has been used for many years in industry, agriculture, and complementary medicine. In this study, cytogenetic effects of fulvic acid purified from Muğla Milas Hüsamlar leonardite (TURKEY) on *Allium cepa* root tip meristem cells were investigated using the Allium test. For this purpose, 10 mg/ml stock solution of fulvic acid was prepared by dissolving in citric acid and it was diluted with distilled water to 10, 20, 40, 80 and 100 µg/mL concentrations. Onion bulbs were exposed to these concentrations of the fulvic acid for macroscopic and microscopic analysis. Tap water was used as a negative control, 40 µg/mL citric acid was used as solvent control (fulvic acid solvent), and 0.02M Ethyl methane sulfonate (EMS) (a mutagenic, teratogenic, and possibly carcinogenic organic compound) was used as a positive control. There has been statistically significant stimulation of root growth depending on fulvic acid concentration in comparison with the control groups ($p<0.05$). Furthermore, in fulvic acid treatment groups, breaks, stickiness and polar deviations appeared at very low rates, and total chromosome aberration ratios were insignificant compared to the control groups. These results suggest that fulvic acid does not have cytotoxic and genotoxic effects on *A. cepa*.

Keywords. Allium test, Chromosome aberrations, Fulvic acid, Mitotic index.

1. INTRODUCTION

Fulvic acid is a class of compounds of humic substances, and it is a mixture of polyphenolic compounds formed through the degradation of organic substances such as plants, microbes and animals by chemical and biological processes (Motojima et al. 2011). It is a type of humic acid. Compared to other humic acid types, the fulvic acid is soluble in both acid and alkaline solutions, is lower in molecular weight, and has a greater biological activity (Stevenson, 1994; Bai et al. 2013; Yong 2001; Zhang et al. 2011). Piccolo (2002) redefined fulvic acid as associations of small hydrophilic molecules in which there are enough acid functional groups to keep the fulvic clusters dispersed in solution at any pH. Because, while humic acids precipitate when the pH is adjusted to 1-2, fulvic acids remain in solution after the alkaline extracts are acidified (Canellas et al. 2015).

Recently, it has been reported that fulvic acid has nutraceutical, neuroprotective (Cornejo et al. 2011; Guzmán-Martinez et al. 2013), antimicrobial, antioxidant, and anti-inflammatory properties (Van Rensburg et al. 2001; Yamada et al. 2007; Sherry et al. 2013). Fulvic acid has also been used as a medicine by people in China, Mexico, India, South America and Russia for centuries. Fulvic acid has a large capacity to retain transition metals, forming metalorganic complexes, which cause these metals to be more or less available for plants which include them into the food chain. The food industry also uses it as an ion exchanger, because it holds heavy metals very well (Pena-Mendez et al. 2005).

Over these last decades, more than 200 short-term bioassay utilizing plants, microorganisms, and insects have been developed and used to evaluate the environmental risks (Marcato-Romain et al. 2009). Plant assays are highly sensitive, easy to use in an experiment, inexpensive, and good predictors of genotoxicity and carcinogenicity (Ennever et al. 1988). The Allium test has been used by many researchers as a bioindicator of environmental pollution (Bagatini et al. 2009; Leme and Marin-Morales 2009) and genotoxicity of various agents (Aşkın Çelik and Aslantürk 2007, 2009, 2010) for a long time. With this test, mutagenic effects of substances may be analyzed by monitoring macroscopic parameters, like the appearance and growth of the roots or by genotoxic parameters, like type and frequency of chromosome aberrations, and abnormal cell division. Another advantage of this test is the presence of an oxidase enzyme system, which is essential for promutagen evaluations (Fiskesjö, 1985; Nielsen and Rank,1994). The Allium test is important, since it is an excellent model *in vivo*, where roots grow in direct contact with the test substance enabling possible damage to DNA of eukaryotes to be predicted. Therefore, results from this test can be extrapolated for all animal and plant biodiversity (Tedesco and Laughinghouse IV 2012).

Although fulvic acid is found in a significant proportion of the substances in the environment, and has been used for many years in industry, agriculture and complementary medicine, there is still minimal scientific evidence of its biological properties. In this study, cytogenetic effects of fulvic acid on *Allium cepa* root tip meristem cells were investigated using the Allium test.

2. MATERIALS AND METHODS

2.1. Supply of Fulvic acid

Fulvic acid purified from Muğla Milas Hüsamlar leonardite (TURKEY) in Chemical Engineering Laboratory of Gazi University in Ankara (TURKEY) was used in this research (Sönmez 2011). This study was conducted between March and December 2017.

2.2. Preparation of the Fulvic acid solution

The 10 mg/ml stock solution of fulvic acid was prepared by dissolving in citric acid, as it has a structure, which is soluble in weak acid. Stock fulvic acid solution was diluted with distilled water to 10, 20, 40, 80 and 100 µg/mL concentrations. Fresh solution was prepared just before the experiment.

2.3. Allium Test

Small bulbs (1.5–2.0 cm in diameter) of the common onion, *A. cepa*, (2n = 16) were purchased at a local supermarket in Aydın, Turkey. Prior to initiating the test, the outer scales of the bulbs and the dry bottom plate were removed without damaging the root primordia.

For each treatment, seven onion bulbs were placed on top of test tubes filled with tap water (pH 7.3) for 48 h. The test tubes were kept in an incubator at 22±1°C. After 48 h, two unhealthy onions with the most poorly growing roots were removed and the other healthy onion bulbs in water were treated with 10, 20, 40, 80 and 100 µg/mL fulvic acid for 24 hours. 0,02M Ethyl methane sulfonate was used as positive control for 3 h, 40 µg/mL citric acid was used as solvent control, and tap water was used as negative control.

Citric acid is a weak organic acid that has the chemical formula $C_6H_8O_7$. It occurs naturally in citrus fruits. In biochemistry, it is an intermediate product in the citric acid cycle, which occurs in the metabolism of all aerobic organisms (Berovic and Legisa, 2007). Ethyl methanesulfonate (EMS) used as positive control in experiment is a mutagenic, teratogenic, and possibly carcinogenic organic compound and its chemical formula $C_3H_8SO_3$. EMS is often used in genetics as a mutagen. Mutations induced by EMS can then be studied in genetic screens or other assays (Merck Index, 1989).

After the completion of treatment the roots were counted and their lengths were measured for each onion. To determine mean root length in a root bundle for each bulb, root lengths of experimental and control bulbs were measured with ruler at the end of treatment time. After then root tips were removed from the bulbs, fixed in 3:1 (v/v) ethanol:glacial acetic acid and stored overnight at 4°C. The next day they were placed in 70% (v/v) aqueous alcohol and refrigerated until use. An average of five slides was made for each bulb using

five root tips which hydrolyzed in 1N hydrochloric acid (HCl) for 3 min, and microscope slides were prepared by squashing the stained root tips in 2% (w/v) acetic orcein. Each slide was examined using Olympus BX51 at a total magnification of 40×10. Chromosomal aberrations were determined by scoring cells with bridges, fragments, sticky chromosomes, and polar deviations in 1000 cells per slide. Also micronucleus formation was determined in 1000 cells per slide. 5000 cells scored in total for each bulb (Fiskesjö 1993, 1997; Pavlica et al. 2000).

2.4. Statistical Analysis

Statistical analyses were performed using the SPSS 20.0 software package program. Data on physicochemical parameters, root length, root number, and mitotic index and chromosomal aberrations were compared using analysis of variance (One Way ANOVA) to confirm the variability of the data and validity of results. Post-hoc test was used to describe the magnitude of variability. Differences between corresponding controls and exposure treatments were considered statistically significant at p <0 .05.

3. RESULTS

3.1. Morphological Analysis

The results of the morphological analysis (root number and root length) are presented in Table 1. These results show that all tested concentrations of fulvic acid caused increase in the root growth, and average root number in comparison to negative control, positive control, and solvent control. The measured average root length is 2.26±1.07 cm in negative control, 1.40±0.40 cm in positive control, and 1.36 cm in solvent control. The average root length after 20 and 40 µg/ml fulvic acid treatment is found very high (4.10±0.41 and 4.22±0.69 cm, respectively) compared to controls (Table 1). The number of roots also increased in fulvic acid treatment groups compared to control groups. The highest root number is found in group treated with 80 µg/ml fulvic acid (Table 1). The root morphology in fulvic acid treated groups was thinner and more fragile compared to the negative control group.

Table 1. The average root numbers and root lengths in control and treatment groups after 24h treatment (Analysis were carried by One Way ANOVA).

Concentrations	Average root number ± SD	Average root lengths (cm ± SD)
Negative control	19.2 ± 8.07	2.26 ± 1.07
Solvent control	20.2 ± 8.87	1.36 ± 0.24
EMS (positive control)	21.0 ± 7.81	1.40 ± 0.40
FA10	37.2 ± 4.43*	3.36 ± 0.54
FA20	31.8 ± 4.56	4.10 ± 0.41*
FA40	37.6 ± 5.92*	4.22 ± 0.69*
FA80	39.2 ± 5.17*	3.98 ± 1.29*
FA100	34.8 ± 6.14*	3.68 ± 0.68

One Way ANOVA Analysis *p<0.05 is significant (EMS: 0.02M Ethyl methane sulfonate; Solvent control: 40 µg/ml citric acid; FA10: 10 µg/ml fulvic acid; FA20: 20 µg/ml fulvic acid; FA40: 40 µg/ml fulvic acid; FA80: 80 µg/ml fulvic acid; FA100: 100 µg/ml fulvic acid).

3.2. Cytogenetic Analysis

With the objective of investigating the possible mechanism involved in root growth stimulation, cytogenetic analysis was performed. Fulvic acid was found to stimulate mitotic index. A statistically significant difference in the mitotic index of root meristems was found in negative, positive and solvent control. The increase in the mitotic index was found to be positively correlated with the increase in concentration of the fulvic acid (Table 2). In the positive and solvent control groups, the mitotic index decreased significantly compared to the control group, and the mitotic index value approached zero in the solvent control group (Table 2).

Cytogenetic alterations were investigated, and the results are described in Table 2 and Figure 1. Table 2 presents the percentage of the aberrant cells in dividing cells. Very few cells with polar deviation were observed in the negative control group. No chromosome aberration was observed except for polar deviation. In this group, total chromosome aberration was found very low (0.07%). The chromosome aberration rate in the positive control group was found to be significantly higher than the control group (36.09%). Especially the anaphase bridge and stickiness have been observed to appear at a very high rate ($p<0.05$). In addition, breaks and polar deviations were observed in the positive control group. No chromosome aberration was observed in the solvent control group (citric acid), because there were only two divided cells in total and the mitotic index value was near zero in this group. The cell membrane and nucleus were deformed (Fig. 1a).

In the groups treated with fulvic acid, breaks, stickiness and polar deviations appeared at very low rates. Total chromosome aberration percentages in these groups were insignificant compared to control and solvent control groups. The highest total chromosome aberration percentage in fulvic acid treated groups was 20

Table 2. Mitotic index values, percentage of chromosomal aberrations and thousandths of micronuclei in control and treatment groups after 24h treatment.

Concentrations	Total cells	Total dividing cells	Mitotic index (MI ± SD)	Breaks (%± SD)	Anaphase bridge (%± SD)	Stickiness (%± SD)	Polar deviation (%± SD)	Total aberrant cells (%± SD)	Micronuclei (‰ ± SD)
Negative control	25000	1241	4.96 ± 0.31	0 ± 0	0 ± 0	0 ± 0	0.07 ± 0.03	0.07 ± 0.03	0 ± 0
Solvent control	25000	2	0.01 ± 0.17*	0 ± 0	0 ± 0	0 ± 0	0 ± 0	0 ± 0	0 ± 0
EMS (positive control)	25000	209	0.83 ± 0.11*	1.17± 0.26	10.47 ± 9.59*	20.05 ± 6.90*	4.39 ± 6.03	36.09 ± 5.48*	0 ± 0
FA10	25000	2893	11.57 ± 1.93*	0.04 ± 0.01	0 ± 0	0± 0	0.51 ± 0.61	0.52 ± 0.60	0.04 ± 0.01
FA20	25000	3111	12.44 ±0.51*	0 ± 0	0 ± 0	0.03 ± 0.07	2.87 ± 0.53	2.90 ± 0.52	0 ± 0
FA40	25000	3559	14.23± 0.41*	0 ± 0	0 ± 0	0 ± 0	2.90 ± 0.42	2.90 ± 0.42	0 ± 0
FA80	25000	3566	14.26 ± 0.35*	0.03 ± 0.06	0 ± 0	0.03 ± 0.06	2.68 ± 0.51	2.73 ± 0.61	0 ± 0
FA100	25000	2988	11.95 ± 0.54*	0.03 ± 0.08	0 ± 0	0 ± 0	2.38 ± 0.17	2.41 ± 0.21	0 ± 0

One Way ANOVA Analysis *p<0.05 is significant (EMS: 0.02M Ethyl methane sulfonate; Solvent control: 40 µg/ml citric acid; FA10: 10 µg/ml fulvic acid; FA20: 20 µg/ml fulvic acid; FA40: 40 µg/ml fulvic acid; FA80: 80 µg/ml fulvic acid; FA100: 100 µg/ml fulvic acid. 25000 cells/group were evaluated for MI and CA)

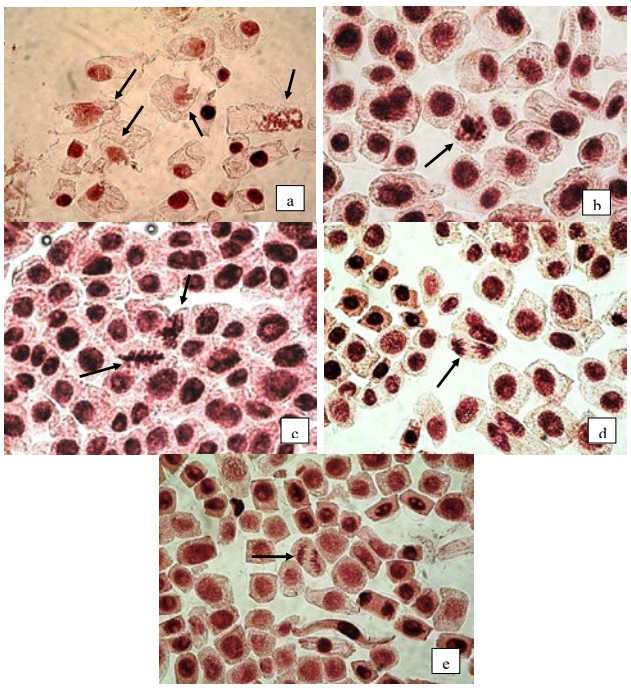

Fig. 1. a: membrane and nucleus deformation in solvent control (citric acid) group; b: stickiness; c: stickiness and polar deviation in positive control group; d: polar deviation in 20 µg/ml fulvic acid treatment group; e: polar deviation 80 µg/ml fulvic acid treatment group.

and 40 µg/ml, respectively (Fig. 1d, e). This percentage is statistically insignificant when compared to the control and solvent control group. In addition, this percentage is very low compared to the chromosome aberration value obtained from the positive control group (EMS), and the difference is statistically significant ($p < 0.05$). In the positive control group (EMS), chromosome aberration percentage has been found high, especially stickiness and anaphase bridge.

Micronucleus formation results are also present in Table 2. Micronucleus formation was found at a very low level of 0.04 ‰ in 10 µg/ml fulvic acid treated group only which was statistically not significant. No micronucleus formation was found in other experimental groups (including negative, positive and solvent controls).

As a result of this study, root length and mitotic index results show that fulvic acid promotes root growth by inducing division in *Allium cepa* root meristem cells. Chromosome aberration and micronucleus results also indicate that fulvic acid does not induce cytotoxic and genotoxic effects in the root meristem cells.

4. DISCUSSION

In this study, cytogenetic effects of fulvic acid were evaluated by analyzing root growth and root morphology. Fulvic acid caused an increase in root growth and number, and there was a statistically significant difference between fulvic acid and control groups (negative, positive and solvent controls). Cyto- and genotoxicity were estimated by observing cytological parameters, such as the mitotic index and number of chromosome abnormalities, including chromosome breaks, stickiness, and polar deviations. The mitotic index (MI) of *A. cepa* meristem cells treated with the EMS and citric acid (solvent control) was significantly decreased (0.83% and 0.01%, respectively) in comparison to negative control. Although EMS and citric acid significantly decreased the

mitotic index, fulvic acid treatment increased the mitotic index in *A. cepa* meristem cells at all concentrations significantly (Table 2). The mitotic index is measure of the mitotic activity of a cell population. It measures the proportion of cells in the M-phase of the cell cycle (Rojas et al. 1993). Therefore, the increase of MI in groups treated with fulvic acid, in comparison to negative control, suggests that fulvic acid could have proliferative effect on the meristem cells of *A. cepa*. The increased mitotic index in *A. cepa* root tip cells treated with fulvic acid is probably due to induction of DNA synthesis and promotion of cell cycle. The MI results of fulvic acid treatment groups are consistent with literature data. Previous studies suggest that humic substances including fulvic acid enhanced stimulation of seedling germination and growth of plants (Kulikova et al. 2002; Pena-Méndez et al. 2005; Van Rensburg 2015). Humic substances affect the development of organisms. Being utilized as a substrate (a source of organic carbon) or nutrient source (N, P, trace elements and vitamins), humic substances can serve as a moiety of the biosynthesis chains. On the other hand, beneficial effects of humic substances on the plants are often attributed to hormone-like activity of these substances (Nardi, 1994; Nardi et al. 2002; Piccolo et al. 1992; Kulikova et al. 2002). Since humic substances originate from the chemical and biological decomposition of plant and animal residues, and from metabolic activities of microorganisms, they might have characteristics of hormones. It was shown that humic substances enhanced plant growth by exhibiting auxin-like activity (Kulikova et al. 2002). Some researchers reported that humic and, in particular, fulvic acids showed some auxin, gibberellin or cytokinin-like activity (Phuong and Tichy 1973; Nardi, 1994; Kulikova et al. 2002). Furthermore, fulvic acid, as a plant growth regulator, is involved in plant response to several environmental stress factors, and is reported to affect growth and development of plants (Heil 2005; Shahid et al. 2012).

There are also studies of growth promoting effects of fulvic acid on plants as well as growth enhancing effects on animals (Nardi et al. 2002; Heil 2005; Bai et al. 2013), because of its antioxidant, antimicrobial and anti-inflammatory properties (Yamada et al. 2007; Van Rensburg et al. 2001; Sherry et al. 2013).

Gao et al. (2017) have shown that when fulvic acid is used as food supplements for 60 days, it increases growth performance of *Paramisgurnus dabryanus* (Sauvage) and improves its intestinal health conditions (Gao et al., 2017). Also, Bai et al. (2013) reported that supplementation of diets with fulvic acid is an effective way to increase growth performance, reduce backfat thickness, and improve meat quality in growing-finishing pig (Bai et al. 2013).

Chromosome aberration and micronucleus results of this study show that fulvic acid does not induce genotoxic effects in the root meristem cells in comparison with control groups. Although in the positive control group (EMS), chromosome aberration rate (especially stickiness and anaphase bridges) has been found high, but in the fulvic acid treatment groups, breaks, stickiness and polar deviations appeared at very low rates. The total chromosome aberration percentages in fulvic acid treatment groups were found insignificant compared to control and solvent control groups (Table 3).

As a result of literature screening, different data on cytotoxic, genotoxic and mutagenic effects of fulvic acid have been reached. Qui et al. (2007) reported that fulvic acid has protective effect against copper toxicity to the polychaete *Hydroidas elegans* larvae, and such an effect is caused by the reduction in labile copper due to Cu-FA (copper-fulvic acid) complexation (Qui et al. 2007). Also, it has been suggested that humic and fulvic acids have desmutagenic effect (inactivation of mutagens outside the cell) on *Vicia faba* root tip cells treated with maleic hydrazide, whereas they have no antimutagenic effect (Ferrara et al. 2000). Ferrara et al. (2004) reported anticlastogenic, antitoxic and sorption effects of humic substances (soil humic acid, peat humic acid and peat fulvic acid) on the maleic hydrazide tested in leguminous plants, *Vicia faba* and *Pisum sativum* L (Ferrara et al. 2004). However, no data has been found on the direct cytogenetic effects of fulvic acid in the literature. Therefore, the data obtained in this study is important in terms of its contribution to the scientific literature in this regard. Furthermore, fulvic acid is currently being used in planting and growing plants, especially in agriculture, and as complementary in treatment of human and animal health. Its use is becoming increasingly widespread. Therefore, it is important to determine whether this substance is safe for the environment, and animal and human health. The results of this study suggest that fulvic acid stimulate the root growth in *A. cepa*, and it does not have cytotoxic and genotoxic effects on *A. cepa* root meristem cells. These results are important, because it is a preliminary study on the safety of using of fulvic acid. However, in order to be able to say that the use of fulvic acid is safe, more detailed studies have to be carried out using different test systems.

ACKNOWLEDGEMENT

I would like to thank the Chemical Engineer Yusuf Mert SÖNMEZ who donated the pure fulvic acid for use in this study. Also I would like to thank Assoc. Prof. Dr.

Tülay AŞKIN ÇELİK for her helpful advice in this manuscript.

DISCLOSURE STATEMENT

No potential conflict of interest was reported by the author.

REFERENCES

Aşkın Çelik T, Aslantürk ÖS. 2007. Cytotoxic and genotoxic effects of *Lavandula stoechas* aqueous extracts. Biologia. 62(3): 292-296.

Aşkın Çelik T, Aslantürk ÖS. 2009. Investigation of Cytotoxic and Genotoxic Effects of *Ecballium elaterium* Juice Based on Allium Test. Methods Find Exp Clin Pharmacol. 31(9): 591-596.

Aşkın Çelik T, Aslantürk ÖS. 2010. Evaluation of cytotoxicity and genotoxicity of *Inula viscosa* leaf extracts with Allium test. Journal of BioMed Research. doi:10.1155/2010/189252

Bagatini MD, Vasconcelos TG, Laughinghouse IV HD, Martins AF, Tedesco SB. 2009. Biomonitoring hospital effluents by *Allium cepa* L. test. Bulletin of Environmental Toxicology and Contamination. 82: 590-592.

Bai HX, Chang QF, Shi BM, Shan AS. 2013. Effects of fulvic acid on growth performance and meat quality in growing-finishing pigs. Livestock Science, 158: 118-123.

Berovic M, Legisa M. 2007. Citric acid production. Biotechnology Annual Review, 13: 303-343.

Canellas LP, Olivares FL, Aguiar NO, Jones DL, Nebbioso A, Mazzei P, Piccolo A. 2015. Humic and fulvic acids as biostimulants in horticulture. Scientia Horticulturae, 196: 15-27.

Cornejo A, Jiménez JM, Caballero L, Melo F, Maccioni RB. 2011. Fulvic acid inhibits aggregation and promotes disassembly of tau fibrils associated with Alzheimer's disease. J Alzheimers Dis., 27: 143-153.

Ennever FK, Andreano G, Rosenkranz HS. 1988. The ability of plant genotoxicity assays to predict carcinogenicity Mutat Res/Gen Tox Environ Mutagen. 205: 99-105.

Ferrara G, Loffredo E, Simeone R, Senesi N. 2000. Evaluation of antimutagenic and desmutagenic effects of humic and fulvic acids on root tips of *Vicia faba*. Environmental Toxicology. 15(5): 513-517.

Ferrara G, Loffredo E, Senesi N. 2004. Anticlastogenic, antitoxic and sorption effects of humic substances on the mutagen maleic hydrazide tested in leguminous plants. Eur J Soil Sci. 55: 449-458.

Fiskesjo G. 1985. The Allium test as a standard in environmental monitoring. Hereditas.102: 99-112.

Fiskesjö G. 1993. Allium test I: a 2–3 day plant test for toxicity assessment by measuring the mean root growth of onions (Allium cepa L). Environ. Toxicol. Wat. Qual. 8: 461–470.

Fiskesjo G. 1997. "Allium test for screening chemicals; evaluation ¨ of cytological parameters," in Plants for Environmental Studies, W. Wang, J. W. Gorsuch, and J. S. Hughes, Eds., pp. 308–333, Lewis, New York, NY, USA, 1997.

Gao Y, He J, He Z, Li Z, Mu Y, Lee JY, Chu Z. 2017. Effects of fulvic acid on growth performance and intestinal health of juvenile loach *Paramisgurnus dabryanus* (Sauvage). Fish and Shellfish Immunology. 62: 47-56.

Guzmán-Martinez L, Farías GA, Maccioni RB. 2013. Tau oligomers as potential targets for Alzheimer's diagnosis and novel drugs. Frony Neurol., 4: 167.

Heil CA. 2005. Influence of humic, fulvic and hydrophilic acids on the growth, photosynthesis and respiration of the dinoflagellate *Prorocentrum minimum* (Pavillard) Schiller. Harmful Algae, 4: 603-618.

Kulikova NA, Stepanova EV, Koroleva OV. 2002. Mitigating Activity of Humic Substances: Direct Influence on Biota. In: Use of Humic Substances to Remediate Polluted Environments: From Theory to Practice. Eds., Irina V. Perminova, Kirk Hatfield and Norbert Hertkorn. 2012. Springer, Germany. Pp: 285-309.

Leme DM, Marin-Morales MA. 2009. *Allium cepa* test in environmental monitoring: a review on its application. Mutat. Res. 682(1): 71-81.

Marcato-Romain C, Pinelli E, Pourrut B, Silvestre J, Guiresse M. 2009. Assessment of the genotoxicity of Cu and Zn in raw and anaerobically digested slurry with the *Vicia faba* micronucleus test. Mutat Res Genet Toxicol Environ Mutagen 672:113–118.

Merck Index. 1989. 11th Edition, 3782. ISBN: 0-911910-28-X

Motojima HO, Villareal M, Han J, Isoda H. 2011. Microarray analysis of immediate-type allergy in KU812 cells in response to fulvic acid. Cytotechnology, 63: 181-190.

Nardi S, Panuccio MR, Abenavoli MR, Muscolo A. 1994. Auxin-like effect of humic substances extracted from faeces of *Allolobophora caliginosa* and *A. rosea*. Soil Biology and Biochemistry, 26: 1341-1346.

Nardi S, Pizzeghello D, Muscolo A, Vianello A. 2002. Physiological effects of humic substances on higher plants. Soil Biology and Biochemistry, 34: 1527-1536.

Nielsen MN, Rank J. 1994. Screening of toxicity and genotoxicity in wastewater by the use of Allium test. Hereditas. 121: 249-254.

Pavlica M, Besendorf V, Roša J & Papeš D. 2000. The cytotoxic effect of wastewater from the phosphoric gypsum depot on common oak (*Quercus robur* L.) and shallot (*Allium cepa* var. ascalonicum). Chemosphere 41: 1519-1527.

Pena-Méndez EM, Havel J, Patoćha J. 2005. Humic substances- compounds of still unknown structure: applications in agriculture, industry, environment and biomedicine. J. Appl Biomed., 3: 13-24.

Phoung HK, Tichy V. 1976. Activity of humic acids from peat as studied by means of some growth regulator bioassay. Biol. Plant (Prague), 18: 195-199.

Piccolo A, Nardi S, Concher G. 1992. Structural characteristics of humus and biological activity. Soil Biology and Biochemistry, 24: 273-280.

Piccolo A. 2002. The supramolecular structure of humic substances. A novel understanding of humus chemistry and implications in soil science. Adv. Agron., 75: 57-134.

Qui JW, Tang X, Zheng C, Li Y, Huang Y. 2007. Copper complexation by fulvic acid affects to the larvae of the polychaete *Hydroides elegans*. Marine Environmental Research, 54: 563-573.

Rojas E, Herrera L A, Sordo M. et al. 1993. Mitotic index and cell proliferation kinetics for identification of antineoplastic activity. Anti-Cancer Drugs, 4(6): 637-640.

Shahid M, Dumat C, Silvestre J, Pinelli L. 2012. Effect of fulvic acids on lead-induced oxidative stres to metal sensitive *Vicia faba* L. plant. Biol. Fertil. Soils, 48: 689-697.

Sherry L, Millhouse E, Lappin DF, Murray C, Culshaw S, Nile CJ,Ramage G. 2013. Investigating the biological properties of carbohydrate derived fulvic acid (CHD-FA) as a potential nove therapy fort he management of oral biofilm infections. BMC Oral Health, 13: 47.

Sönmez YM. 2011. Fülvik Asit Prosesinin Geliştirilmesi ve Tasarımı. Yüksek Lisans Tezi, Gazi Üniversitesi Fen Bilimleri Enstitüsü, Ankara.

Stevenson FJ. 1994. Humus Chemistry: Genesis, Composition, Reactions. John Wiley&Sons, NewYork.

Tedesco SB, Laughinghouse IV HD. 2012. Bioindicator of Genotoxicity: The *Allium cepa* Test. Environmental Contamination, InTechOpen, pp, 137-156.

Van Rensburg CEJ, Malfeld SCK, Dekker J. 2001. Topical application of oxifulvic acid suppressess the cutaneous immune response in mice. Drug Dev Res., 53: 29-32.

Van Rensburg CEJ. 2015. The anti-inflammatory properties of humic substances: A mini review. Phytotherapy Research, 29: 791-795.

Yamada P, Isoda H, Han JK, Talorete TP, Abe Y. 2007. Inhibitory effect of fulvic acid extracted from Canadian Sphagnum peat on chemical mediator release by RBL-2H3 and KU812 cells. Biosci Biotechnol Biochem., 71: 1294-1305.

Yong RN. 2001. Geoenvironmental Engineering, Contaminated Soils, Pollutant Fate, and Mitigation. CRC Press, Boca Raton, Florida.

Zhang YL, Du JZ, Zhang FF, Yu YH, Zhang J. 2011. Chemical characterization of humic substances isolated from mangrove swamp sediments: the Qinglan area of Hainan Island, China. Estuar Coast. Shelf Sci., 93: 220-227.

Caryologia
International Journal of Cytology, Cytosystematics and Cytogenetics

Firenze University Press
www.fupress.com/caryologia

Citation: I. Sarac, E. Bonciu, M. Butnariu, I. Petrescu, E. Madosa (2019) Evaluation of the cytotoxic and genotoxic potential of some heavy metals by use of *Allium* test. *Caryologia* 72(2): 37-43. doi: 10.13128/cayologia-256

Published: December 5, 2019

Data Availability Statement: All relevant data are within the paper and its Supporting Information files.

Competing Interests: The Author(s) declare(s) no conflict of interest.

Evaluation of the cytotoxic and genotoxic potential of some heavy metals by use of *Allium* test

Ioan Sarac[1], Elena Bonciu[2,*], Monica Butnariu[1], Irina Petrescu[1], Emilian Madosa[1]

[1] *Banat's University of Agricultural Science and Veterinary Medicine "King Michael I of Romania" Timisoara, Romania*
[2] *Department of Agricultural and Forestry Technology, University of Craiova, Craiova, Romania*
*Corresponding author: elena.agro@gmail.com

Abstract. The present study aimed to evaluate the cytogenetic effects induced by heavy metals nickel (Ni) and lead (Pb) to crop plants, using the *Allium sativum* (garlic) as a test plant. For this purpose, were used solutions of nickel nitrate - $Ni(NO_3)_2$ - and lead nitrate - $Pb(NO_3)_2$ - at concentrations of 50, 150 and 450 ppm for 72 hours, along with an untreated control variant immersed in plain water. The biological material was immersed from the beginning in the tested solutions. The results obtained showed a strong inhibitory effect of these heavy metals on the process of rhizogenesis, as well as a significant mitodepresive effect in the meristematic cells, both phenomena being correlated with increasing concentration of the tested solutions. At the same time, several types of chromosomal aberrations (c-mitosis, vagrants, star-anaphase, star-telophase, fragments, clumping, stickiness, bridges) have been recorded in all treatment variants. The presence of these chromosomal aberrations in all treatment variants indicates the aneugenic effects of nickel nitrate and lead nitrate in the meristematic cells of *A. sativum*. The results suggest the ecotoxicity potential of nickel and lead on plants even at low concentrations and confirm the suitability of *A. sativum* as a test plant for assessing the cytotoxicity and genotoxicity of heavy metals to plants.

Keywords. Genotoxicity, chromosomal aberrations, lead, mitotic index, nickel.

INTRODUCTION

The concept of heavy metals has refers to any metallic chemical element that has a relatively high density and is toxic or poisonous in low concentrations. As natural water pollutants, heavy metals are among the most toxic pollutants due to their prolonged persistence in solutions and the difficulty of being converted into insoluble compounds in surface waters (Bilal et al. 2014). The contamination of soil by heavy metals is also a major environmental problem (Lassoued et al. 2014) and have a toxic action on the aquatic organisms, meanwhile inhibiting the self-purification processes (Nemcsók

et al. 2010). Heavy metals are dangerous because they tend to bioaccumulate (Coroian et al. 2017; Hariri et al. 2018; Marinova et al. 2018). Bioaccumulation means the increase in time in biological organisms of the concentration of the substance in an amount compared to the concentration of this substance in the environment.

The presence of heavy metals in soil, is one important factor that can cause altered physiological and metabolic processes to plants or disturbing the metabolism of essential elements (Dong et al. 2006; Mohanpuria et al. 2007; Wójcik and Tukiendorf 2014; Petrescu et al. 2015; Sarac et al. 2015; Georgieva et al. 2018; Nikolova and Georgieva 2018).

Symptoms of heavy metal toxicity are the result of harmful effects of metals on physiological processes including: inhibiting respiration and photosynthesis, altering the plant-water relationship that causes stress, decreased plasma membrane permeability in the root cells, adverse effects on the metabolic activities of enzymes (Arduini 1994).

Lead (Pb) is one of the ubiquitously distributed most abundant toxic elements in the soil. Pb inhibits the activity of enzymes at cellular level by reacting with their sulfhydril groups (Yadav 2010). High lead exposure is harmful, particularly for children; its effects include damage to the nervous system, liver and kidney damage and developmental delays. Also, the lead exposure is associated with an increased risk of several cancers, in particular, meningioma, brain cancer, and kidney cancer (Liao et al. 2016).

Nickel (Ni) is considered to be an essential micronutrient for plants (Eskew et al. 1983) but at excess concentrations this metal becomes toxic for majority of plant species and triggers oxidative damage (Zornova et al. 1999; Nakazawa et al. 2004; Gajewska et al. 2006; Sachan and Lal 2017). On the other hand, some authors reported cytotoxic effects even at low doses (20 to 100μM) of nickel ions as well as antioxidative enzyme changes in *Allium cepa* roots (Gantayat et al. 2017). Concentrations of Ni could increase by human activities such as application of phosphate fertilizers and pesticides (Gimeno-García et al. 1996) or industrial and agricultural wastewater discharges, domestic sewage discharge and atmospheric deposition (Yan et al. 2018).

The vegetal meristematic tissues that are used for testing the effects of chemicals on chromosomes should be easy to obtain and less expensive. From this point of view, the species *A. sativum* and *A. cepa* are well suited to cytogenetic studies because the meristematic roots appear lightly, have relatively large chromosomes in small numbers and can be easily observed by optical microscope (Doroftei et al. 2010; Bonciu 2012; Bonciu et al. 2018).

MATERIALS AND METHODS

Plant material

The biological material consisted of garlic bulbs, clean and without traces of pests or diseases that had been spread in several bulbils. They were cleaned from the dried leaves and formed by removing any roots after which they were transferred to small glass bottles containing the heavy metal solutions: nickel nitrate - $Ni(NO_3)_2$ and lead nitrate - $Pb(NO_3)_2$ in concentrations of 50, 150 and 450 ppm for each of them.

Three treatment variants with 4 repetitions were performed for each of the heavy metals experienced, along with an untreated control immersed in plain water. In each variant, four garlic bulbils were immersed directly into the treatment solutions for 72 hours, time required for the meristematic roots to be emitted.

Microscopic preparations

After sampling, the meristematic roots were fixed with a mixture of absolute ethyl alcohol and glacial acetic acid in a volume ratio of 3: 1 for 16 hours in the refrigerator, followed by acid hydrolysis with 1 N HCl for 5 minutes and HCl 50% consisting of equal parts of HCl and distilled water for 16 min at room temperature. Roots' staining was performed by the Feulgen technique with Schiff's reagent; the staining time was 90 minutes, followed by the intensification of the coloration in plain water for 20 minutes.

Statistical analyses

After 72 hours, the meristematic roots were counted and measured at each variant. The cytogenetic effects of heavy metals were assessed by calculating the mitotic index (MI) and analysing the chromosomal aberrations observed in the various stages of mitosis. The microscopic preparations have been studied using a microscope with digital camera Kruss (Kruss manufacturer Hamburg, Germany). Five preparations for each variant and 500 cells were analysed for calculating the mitotic index and the chromosome aberration frequency.

Statistical analysis was done using MS Excel 2007. The obtained data were analysed statistically with one-way analysis of variance (ANOVA). The differences between treatment means were compared using the LSD-test at a probability level of 0.05% subsequent to the ANOVA analysis.

The mitotic index and chromosomal aberrations were calculated using the following formulas:

Mitotic index (MI%) = total number of cells in division / total number of analysed cells x 100;

Chromosomal aberrations (CA%) = total number of aberrant cells / total number of cells in division × 100.

RESULTS

The treatment of *A. sativum* bulbils with nickel and lead depending on the concentration negatively influenced the process of issuing meristematic roots.

The treated roots was smaller in size and they had a smaller number than the control. Thus, their number decreased as the concentration of the heavy metal solutions tested in all variants increased: from 46 registered roots to the control variant, to 14-28 roots to the variant treated with $Ni(NO_3)_2$ respectively 5-18 roots to the variant treated with $Pb(NO_3)_2$ (Figure 1).

The results showed that both heavy metals treatments caused a decrease in MI at all the treatment groups (Table 1). Thus, the value of the MI decreased with the increase concentration of heavy metal solutions. The intensity of mitotic activity was decreasing in order of treatment with lead nitrate to nickel nitrate treatment. However, the strongest mitodepresive effect was seen in the treatment of $Pb(NO_3)_2$ at the concentration of 450 ppm, when MI was 5.32%, ie with 46.4% lower mitotic activity compared to the control variant.

Heavy metals tested induced a high number of CA when compared with control. The increase of CA was dependent on the increasing treatment concentrations (Table 1). The types of CA identified in meristematic cells of *A. sativum* were the following: C-Mitosis (Figure 2A); fragments and vagrants (Figure 2B); star-anaphase; star-telophase (Figure 2C); clumping; stickiness (Figure 2D); bridges (Figure 2E).

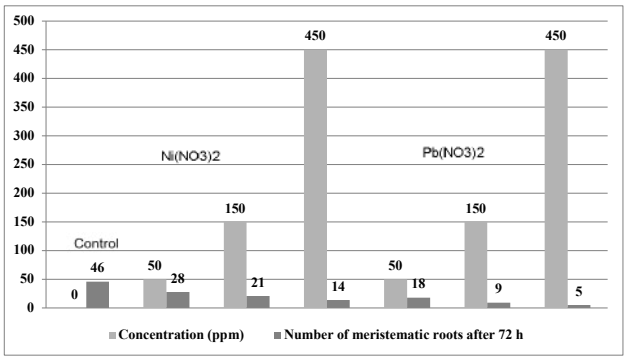

Fig. 1. The inhibitory effect of different concentrations of $Ni(NO_3)_2$ and $Pb(NO_3)_2$ on the rhizogenesis to *A. sativum.*

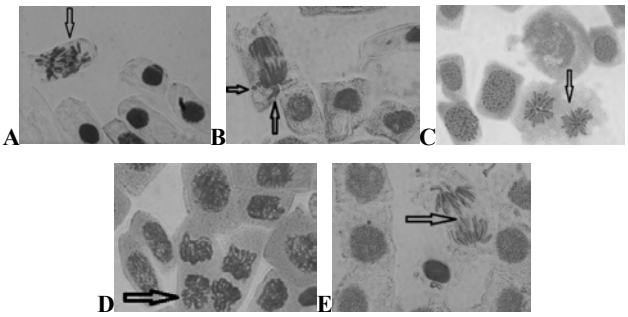

Fig. 2. Some chromosomal aberrations identified in meristematic cells of *A. sativum* exposed to $Ni(NO_3)_2$ and $Pb(NO_3)_2$: C-Mitosis (A), fragments and vagrants (B), star-telophase (C), stickiness in telophase (D), anaphase bridge (E).

As can be seen from the data of Table 1, the most common types of CA were stickiness, C-Mitosis and bridges, and the least frequent were vagrants chromosomes. Compared with the control variant, the total CA rate recorded insignificant values for the variant treated with 50 ppm $Ni(NO_3)_2$, significant for the variant treated with 150 ppm $Ni(NO_3)_2$ and distinctly significantly positive for the variant treated with 450 ppm $Ni(NO_3)_2$. On the other hand, in case of the $Pb(NO_3)_2$ treated variants compared to the control variant, the total CA recorded significantly positive values for the variant treated with 50 ppm $Pb(NO_3)_2$ and strongly positive for the variants treated with 150 and 450 ppm $Pb(NO_3)_2$ respectively.

DISCUSSION

We chose to study the cytotoxic effects of Ni and Pb heavy metals on *A. sativum* because, according to many authors (Saxena et al. 2004; Gul et al. 2006; Unyayar et al. 2006; Liu et al. 2009), the evaluation of CA in *A. sativum* meristematic roots is a reliable biotest example that can be applied to detect a wide range of genetic damage.

At a macroscopic level, heavy metals induced inhibition of the growth of meristematic garlic roots. Generally, heavy metals are known to decreasing the plant growth and ground cover (McGrath et al. 2001). Some effects of lead on growth, physiology, metabolism and yield attributes of plants are the following: inhibition in seed germination, fresh and dry biomass, leaf area, chlorophyll and growth to *Helianthus annuus* (Mahmood et al. 2013); decline in growth, chlorophyll, carotenoids and prolinecontent to *Brassica juncea* (John et al. 2009); decrease in plant growth, root hair to *Vigna unguiculata* (Kopittke et al. 2007), etc.

In our experiment, reducing the number of meristematic root has been accentuated with increasing con-

Table 1. Mitotic index, type and percentage of mitotic aberrations induced by some heavy metals on the meristematic roots to *A. sativum.*

Treatment / Exposure time (hours)	Conc. (ppm)	MI ± SD (%)	CA (%)								Total aberrations (%)
			C-M	V	S-A	S-T	F	CL	S	B	
Ct / 72	0	11.45±0.5	2.35	0	0	0	0	0	0	0	2.35
$Ni(NO_3)_2$ / 72	50	10.66±0.4	1.61	0.65	0.42	0	0	0	3.62	2.31	8.61
	150	8.13±0.3	1.90	0.83	1.81	0.83	0	1.23	5.11	3.22	14.93*
	450	6.84±0.8	3.15	1.40	2.73	1.43	2.11	3.41	5.42	3.91	23.56**
$Pb(NO_3)_2$ / 72	50	8.73±0.4	4.65	1.62	3.90	1.70	2.80	3.96	6.28	4.82	29.73**
	150	6.51±0.8	6.23	2.11	4.31	2.82	3.70	4.20	6.50	5.31	35.18***
	450	5.32±0.5	7.51	2.64	4.85	4.20	4.21	6.52	7.40	6.10	43.43***

Ct = Control; Conc. = Concentration; MI = Mitotic index; SD = Standard deviation;
CA = Chromosomal aberrations; C-M = C-Mitosis; V = Vagrants; S-A = Star-Anaphase; S-T = Star-Telophase; F = Fragments; CL = Clumping; S = Stickiness; B = Bridges;
The differences between treatment means were compared using the LSD-test at a probability level of 0.05%: *significant at P<0.05, **significant at P<0.01, ***significant at P<0.001 as compared to the control variant.

centrations of test solutions (especially to treatments with lead nitrate). Proportionately with increasing concentrations, intensity of the mitotic division has been decreased to all variants, as an active protection reaction of the plants exposed to heavy metals action. These findings are in agreement with Doroftei et al. (2010) who have tested the cytogenetic effects of lead nitrate to *A. cepa*. The lead and nickel inhibited cell division to other plants too, like *Zea mays* (Kozhevnikova et al. 2007).

The root growth is an integrative process depending on whole-organism signalling and individual growth trajectories of cells (Beemster et al. 2003). The intensity of the mitotic division is directly related to the growth of plant roots; conceptually, mitotic division in the apical root meristem provides cells during longitudinal growth (Sanz et al. 2012). The number of dividing cells in the root apical meristem generates a cell flux with importance in modulating root growth (Baskin, 2013). Studies of cell length profiles have shown that the proliferative fraction of dividing cells in the apical root meristem proliferation domain is indistinguishable from one, even in response to moderate levels of stress (Ivanov and Dubrovsky 2013).

The results of this study highlight the increasing of CA frequencies to *A. sativum* dependent on different concentrations of nickel nitrate and lead nitrate. Stickiness, C-mitosis and bridges were most often identified in all treatment variants but the highest frequency was recorded to variants treated with lead nitrate. According to some authors, sticky chromosomes might have resulted from increased chromosome contraction and condensation or possibly from depolymerisation of DNA and partial dissolution of nucleoproteins (Kuras et al. 2005; Turkoglu 2013b). Asita and Mokhobo (2013) suggested that the induction of *Allium*'s sticky chromosomes under the influence of pesticides indicates abnormal DNA condensation, abnormal chromosomal wrapping, and inactivation of the axes, and all these anomalies cell division can have adverse effects on the environment. C-Mitosis indicates a chemical-inhibited spindle formation similar to the effect of colchicine and induction of these aberrations suggests a turbogenic effect (Shahin and El-Amoodi 1991; Turkoglu 2013b). Regarding the anaphase bridges, these chromosomal aberration cause structural chromosome mutations and may lead to loss of genetic material (George 2000; Pampalona et al. 2016). According to Turkoglu (2013b), bridges could form due to dicentric chromosome presence or due to the breakage and fusion of chromosomes and chromatids.

In our experiment, the stickiness had a frequency of 3.62-5.42% at the nickel nitrate treatment, while for treatment with lead nitrate the frequency of these CA was at the level of 6.28-7.40% at all concentrations (50, 150, 450 ppm). Sticky chromosomes can probably lead to cell death (Singh 2015). These results suggest the strong genotoxic effect of lead nitrate even at low concentrations of 50 and 150 ppm. The current findings agreed well with other reports which showed cytotoxicity and genotoxicity of lead in plant cells (Choudhury and Panda 2004; Arya et al. 2013).

Some nickel compounds have been established as human carcinogens (Coogan et al. 1989), but at the same time, some plant seeds, such as soybeans, can act as protectors when introduced into diet of treated mice, by reducing the percentage of CA (Fahmy et al. 2014). Certain hormones can act as agents for inducing resistance

of plants to heavy metal toxicity. Thus, some authors have reported that *Brassica juncea* plants sprayed with 28-homobrassinolide hormone, showed improved resistance against the some heavy metal toxicity (Hayat et al. 2007). Also, the organic acids (citrate and malate) have been reported to have a role in the plant protection against heavy metal stress (Haydon et al. 2007).

CA called C-mitosis had a frequency of 1.61-3.15% at the nickel nitrate treatment, while for treatment with lead nitrate the frequency of C-mitosis was at the level of 4.65-7.51%, these results demonstrating the high genotoxic potential of lead to plants. C-mitosis is the result of damaged mitotic apparatus due to genotoxic substances in the cells and is stimulated by many chemicals (Fiskesjö 1993; Firbas and Amon 2014).

Cytogenetic tests on *A. sativum* reveal a decrease in the mitotic index following heavy metal treatments. Mitosis analysis indicates the occurrence of a large number of CA identified at various stages of mitosis, the cell division process being significantly affected. The most of the CA identified indicates aneugenic effects, because of in the mitotic spindle disorders (Sharma and Panneerselvan 1990; Fernandes et al. 2007).

The results obtained in this study reflect cytotoxic and genotoxic potential of Ni and Pb to higher plant A. *sativum*. Changes induced by the heavy metals analysed in the genetic material can be much deeper but unnoticeable with our investigative means.

REFERENCES

Arduini I, Goldbold DL, Onnis A. 1994. Cadmium and cooper change root growth and morphology at *Pinus pinea* and *Pinus pinaster* seedling. Physiol Plant. 92(4): 675-680.

Arya SK, Avisek Basu A, Mukherjee A. 2013. Lead induced genotoxicity and cytotoxicity in root cells of *Allium cepa* and *Vicia faba*. *Nucleus*. 56(3): 183-189.

Asita AO, Mokhobo MM. 2013. Clastogenic and Cytotoxic Effects of Four Pesticides Used to Control Insect Pests of Stored Products on Root Meristems of *Allium cepa*. Environ Nat Resources Res. 3(2):133-145.

Baskin TI. 2013. Patterns of root growth acclimation: constant processes, changing boundaries. Developmental Biology 2(1): 65–73.

Beemster GTS, Fiorani F, Inzé D. 2003. Cell cycle: the key to plant growth control? Trends in Plant Science 8(4): 154–158.

Bilal E, Guenolé–Bilal I, Bounahkla M, Iatan LE, Machado de Mello F, Doumas M, Tahri M, Gallice F, Grail-lot D, Piegay H, Lassoued N. 2014. The freshwater mussels are a good bioindicator for monitoring the water pollution by heavy metal (the Saint–Victor–sur–Loire Lake, France). Banat¢s Journal of Biotechnology. 5(10): 5–11.

Bonciu E, Firbas P, Fontanetti CS, Wusheng J, Karaismailoğlu MC, Liu D, Menicucci F, Pesnya DS, Popescu A, Romanovsky AV, Schiff S, Ślusarczyk J, de Souza CP, Srivastava A, Sutan A, Papini A. 2018. An evaluation for the standardization of the *Allium cepa* test as cytotoxicity and genotoxicity assay. Caryologia. 71(3): 191-209.

Bonciu E. 2012. Cytological effects induced by Agil herbicide to onion. J Horticult For Biotechnol. 16(1):68-72.

Choudhury S, Panda SK. 2004. Induction of oxidative stress and ultrastructural changes in moss *Taxithelium nepalense* (Schwaegr) broth under lead and arsenic phytotoxicity. Curr Sci 87(3): 342-348.

Coogan TP, Latta DM, Snow ET, Costa M. 1989. Toxicity and carcinogenicity of nickel compounds. Crit Rev Toxicol. 19(4): 341-384.

Coroian A, Miresan V, Cocan D, Raducu C, Longodor AL, Pop A, Feher G, Andronie L, Marchis Z. 2017. Physical-chemical parameters and the level of heavy metals in cow milk in the Baia Mare area. Banat¢s Journal of Biotechnology. 8(16): 69–74.

Dong J, Wu FB, Zhang GP, 2006. Influence of cadmium on antioxidant capacity and four microelement concentrations in tomato seedlings (*Lycopersicon esculentum*). Chemosphere. 64(10): 1659-1666.

Doroftei E, Antofie MM, Sava D, Arcus M. 2010. Cytogenetic effects induced by Manganese and Lead microelements on germination at *Allium cepa*. Botanica Serbica. 34(2): 115-121.

Eskew DL, Welch RM., Cary EE. 1983. Nickel: an essential micronutrient for legumes and possibly all higher plants. Science. 222(4624): 621-623.

Fahmy MA, Hassan NHA, Melek FR, Hassan ZM, Al-Ashaal HA. 2014. Studies on the Genotoxic Effect of Nickel Chloride in Mice and the Possible Protective Role of Soybean Seeds Extracts. Global J Pharmacol. 8(4): 625-634.

Fernandes TCC, Mazzeo DEC, Marin-Morales MA. 2007. Mechanism of micronuclei formation in polyploidizated cells of *Allium cepa* exposed to trifluralin herbicide. Pesticide Biochemistry and Physiology. 88(3): 252-259.

Firbas P, Amon T. 2014. Chromosome damage studies in the onion plant *Allium cepa* L. Caryologia. 67(1): 25-35.

Fiskesjö G. 1993. The *Allium* test – A potential standard protocol of assessment of environmental tox-

icity. In: Gorsuch JW, Dwyer FJ, Ingorsoll CG, La Point TW, editors. Environ Toxicol and Risk Assess, Vol. 2. Philadelphia: American Society for Testing and Materials. p. 331–345.

Fisjekö G. 1982. Evaluation of short term tests of toxicity and mutagenity with special reference to mercury and selenium. Hereditas. 95: 155-162.

Gajewska E, Sklodowska M, Slaba M, Mazur J. 2006. Effect of nickel on antioxidative enzyme activities, proline and chlorophyll contents in wheat shoots. Biologia Plantarum. 50(4): 653-659.

Gantayat S, Mania S, Pradhan C, Das AB. 2017. Ionic Stress Induced Cytotoxic Effect of Cadmium and Nickel Ions on Roots of *Allium cepa* L. Cytologia 83(2):143-148.

George NM. 2000. Evaluation on Mutagenic Effects of the Three Heavy Metals on *Vicia faba* Plants. Cytologia 65(1): 75-82.

Georgieva N, Nikolova I, Naydenova Y. 2018. Possibility for weed control by using of an organic product with herbicidal effect. Banat¢s Journal of Biotechnology 9(17): 40-49.

Gimeno-García E, Andreu V, Boluda R. 1996. Heavy metals incidence in the application of inorganic fertilizers and pesticides to rice farming soils. Environ Pollut. 92(1): 19-25.

Gul T, Kaymak F, Fulya D, Muranli G (2006). Genotoxic Effects of Avenoxan on *Allium cepa* L. and *Allium sativum* L. *Caryologia.* 59(3): 241-247.

Hariri Moghadam F, Khalghani J, Moharramipour S, Gharali B, Mostashari Mohasses M. 2018. Investigation of the induced antibiosis resistance by zinc element in different cultivars of sugar beet to long snout weevil, *Lixus incanescens* (Col: *Curculionidae*). Banat¢s Journal of Biotechnology. 9(17): 5–12.

Hayat S, Ali B, Hasan SA, Ahmad A. 2007. Brassinosteroid enhanced the level of antioxidants under cadmium stress in *Brassica juncea*. Environ Exp Bot. 60(1): 33–41.

Haydon MJ, Cobbett CS. 2007. Transporters of ligands for essential metal ions in plants. New Phytol. 174(3): 499–506.

Ivanov VB, Dubrovsky JG. 2013. Longitudinal zonation pattern in plant roots: conflicts and solutions. Trends in Plant Science 18(5): 237–243.

John R, Ahmad P, Gadgil K, Sharma S. 2009. Heavy metal toxicity: Effect on plant growth, biochemical parameters and metal accumulation by *Brassica juncea* L. Int J Plant Product. 3(3): 65-76.

Kopittke PM, Asher CJ, Kopittke RA, Menzies NW. 2007. Toxic effects of Pb2+ on growth of cowpea (Vigna unguiculata). Environ Pollut. 150(2): 280-287.

Kozhevnikova AD, Seregin IV, Bystrova EI, Ivanov VB. 2007. Effects of heavy metals and strontium on division of root cap cells and meristem structural organization. Russ J Plant Physiol. 54(2): 257–266.

Kuraś M, Nowakowska J, Sliwinska E, Pilarski R. 2005. Changes in chromosome structure, mitotic activity and nuclear DNA content from cells of *Pallium* Test induced by bark water extract of *Uncaria tomentosa* (Willd.) DC. J of Ethnopharmacol. 107(2): 211-221.

Lassoued N, Khelil MN, Rejeb S, Bilal E, Chaouachi M, Rejeb MN, Guenolé–Bilal I. 2014. Transfert heavy metal sewage sludge as fertilizer from soil to ray grass. Banat¢s Journal of Biotechnology. 5(9): 86–95.

Liao LM, Friesen MC, Xiang YB, Cai H, Koh DH, Ji BT, Yang G, Li HL, Locke SJ, Rothman N, Zheng W, Gao YT, Shu XO, Purdue MP. 2016. Occupational Lead Exposure and Associations with Selected Cancers: The Shanghai Men's and Women's Health Study Cohorts. Environ Health Perspect. 124(1): 97-103.

Liu D, Jiang W, Meng Q, Zou J, Gu J, Zeng M (2009). Cytogenetical and ultrastructural effects of copper on root meristem cells of *Allium sativum* L. *Biocell.* 33(1): 25-32.

Mahmood S, Ishtiaq S, Malik MI, Ahmed A. 2013. Differential growth and photosynthetic responses and pattern of metal accumulation in sunflower (*Heliathus annuus* L.) cultivars at elevated levels of lead and mercury. Pak J Bot. 45(SI): 367-374.

Marinova DH, Ivanova II, Zhekova ED. 2018. Evaluation of Romanian alfalfa varieties under the agro–environmental conditions in northern Bulgaria. Banat¢s Journal of Biotechnology 9(18): 56-64.

McGrath SP, Zhao FJ, Lombi E. 2001. Plant and rhizosphere processes involved in phytoremediation of metal-contaminated soils. Plant and Soil. 232(1-2): 207-214.

Mohanpuria P, Rana NK, Yadav SK 2007. Cadmium induced oxidative stress influence on glutathione metabolic genes of *Camellia sinensis* (L.) O. Kuntze. Environ Toxicol. 22(4): 368-374.

Nakazawa R, Kameda Y, Ito T, Ogita Y, Michihata R, Takenaga H. 2004. Selection and characterization of nickel-tolerant tobacco cells. Biol Plant. 48(4): 497-502.

Nemcsók J, Editare H, Zsanett J, Băneş A, Horablaga M, Bostan C. 2010. The pollution of the soils, the underground and surface waters, from Hungarian–Romanian Cross–Border area. Banat¢s Journal of Biotechnology. 1(2): 70-78.

Nikolova I, Georgieva N. 2018. Effect of biological products on the population of aphids and chemical components in alfalfa. Banat¢s Journal of Biotechnology 9(18): 38-45.

Pampalona J, Roscioli E, Silkworth WT, Bowden B, Genescà A, Tusell L, Cimini D. 2016. Chromosome Bridges Maintain Kinetochore-Microtubule Attachment throughout Mitosis and Rarely Break during Anaphase. PLOSOne. 11(1): e0147420.

Petrescu I., Sarac I, Chereches B, Madosa E. 2015. Effect of lead on the growth of *Coriandrum sativum* L. J Horticult For Biotechnol. 19(4): 93-95.

Sachan P, Lal N. 2017. An Overview of Nickel (Ni2+) Essentiality, Toxicity and Tolerance Strategies in Plants. Asian J Biol. 2(4): 1-15.

Sanz L, Murray JAH, Dewitte W. 2012. To Divide and to Rule; Regulating Cell Division in Roots during Post-embryonic Growth. In: Lüttge U, Beyschlag W, Büdel B, Francis D (Eds.), Progress in Botany: 73: 57-80. Springer-Verlag Berlin Heidelberg.

Sarac I, Petrescu I, Madosa E, Antonie IF. 2015, *Copper effects at seed germination of Secale cereale* L. J Horticult For Biotechnol. 19(4): 84-88.

Saxena PN, Chauhan LKS, Chandra S, Gupta SK. 2004. Genotoxic effects of diuron contaminated soil on the root meristem cells of *Allium sativum*: a possible mechanism of chromosome damage. *Toxicology Mechanisms and Methods.* 14(5): 281-286.

Shahin SA, El-Amoodi KHH. 1991. Induction of numerical chromosomal aberrations during DNA synthesis using the fungicides Nimrod and Rubigan-4 in root tips of *Vicia faba* L. Mutation Research 261(3): 169–176.

Sharma CBSR, Panneerselvan N. 1990. Genetic toxicology of pesticides in higher plant systems. Critical Reviews in Plant Sciences. 9(5): 409-442.

Singh P. 2015. Toxic effect of chromium on genotoxicity and cytotoxicity by use of Allium cepa L. IJREAS. 5(10): 1-10.

Unyayar S, Celik A, Cekic FO, Gozel A. 2006. Cadmium-induced genotoxicity, cytotoxicity and lipid peroxidation in *Allium sativum* and *Vicia faba*. Mutagenesis. 21(1): 77–81.

Türkoglu S. 2013b. Evaluation of genotoxic effects of five flavour enhancers (glutamates) on the root meristem cells of *Allium cepa*. Food and Chemical Toxicol. 49(4): 763 – 769.

Wójcik M, Tukiendorf A. 2014. Phytochelatin synthesis and cadmium localization in wild type of *Arabidopsis thaliana*. Plant Growth Regulation. 44(1): 71-80.

Yadav SK. 2010. Heavy metals toxicity in plants: An overview on the role of glutathione and phytochelatins in heavy metal stress tolerance of plants. South African Journal of Botany. 76(2): 167-179.

Yan X, Liu M, Zhong J, Guo J, Wu W. 2018. How Human Activities Affect Heavy Metal Contamination of Soil and Sediment in a Long-Term Reclaimed Area of the Liaohe River Delta, North China. Sustainability: 10(2): 338.

Zornoza P, Robles S, Martin N, 1999. Alleviation of nickel toxicity by ammonium supply to sunflower plants. Plant and Soil. 208(2): 221-226.

Caryologia
International Journal of Cytology, Cytosystematics and Cytogenetics

Firenze University Press
www.fupress.com/caryologia

Citation: L. Verschaeve, R.Antonissen, A. Baeyens, A. Vral, A. Maes (2019) Fluorescence In Situ Hybridisation Study of Micronuclei in C3A Cells Following Exposure to ELF-Magnetic Fields. *Caryologia* 72(2): 45-51. doi: 10.13128/cayologia-254

Published: December 5, 2019

Data Availability Statement: All relevant data are within the paper and its Supporting Information files.

Competing Interests: The Author(s) declare(s) no conflict of interest.

Fluorescence In Situ Hybridisation Study of Micronuclei in C3A Cells Following Exposure to ELF-Magnetic Fields

Luc Verschaeve[1,2,*], Roel Antonissen[1], Ans Baeyens[3], Anne Vral[3], Annemarie Maes[1]

[1] *Sciensano, Risk and Health Impact Assessment Service, Brussels, Belgium*
[2] *Department of Biomedical Sciences, University of Antwerp, Antwerp, Belgium*
[3] *Department of Basic Medical Sciences, Ghent University, B-9000 Ghent, Belgium*
*Corresponding author: Luc.verschaeve@sciensano.be

Abstract. Human C3A cells were exposed to extremely low frequency (50 Hz) magnetic fields (ELF-MF's) up to 500 μT. They were subjected to the micronucleus assay using a Fluorescence In Situ Hybridization (FISH) technique with an in-house pan-centromere probe. We found no increased frequency in micronucleated cells and no change in the proportion of centromere positive over centromere negative micronuclei compared to the unexposed control cells. These results are in accordance with some, but in contradiction with other previously published investigations underlining that effects of environmental ELF-EMF's on cellular DNA may be very subtle and that small changes or environmental influences may determine the outcome of a (geno)toxicity study. Interestingly, a low-level (5μT) exposure resulted in less than the background micronucleus frequency.

Keywords. 50 Hz magnetic fields, FISH staining, micronuclei, centromere staining, genotoxicity.

INTRODUCTION

Overall, there is little experimental or theoretical evidence that extremely low frequency magnetic fields (ELF-MF's) from power lines or other man made sources in the environment can be genotoxic. Given the level of energy involved, it is difficult to accept that they are able to directly interact with genomic structures. The results of most *in vitro* and *in vivo* genetic toxicology studies involving ELF-MF's have been negative and therefore there is a general consensus that they, especially at normal (moderate) exposure levels, are not directly mutagenic (Bergqvist et al. 2003; Vijayalaxmi and Prihoda 2009). Yet, some papers did report effects suggesting that ELF magnetic fields may interact with DNA or, most often, with DNA-damaging agents, hence being co-genotoxic (e.g., Tofani et. al. 1995; Lai and Singh 1997; Singh and Lai 1998; Bergqvist et al. 2003; Cho and Chung 2003; Ding et al. 2003;

Moretti et al. 2005; Vijayalaxmi and Obe 2005; Juutilainen et al. 2006; EHC 2007; Ruiz-Gómez and Martinez-Morillo 2009; Markkanen 2009; Udroiu et al. 2006). According to some of these studies ELF-magnetic fields are able to enhance, but not to start a mutagenic (DNA damaging) effect. Some of the above mentioned papers also indicate that EMF-MF's exposure may, alone or in conjunction with another agent, be able to promote the occurrence of aneuploidy caused by an aneugen via a mechanism involving the neuroendocrine system (Maes et al. 2016a). Jin et al. (2015) however, provided evidence that ELF-MF's alone do not induce either G2/M arrest or aneuploidy, even when administered in combination with different stressors. Only a few papers reported so far on possible aneugenic or co-aneugenic effects of electromagnetic fields (Udroiu et al. 2006; Maes and Verschaeve 2012; Maes et al. 2016a). On previous investigations (Maes et al. 2016a,b) we reported increased levels of especially nuclear buds and large micronuclei in cells that were exposed to 50 Hz ELF-MF's. This indicated that the magnetic fields may, at least in particular cells, situations and exposure levels induce gene amplification (buds) and aneuploidy. In the present paper we further explore this possibility by using fluorescence in situ hybridisation (FISH) with a pan-centromeric probe. The main objective was to verify our previous results and to investigate whether potential ELF-MF's induced micronuclei (MN) were predominantly centromere-positive or centromere-negative, respectively suggesting an aneugenic or clastogenic effect.

MATERIALS AND METHODS

ELF-MF exposure unit

The exposure unit was a cylindrical coil (380 turn coil, 42 cm long, 20 cm inner diameter) which allowed the exposure of cell cultures to a nearly constant magnetic field (with a tolerance of a few percent). With this device, cell cultures could be exposed to different 50 Hz magnetic field amplitudes ranging from 0 up to about 2500 μT. More details about the exposure unit can be found elsewhere (Maes et al. 2000; Verheyen et al. 2003; Mineur 2009). We exposed cell cultures to magnetic fields of 5, 10, 50, 100 and 500 μT. The ambient magnetic field was 0.02±0.01 mT.

Cell cultures and ELF-MF exposure

Human hepatic C3A cells (Brunschwig Chemie B.V, Amsterdam, the Netherlands) were grown in 24 well plates in Dulbecco's modified Eagle's culture medium supplemented with 10% foetal calf serum. The cell density was 200.000 cells/well. Plates were incubated at 37°C and 5% CO_2. Humidity was maintained using a water bath containing milli-Q water inside the incubator. After 24 h of incubation, a magnetic field producing a determined magnetic flux density (5, 10, 50, 100, or 500 μT) was applied for another 24 h. Following exposure to the magnetic field, cells were blocked in their binucleated (BN) telophase stage with cytochalasin B (4.5 μg/ml, Merck). Another 24h later cells were fixed with methanol/acetic acid (3/1) and spread onto well-cleaned microscope slides. Magnetic flux densities were chosen based on our previous experiments (Maes et al. 2000, 2016a,b; Verheyen et al. 2003). Each exposure was accompanied by its own unexposed (negative) control culture (0 μT). Methyl methane sulfonate (MMS, 15μg/ml) was used as a positive control. It was found to induce micronuclei as expected (results not shown). Both control cultures were incubated away from the coil at a distance where no ELF-MF, other than the ambient field could be measured.

Two independent investigations were conducted. In the first experiment magnetic flux densities of 5, 10, 50, 100 and 500 μT were investigated. The second study was conducted on new exposed cell cultures and fresh slides using magnetic flux densities of 5, 50 and 500 μT.

Fluorescence In Situ Hybridization (FISH)

In the first set of experiments, FISH was performed on the slides using an in-house pan-centromeric probe, labelled with spectrum orange. For more details about this probe and the FISH protocol we refer to Baeyens et al. (2011) and Vral et al. (2016). In the repeat study, FISH was performed using a FITC-labeled PNA (peptide nucleic acid) probe, specific for centromeric sequences, from Panagene (centFAM 5nmol, PN-CN001-005 Eurogentec, Belgium). The protocol, described in detail by M'Kacher et al. (2014), for centromere staining of dicentric chromosomes was followed. At the end of both FISH procedures, the slides were counterstained and mounted with DAPI-vectashield (H-1200, Labconsult, Belgium).

FISH-DAPI stained slides were analysed with the Metafer 4 platform (MetaSystems GmbH, Altlussheim, Germany) connected to a motorized Zeiss AxioImager M1 microscope (Zeiss, Oberkochen, Germany). Detailed information regarding the MSearch slide scanning procedure, stage movement, focusing and image acquisition are detailed in Willems et al. (2010). For analyses of micronuclei the MNScore module for Metafer MSearch was used. This software allows automated MN scoring in binucleated (BN) cells using a 10x objective. The auto-

matically selected BN cells were then checked manually (false BN cells and false positive or negative micronuclei were removed) and only confirmed BN cells with micronuclei were scanned via the Autocapt image acquisition software using a 40x objective. The autocapt images were then manually viewed for the presence of centromeres. Bad/non-interpretable FISH images were rejected. For more details about the MN-centromere analysis we refer to Vral et al. (2016). The number of investigated cells was set to 2.500 but the actual number of analysed cells was sometimes less (see Table 1). Two slides (approximately 1.250 cells) were analysed per exposure.

RESULTS AND DISCUSSION

The results of the two independent investigations are summarized in Table 1. The table data indicate that micronucleus frequencies were not increased following ELF-MF's exposures up to 500 μT. According to this analysis we observe no clear differences in number of MN between the tested situations. No clear difference or trend in the percentage of centromere-negative or centromere-positive MN can be observed as well. According to these data 50 Hz ELF-MF's do not change the proportion of centromere-positive over centromere-negative MN, neither do they induce elevated micronucleus frequencies.

This does not coincide with our previous results on the same cells that were exposed in the same way to magnetic fields of the same magnetic flux densities. In our previous investigation (Maes et al. 2016b) we also performed two independent experiments but slides were stained with Giemsa. Currently we used a fluorescence in situ hybridisation procedure but there is no reason why the different staining methods should influence the results. Both investigations were also performed by the same persons ruling out the possible variation in micronucleus frequencies obtained by individual laboratories and scorers (Fenech et al. 2003).

As mentioned before, the literature reveals the presence of positive as well as negative results following exposure of cells or organisms to (weak) ELF-MF's. We, for example, did not find increased micronucleus frequencies in peripheral human white blood cells after exposure to ELF-MF's up to 800 μT using the same experimental set up (Verheyen et al. 2003). Moreover, Loberg et al. (2000) also did not find evidence for the hypothesis that magnetic fields interact with genotoxic agents to induce adverse biological effects in either normal or genetically susceptible human cells. The same holds true for the investigation of Ding et al. (2003)

Table 1. Summary of two independent experiments on ELF-MF's exposed C3A cells following FISH-staining of micronuclei.

	Number of Binucleated cells	MN/1000 cells	MN+	MN-	% CM+	% CM-	MN+/ MN-
Experiment 1							
5 μT	2500	10	5.2	4.8	52	48	1.1
control	2500	19.2	14	5.2	72.17	27.08	2.7
10 μT	2500	12	7.2	4.8	60	40	1.5
control	2500	14	8.8	5.2	62.86	37.14	1.7
50 μT	2500	18	14.4	3.6	80	20	4
control	2500	13.6	11.2	2.4	82.35	17.65	4.7
100 μT	2500	16.8	12.8	4	76.19	23.81	3.2
control	2500	18.8	13.6	5.2	72.34	27.66	2.6
500 μT	2500	12	8	4	74.29	25.71	2
control	2500	14	10.4	3.6	66.67	33.33	2.9
Experiment 2							
5 μT	3432	20.69	15.15	5.54	73.24	26.76	2.7
Control	3423	21.62	16.36	5.26	75.68	24.32	3.1
50 μT	1629	22.71	14.12	2.46	89.19	10.81	5.7
Control	1093	20.13	16.47	3.66	81.82	18.18	4.5
500 μT	2193	22.8	15.04	7.75	66	34	1.9
control	3021	28.8	16.88	5.3	81.61	18.39	3.2

where Chinese hamster ovary cells were exposed to a 60 Hz ELF-MF at 5 mT field strength. In this investigation, MN were evaluated by immunofluorescence staining using anti-kinetochore antibodies from the serum of Scleroderma (CREST syndrome) patients. No statistically significant difference in the frequency of MN was observed between sham exposed and 24 h ELF-MF's exposed cells. The number of spontaneous kinetochore-positive and kinetochore-negative MN was, as in our present investigation, not affected by exposure to an ELF magnetic field alone. However, Kesari et al. (2016) reported increased micronucleus frequencies at 10 and 30 μT in SH-SY5Y neuroblastoma cells using a flow cytometry method. Other examples of positive and negative results on ELF-MF's exposed cells and organisms were presented by Heredia-Rojas et al. (2017).

Actually, the absence of independent replication has been a consistent feature of experimental studies searching for biological effects of weak ELF-(electro) MF's (ELF-EMF's). As pointed out by Foster and Skufca (2016) many scientific results can't be replicated, leading to serious questions about what's true and false in the world of research. Many reasons, especially involving statistical inadequacies or different experimental factors

or errors of unknown nature, can be evoked. Effects of environmental ELF-EMF's on cellular DNA are believe to be very subtle (Heredia-Rojas et al. 2018) and therefore small experimental changes or environmental influences may determine the outcome of a (geno)toxicity study. Also, different cell types (e.g., healthy lymphocytes versus a cancer cell line), but especially the different physiological state of the cells may account for different susceptibilities and consequently different results (Fenech 1998). It was for example shown that cells from aged donors and leukemic patients respond to ELF-EMF's exposure differently than 'other' (normal) cells (Cadossi et al. 1992), and that DNA damage was found in cells from Turner syndrome patients but not in cells from healthy individuals (Scarfi et al. 1997a). The same authors found that Turner syndrome subjects showed a lower spontaneous and mitomycin C-induced micronucleus frequency, in comparison with healthy subjects (Scarfi et al. 1996). On the other hand, in another publication they did not report a different response between normal cells and cells from Turner syndrome patients (Scarfi et al. 1997b). The viability of goldfish that were infected by a parasite increased substantially when the fish were exposed to very low levels of ELF-MF's (Cuppen et al. 2007) giving another example of possible different effects according to the health status of a cell or organism. Some more cases are also reported in the literature.

We used HepG2/C3A cells mainly because they have nitrogen metabolizing activity comparable to perfused rat livers, which was an important asset in some of our other studies. They are a clonal derivative of Hep G2 hepatocellular carcinoma cells, with an unstable chromosome number of 45-60. Perhaps another batch and cell passage may also be responsible for small physiological changes that ultimately may influence the MN frequency. Although cellular passaging was not found to influence significantly hASCs's secretome properties (Serra et al., 2018), increased cell passage number was found to alter P-glycoprotein expression in Caco2 cell (Senarathna and Crowe, 2015). Previously, Gloy et al. (1994) already reported that the response of membrane voltage to ATP and angiotensin II in rat mesangial cells was influenced by cell culture conditions and passage number. Furthermore, Peiser et al. (1993) reported that more micronuclei were always detected in cells of higher passages than of lower passages showing that metabolic and genetic characteristics of permanently growing cells differ remarkably depending on the culture passage. Unfortunately, we do not recall whether the cells used in our independent investigations were from a different batch and/or different cell passages. The different background levels of MN found in our different investigations may yet show that there are some differences in cell behaviour from one experiment to the other. In our previous investigation (Maes et al., 2016b) we obtained background MN yields of 5-9MN/1000 BN cells (Giemsa stain; experiment done in 2014-2015), whereas we now had background micronucleus frequencies of approximately 13-19MN/1000 BN cells in the first experiment (2016) and 20-29MN/1000 BN cells (2018) in the second experiment (FISH staining). Examples of micronucleated C3A cells are given in Figure 1.

An important finding of our previous investigation (Maes et al. 2016b) was also that low-level ELF-MF exposures resulted in micronucleus frequencies that were lower than in the unexposed control cells. Actually, this was also observed here. However, this was only substantial (and statistically significant according to the binomial test described by Kastenbaum and Bowman 1970) in our first experiment. Here the micronucleus frequency in cells exposed to 5 μT was 10MN/1000 BN cells compared to almost the double (19.2MN/1000 BN cells) in the controls. This may possibly indicate that low-level exposures to ELF-MF's, as environmental stimuli, can activate DNA repair mechanisms which then result in the repair of 'spontaneous' DNA damage which is not repaired in unexposed cells. This may be more or less comparable to the adaptive response which was already described in earlier investigations. Adaptive response is a phenomenon in which cells that were pre-exposed to extremely low and non-toxic doses of a toxic agent build-up a resistance to the damage induced by subsequent exposure to a

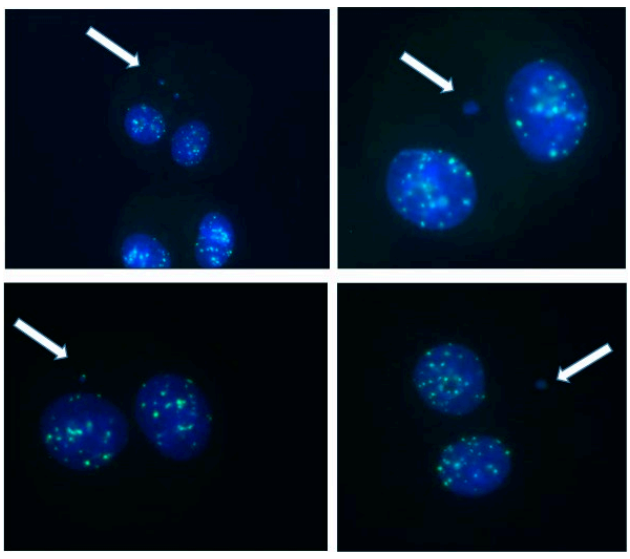

Fig. 1. Examples of binucleated C3A cells with micronuclei following FISH staining. Centromere positive cells are at the left.

higher and toxic dose of the same, similar (in action) or another toxic agent (Vijayalaxmi et al. 2014). There are indications that ELF-EMF's may also elicit such response and therefore may even have beneficial instead of detrimental properties, at least after short exposure times. Some previous research also proposed that low-frequency magnetic fields might play a positive role in cardiac tissue against ischemia reperfusion injury via regulating ROS production and NO/ONOO– balance (Ma et al. 2013).

Although the present study was not able to associate ELF-MF's with genotoxicity it is evident that there is no consensus reached yet on the alleged association between ELF-electromagnetic fields (and ELF-MF's in particular) and adverse health effects in humans. Yet, this remains an important issue, especially in view of the transition from nuclear and fossil to renewable energy sources for power production which leads to the necessity to optimize and expand the existing power grid and to construct several high voltage AC and DC power lines across the concerned countries (for the time being this is for example the case in Germany where nuclear power plants are all about to be dismantled).

ACKNOWLEDGEMENTS

The authors wish to thank Ms. Johanna Aernoudt and Ms. Toke Thiron of the Department of Basic Medical Sciences of Ghent University for their excellent practical assistance.

This paper was part of the research performed within the BBEMG (Belgian BioElectroMagnetics Group); cf. http://www.bbemg.be/.

REFERENCES

Baeyens A, Swanson R, Herd O, Ainsbury E, Mabhengu T, Willem P, Thierens H, Slabbert JP, Vral A. 2011. A semi-automated micronucleus-centromere assay to assess low-dose radiation exposure in human lymphocytes. Int J Radiat Biol. 87:923-931.

Bergqvist U, Brix J, de Gruijl F, de Seze R, Hietanen M, Jeffereys JGR, Lagroye I, Lotz GW, Owen RD, Repacholi MH, et al. 2003. Review of experimental investigations of EMF biological effects (0-100 kHz) – ICNIRP Standing committee II. In: Matthes R, McKinley A, J. Bernhardt, Vecchia P, Veyret B, editors. Exposure to static and low frequency electromagnetic fields, biological effects and health consequences, Oberschleißheim, Germany: ICNIRP13/2003, p. 121-398.

Cadossi R, Bersani F, Cossarizza A, Zucchini P, Emilia G, Torelli G, Franceschi C. 1992. Lymphocytes and low frequency electromagnetic fields. FASEB J. 6:2667-2674.

Cho YH, Chung HW. 2003. The effect of extremely low frequency electromagnetic fields (ELF-EMF) on the frequency of micronuclei and sister chromatid exchange in human lymphocytes induced by benzo(a)pyrene. Toxicol Lett. 143:37-44.

Cuppen JM, Wiegertjes GF, Lobee HWJ, Savelkoul HFJ, Elmusharaf MA, Beynen AC, Grooten HNA, Smink W. 2007. Immune stimulation in fish and chicken through weak low frequency electromagnetic fields. Environmentalist DOI 10.1007/s10669-007-9055-2.

Ding GR, Nakahara T, Miyakoshi J. 2003. Induction of kinetochore-positive and kinetochore-negative micronuclei in CHO cells by ELF magnetic fields and/or X-rays. Mutagenesis 18:439-443.

EHC (2007) Environmental health criteria 238: extremely low frequency fields. World Health Organization, Geneva. ISBN 978-92-4-157238-5.

Fenech M. 1998. Chromosomal damage rate, aging, and diet. Ann N Y Acad Sci. 854:23-36.

Fenech M, Bonassi S, Turner J, Lando C, Ceppi M, Chang WP, Holland N, Kirsch-Volders M, Zeiger E, Bigatti MP et al. 2003. HUman MicroNucleus project. Intra- and inter-laboratory variation in the scoring of micronuclei and nucleoplasmic bridges in binucleated human lymphocytes. Results of an international slide-scoring exercise by the HUMN project. Mutat Res. 534:45-64.

Foster KR, Skufca J. 2016. The problem of false discovery. IEEE Pulse, March/April, 37-40.

Gloy J, Greger R, Schollmeyer P, Huber M, Pavenstädt H. (1994) Influence of cell culture conditions and passage number on the response of membrane voltage to ATP and angiotensin II in rat mesangial cells. Ren Physiol Biochem. 17:62-72.

Heredia-Rojas JA, Beltcheva M, Rodríguez-De la Fuente AO, Heredia-Rodríguez O, Metcheva R, Rodríguez-Flores LE, Santoyo-Stephano MA, Castañeda-Garza E. 2017. Evidence of Genotoxicity Induced by 60 Hz Magnetic Fields on Mice Bone Marrow as Assessed by In Vivo Micronucleus Test. Acta Zool Bulg., Suppl. 8:69-75.

Heredia-Rojas JA, Gómez-Flores RA, De la Cruz-Torres E, Heredia-Rodríguez O, Campos-Góngora E, Cantú-Martínez PC, Rodríguez-Flores LE, Rodríguez de la Fuente AO. 2018. Genotoxicity by Electromagnetic Fields In: Larramendy ML, Soloneski S., Editors. Genotoxicity. A Predictable Risk to Our Actual World, London: IntechOpen, p. 81-94.

Jin H, Yoon HE, Lee JS, Kim JK, Myung SH, Lee YS. 2015. Effects on G2/M phase cell cycle distribution and aneuploidy formation of exposure to a 60 Hz electromagnetic field in combination with ionizing radiation or hydrogen peroxide in l132 nontumorigenic human lung epithelial cells. Korean J Physiol Pharmacol. 19:119-24.

Juutilainen J, Kumlin T, Naarala J. 2006. Do extremely low frequency magnetic fields enhance the effects of environmental carcinogens? A meta-analysis of experimental studies. Int J Radiat Biol. 82:1-12.

Kastenbaum MA, Bowman KO. 1970. Tables for determining the statistical significance of mutation frequencies. Mutat Res. 9:527-549.

Kesari KK, Juutilainen J, Luukkonen J, Naarala J. 2016. Induction of micronuclei and superoxide production in neuroblastoma and glioma cell lines exposed to weak 50 Hz magnetic fields. J R Soc Interface 13: 20150995.

Lai H, Singh NP. 1997. Acute exposure to a 60 Hz magnetic field increases DNA strand breaks in rat brain cells. Bioelectromagnetics 18:156-165.

Loberg LI, Luther MJ, Gauger JR, McCormick DL. 2000. 60 Hz magnetic fields do not enhance cell killing by genotoxic chemicals in Ataxia telangiectasia and normal lymphoblastoid cells. Radiat Res. 153:685-689.

Ma S, Zhang Z, Yi F, Wang Y, Zhang X, Li X, Yuan Y, Cao F. 2013. Protective effects of low-frequency magnetic fields on cardiomyocytes from ischemia reperfusion injury via ROS and NO/ONOO−. Oxid Med Cell Longev. 2013:529173.

Maes A, Collier M, Vandoninck S, Verschaeve L. 2000. Cytogenetic effects of 50 Hz magnetic fields of different magnetic flux densities. Bioelectromagnetics 21:589-596.

Maes A, Verschaeve L. 2012. Can cytogenetics explain the possible association between exposure to extreme low-frequency magnetic fields and Alzheimer's disease? J Appl Toxicol. 32:81-87.

Maes A, Anthonissen R., Verschaeve L. 2016a. On the alleged association between extremely low magnetic fields exposures and an increased risk of Alzheimer's disease. Radiat Applic. 1:151-154.

Maes A, Anthonissen R, Wambacq S, Simons K, Verschaeve L. 2016b. The cytome assay as a tool to investigate the possible association between exposure to extremely low frequency magnetic fields and an increased risk for Alzheimer's disease. J. Alzheimer's Disease 50:741-749.

Markkanen A. 2009. Effects of electromagnetic fields on cellular responses to agents causing oxidative stress and DNA damage. Kuopio University Publications C. Natural Environ Sci. 253: 59 p. ISBN 978-951-27-1191-8.

Mineur P. 2009. Etude des effets biologiques de facteurs physiques environnementaux [Study of the biological effects of environmental physical agents]. PhD thesis, University of Liège, Liège, Belgium. French.

M'kacher R, Maalouf EEL, Ricoul M, Heidingsfelder L, Laplagne E, Cuceu C, Hempel WM, Colicchio B, Dieterlen A, Laure Sabatier L. 2014. New tool for biological dosimetry: Reevaluation and automation of the gold standard method following telomere and centromere staining. Mut Res. 770:45–53

Moretti M, Villarini M, Simonucci S, Fatigoni C, Scassellati-Sforzolini G, Monarca S, Pasquini R, Angelucci M, Strappini M. 2005. Effects of co-exposure to extremely low frequency (ELF) magnetic fields and benzene or benzene metabolites determined in vitro by the alkaline comet assay. Toxicol Lett. 157:119-128.

Peiser C, Riebe-Imre M, Emura M, Mohr U. 1993. Influence of culture passages on growth kinetics, xenobiotic metabolism, chromosomal stability and transformation in a clonal fetal hamster lung epithelial cell line. Mutat Res. 289:281-90.

Ruiz-Gómez MJ, Martínez-Morillo M. 2009. Electromagnetic fields and the induction of DNA strand breaks. Electromagn Biol Med. 28:201-214.

Senarathna SM, Crowe A. 2015. The influence of passage number for Caco2 cell models when evaluating P-gp mediated drug transport. Pharmazie 70:798-803.

Singh N, Lai H. 1998. 60 Hz magnetic field exposure induces DNA crosslinks in rat brain cells. Mutat Res. 400:313-320.

Scarfí MR, Prisco F, Bersani F, Lioi MB, Zeni O, Di Pietro R, Franceschi C, Motta M, Iafusco D, Stoppoloni G. 1996. Spontaneous and mitomycin-C-induced micronuclei in lymphocytes from subjects affected by Turner's syndrome. Mutat Res. 357:183-190.

Scarfi MR, Prisco F, Lioi MB ,Zeni O, Della Noce M, Di Pietro R, Franceschi C, Iafusco D, Motta M, Bersani F. 1997a. Cytogenetic effects induced by extremely low frequency pulsed magnetic fields in lymphocytes from Turner's syndrome subjects Bioelectrochem Bioenerg 4: 221-226.

Scarfi MR, Prisco F, Lioi MB, Zeni O, Della Noce M, Di Pietro R, Franceschi C, Bersani F. 1997b. 50 Hz, 1 mT sinusoidal magnetic fields do not affect micronucleus frequency and cell proliferation in human lymphocytes from normal and Turner's syndrome subjects. Electro Magnetobiol. 16:301–307.

Serra SC, Costa JC, Assunção-Silva R, Teixeira FG, Silva N1, Anjo SI, Manadas B, Gimble J4, Behie LA, Sal-

gado A6. 2018. Influence of passage number on the impact of the secretome of adipose tissue stem cells on neural survival, neurodifferentiation and axonal growth. Biochimie 155:119-128.

Tofani S, Ferrara A, Anglesio L, Gilli G. 1995. Evidence for genotoxic effects of resonant ELF magnetic fields. Bioelectrochem. Bioenerg. 36: 9-13.

Udroiu I, Cristaldi M, Ieradi LA, Bedini A, Giuliani L, Tanzarella C. 2006. Clastogenicity and aneuploidy in newborn and adult mice exposed to 50 Hz magnetic fields. Int J Radiat Biol. 82:561-567.

Verheyen G, Pauwels G, Verschaeve L, Schoeters G. 2003. The effect of co-exposure of 50 Hz magnetic fields and an aneugen on human lymphocytes, determined by the cytokinesis-block micronucleus assay. Bioelectromagnetics 24:160-164.

Vijayalaxmi, Obe G. 2005. Controversial cytogenetic observations in mammalian somatic cells exposed to extremely low frequency electromagnetic radiation: a review and future research recommendations. Bioelectromagnetics 26:412–430.

Vijayalaxmi, Prihoda TJ. 2009. Genetic damage in mammalian somatic cells exposed to extremely low frequency electromagnetic fields: A meta-analysis of data from 87 publications (1990–2007). Int J Radiat Biol. 85:196–213.

Vijayalaxmi, Cao Y, Scarfi MR. 2014. Adaptive response in mammalian cells exposed to non-ionizing radiofrequency fields: A review and gaps in knowledge. Mutation Res. 760:36–45.

Vral A, Decorte V, Depuydt J, Wambersie A, Thierens H. 2016. A semi-automated FISH-based micronucleus-centromere assay for biomonitoring of hospital workers exposed to low doses of ionizing radiation. Mol Med Rep. 14:103-110.

Willems P, August L, Slabbert J, Romm H, Oestreicher U, Thierens H, Vral A. 2010. Automated micronucleus (MN) scoring for population triage in case of large scale radiation events. Int J Radiat Biol. 86:2-11.

Caryologia
International Journal of Cytology, Cytosystematics and Cytogenetics

Firenze University Press
www.fupress.com/caryologia

OPEN ACCESS

Citation: N. Anca Şuţan, I. Fierăscu, R. Fierăscu, D. Ionica, L.C. Soare (2019) Phytochemical analysis and *in vitro* assessment of *Polystichum setiferum* extracts for their cytotoxic and antimicrobial activities. *Caryologia* 72(2): 53-61. doi: 10.13128/cayologia-255

Published: December 5, 2019

Data Availability Statement: All relevant data are within the paper and its Supporting Information files.

Competing Interests: The Author(s) declare(s) no conflict of interest.

Phytochemical analysis and *in vitro* assessment of *Polystichum setiferum* extracts for their cytotoxic and antimicrobial activities

Nicoleta Anca Şuţan[1,*], Irina Fierăscu[2], Radu Fierăscu[2], Deliu Ionica[1], Liliana Cristina Soare[1]

[1] *University of Piteşti, Faculty of Sciences, Physical Education and Informatics, Department of Natural Sciences, 1 Targu din Vale Str., 110040 Pitesti, Romania*
[2] *The National Institute for Chemistry and Petrochemistry – ICECHIM, 202 Spl. Independentei, 060021, Bucharest, Romania*
*Corresponding author: ancasutan@yahoo.com

Abstract. Ferns are traditionally used by some nations to treat rheumatism, lungs, gynecology, blood and digestion dysfunctions, and several others illnesses. The present study evaluates the bioactivity of methanol and ethanol extracts from *Polystichum setiferum* (Forssk.) Moore ex Woyn. in an *Allium cepa* test and disk diffusion test. In the *Allium cepa* test the methanol and ethanol extracts induced a significant time-related increase in the mitotic index. The tested extracts were non-mutagenic by used assay, with no occurrence either the structural or numerical aberrations detected. The extracts were also evaluated in terms of trace elements (by EDXRF) and qualitative composition (by UV-VIS, FTIR and total phenolic content). In the disk diffusion test, methanol extracts from leaves determined a small inhibition of bacterial growth for *Enterobacter cloacae* and *Citrobacter freundii* strains relatively to control sample (methanol). The ethanol extracts were more efficient, the diameter of inhibition growth zones measured from 7 to 10 mm, the most affected strain was *Chryseobacterium meningosepticum*.

Keywords. *Polystichum*, extracts, FTIR, EDXRF, UV-VIS, cytogenotoxicity, antimicrobial activity.

INTRODUCTION

Appearance of antibiotic microbial resistance is present all over the world and is an increasingly serious threat to global public health. From the developing countries to the developed ones, bacterial antibiotic resistance problem it is very serious because cases of infection are treated by the lack of medicines or using them in excess (Mundy et al. 2016). Nosocomial infections usually represent an infrequent phenomenon. If it most developed countries this phenomenon is controlled, in many developing countries it is not reported (Serban et al. 2012).

In order to obtain alternative ways to combat bacteria that cause infections, herbal medicine represents one of the most important fields of tradi-

tional medicine all over the world, special attention has being paid to natural extracts with potential antimicrobial biological active compounds (Chanda et al. 2011; Jeyaseelan et al. 2012; Chanda et al. 2013; Fierascu et al. 2015).

The natural products have been considered as a source of potential medicines, specific for each region or country (Dubey and Padhy 2013; Panahi et al. 2014; Gyawali and Ibrahim 2014; Georgiev 2014; Schnekenburger et al. 2014; Atanasov et al. 2015).

In this context the study of ferns can be beneficial for this domain. Studies focused on some ferns used as crude extracts, standardized extracts, purified substances or in the form of nanoparticles showed pharmacological activity (Santos et al. 2010; Soare and Sutan 2018). The total flavonoid contents, antioxidant and anticancer activities, and acetylcholinesterase (AChE) inhibition potential of fern extracts were investigated in detail (Xia et al. 2014), but not the antimicrobial effect and cytotoxicity.

Some ferns species were traditionally used for scabies, eczema, jaundice including wounds and skin disease (Kirtikar and Basu 1999). *Polystichum* is one of the most diverse genera of ferns with 360–400 species distributed worldwide (Morero et al. 2015). *Polystichum setiferum* (Forssk.) Moore ex Woyn. is an evergreen or semi-evergreen fern native to southern and western Europe. Of the four species of *Polystichum* present in Romania, *Polystichum setiferum* (Forssk.) Moore ex Woyn. is the most common species (Sârbu et al. 2013). Totally, one hundred fern species have been described for their ethnomedicinal applications and chemical constituents in a fern ethnomedicinal plant database (Thakar et al. 2015). Rhizomes of *Polystichum setiferum* (Forssk.) Moore ex Woyn. tied around the neck of child are used to cure dysentery during the primary teeth development (Kumar et al. 2013), parts of *Polystichum pungens* (Kaulf.) C. Presl are used for the treatment of wounds (Grierson and Afolayan 1999), aerial parts of *Polystichum munitum* (Kaulf.) C. Presl are used to stimulate digestion (Lans et al. 2007), decoctions obtained from the rhizomes of *Polystichum pungens* (Kaulf.) C. Presl Roth are used to treat intestinal worms and as a general anthelminthic, powdered dried fronds to heal wounds, and fresh fronds as poultice (Lall and Kishore 2014), sporophyll extracts of *Polystichum squarrosum* (D. Don) Fee and *Polystichum moluscens* (Bl.) T. Moore are used as antibacterial agent (Singh 1999), decoction obtained from fronds of *Polystichum woronowii* Fomin is used as antiinflamatory and anti-hepatitis agent and decoction obtained from leaf of *Polystichum aculeatum* (L.) Schott as anthelminthic (Bahadori et al. 2015).

The present study aims to comparative analyse the chemical composition of the methanol and ethanol extracts of *Polystichum setiferum* (Forssk.) Moore ex Woyn., their antimicrobial effects on five bacterial strains: *Escherichia coli* (ATCC 25922), *Staphylococcus aureus* (ATCC 25923), *Enterobacter cloacae* and *Citrobacter freundii* (both clinical strains) and *Elizabethkingia meningoseptica* (formerly *Chryseobacterium meningosepticum*, strain isolated from soil) and their cytotoxic effects on meritematic root cells of *Allium cepa* L. assay.

MATERIALS AND METHODS

Preparation of plant extracts

Leaves and rhizomes of *Polystichum setiferum* (Forssk.) Moore ex Woyn. were collected from Vîlsan Valley, Argeş County, Romania from site N 45º25'40.2", E 024º42'33.1", altitude 1062 m. Part of the plant material is preserved (-18 ºC) in Botanic Laboratory of the Department of Natural Sciences, University of Pitesti for future references. The voucher specimen is register at the Botanical Collection of County Museum Argeş with number 11326/25.05.2016. The leaves and rhizomes with scales were washed thoroughly and rinsed with bidistilled water and preserved at -18 ºC. Frozen leaves and rhizomes were chopped at room temperature. Leaves and rhizomes ethanol and methanol extracts (PEL - leaves ethanol extract, PER - rhizomes ethanol extract, PML - leaves methanol extract, PMR - rhizomes methanol extract) were prepared by mixing 100 g of each type of vegetable material in 1000 ml alcohol for 48 h at room temperature (22°C). The obtained extracts were filtered using Whatman filter paper no. 1.

The dried weight was obtained by shade drying to constant mass the plant materials, in order to remove excess moisture. The average dried masses for 15 samples were 29.01%±2.80 for rhizomes and, respectively, 32.25%±2.66 for leaves.

Evaluation of chemical composition of leaf and rhizome extracts

For Fourier transform infrared spectroscopy (FTIR), was used a Varian 3100 Excalibur spectrometer equipped with a Harrick Praying Mantis diffuse reflectance (DRIFT) accessory. The IR spectrum was collected in the region 4000–500 cm-1 at a resolution of 2 cm-1. The spectrum was analysed with the program Analyzer IR – KnowItAll (Bio-Rad 2005).

For UV-Vis evaluation was used an UV - VIS Unicam Helios α Thermo Orion spectrometer from 200 to 900 nm, at the resolution of 1 nm, with 1 nm slit width and automatic scan rate. The obtained results were processed using specific data analysis software (Origin Pro 8.0).

For energy dispersive X-ray fluorescence determinations was used a PW4025 – MiniPal – PANalytical energy dispersive XRF Spectrometer with rhodium anode. The XRF determinations have been carried out in Helium atmosphere, for a period of 300 seconds, without any filter, at proper voltage and current intensity.

Determination of total phenolic contents

The concentration of total phenolic was measured by colorimetric method with Folin- Ciocalteu reagent (Merck KGaA Germany), according with a method previously presented (Fierascu et al. 2015). The method involves the reduction of Folin-Ciocalteu reagent by phenolic compounds, with formation of a blue complex; the absorbance was read at 765 nm on the UV-VIS spectrophotometer. The measurements were compared to a standard curve prepared with gallic acid (99%, Merck KGaA Germany) solutions at different concentrations (10-55 µg/mL). The total phenolic content was expressed as milligrams of gallic acid equivalents per 100 gram of dried weight. The dried weight was obtained by shade drying to constant mass the plant materials, in order to remove excess moisture.

Antioxidant activity

Antioxidant activity of the extracts was determined following the DPPH assay, following a protocol previously exhaustively described (Fierascu et al. 2015, Fierascu et al. 2014). The absorbance was read at 517 nm after an incubation period of 30 minutes. The antioxidant activity (AA %) percentage was calculated using the formula:

$$AA\ (\%) = [(A_{control}\text{-}A_{sample})/A\_control]\times 100,$$

where: $A_{control}$ is the absorbance of the DPPH solution without sample, A_{sample} is the absorbance of the extract mixed with 0.02 mg/mL DPPH solution.

Evaluation of antimicrobial properties

Antibacterial effects of fern methanolic and ethanolic extracts were tested by disk diffusion method on five bacterial strains: *Escherichia coli* (ATCC 25922), *Staphylococcus aureus* (ATCC 25923), *Enterobacter cloacae* and *Citrobacter freundii* (both clinical strains) and *Elizabethkingia meningoseptica* (formerly *Chryseobacterium meningosepticum*, strain isolated from soil). Frequency and rank of isolated bacteria, identified and tested by antibiogram in microbiology laboratories within major hospitals in Bucharest present these strains in the top of the isolated germs that produce nosocomial infections (Serban et al. 2012).

As positive control was used antibiotic (Ampicillin 10µg per disc from Bioanalyse), while the negative control was the solvent specific for each extract (ethanol 96% and methanol 99.8%).

An overnight (16 to 24 h) culture at 37°C of each bacterial strain was used (bacterial suspension was prepared by suspending one wire loop from the stock into 2 mL nutrient broth).

In disk diffusion method sterile filter paper discs with 6 mm diameter were used. For diffusion method was used nutrient agar in Petri dishes. Each bacterial culture was homogeneous inoculated (in three directions) on the entire surface of nutrient agar in Petri dishes.

The disc with Ampicillin (pre-warmed to room temperature) was placed on the surface of inoculated solid medium. Four discs of sterilized filter paper were put on the nutrient agar; 5µL of each fern extract were used to impregnate the discs using micropipette. For negative control, two sterile discs of paper filter were used (5µL ethanol, respectively 5µL methanol). The Petri dishes were incubated inverted for 24 h at 37°C.

The antibacterial effects of fern extracts were estimated by measuring the diameter of inhibition growth zone (in millimeters), as a clear zones surrounding paper filter discs. The experiment was repeated three times and the results were in terms of average of measured values.

Evaluation of cytotoxic activity of leaf and rhizome extracts

Cytotoxic potential of leaf and rhizome extracts was evaluated by changes in mitotic index (MI) and phase indexes (prophase, metaphase, anaphase, telophase), induced in root tips cells of *Allium cepa* L. (Sutan et al. 2016). Equal-sized onion bulbs, from a local variety, were purchased from local market. The outer scales were carefully removed and the bottoms were scraped to expose root primordia. Rhizogenesis and root growth were induced on 30 ml jars filled with distilled water until to 0.5-1cm average length of the roots. After 48 hours, freshly emerged roots were treated with leaf and rhizome extracts for 6, 12 and 24 hours. Distilled water, ethanol and metha-

nol were used as controls. Cytological analysis were performed on squash slides prepared as follow: the root were fixed in a mixture of ethanol + glacial acetic acid (3:1) for 12 hours at 4°C, than were transferred to a watch glass in preheated 1N HCl at 60°C for 14 minutes and subsequently were immersed in preheated aceto-orcein solution at 60°C for 14 minutes. The tips of the roots were cut on a glass slide in a drop of 45% acetic acid, covered with coverglass, and squashed by tapping with matchstick. About 3000 cells from 9 root tips were scored for each treatment. The cells at different stages of mitosis were noticed.

Mitotic index (MI) was computed by determining the mitotic cell frequency (prophase, metaphase, anaphase and telophase) by the total number of cells observed and multiplying the result by 100 (Tedesco and Laughinghouse IV 2012). The number of cells at various mitosis stages (prophase, metaphase, anaphase, telophase) was calculated as percentage to number of dividing cells. Results are presented as the Mean ± standard error of more independent experiments. The data was analysed for statistical significance using analysis of variance (one way ANOVA) and Tukey test was used to determine significant differences among means. Significant differences were set at P≤0.05.

RESULTS

Phytochemical analysis

The mineral content of the extracts was evaluated using a non-destructive technique, X-ray fluorescence. The extracts contain traces (in the ppm concentration range) of Mg, P, Ca, Cr, Mn, Fe, Ni and Cu. Also, PML contains minor traces of K and the ethanol extracts contains traces of Co, not observed for the methanol extracts (Fig. 1A).

The FTIR spectra presented in Fig. 1B showed that the plant have compounds such as aldehyde, ketone, alcohol, carboxylic acid, amides, ethers and phenolic compounds. The peaks in FTIR spectra in Figure 1B are attributed to the following type of compounds, as previously reported (Sutan et al., 2016): hydroxy compounds (OH stretching) – 3649 cm^{-1}, carboxylic acid (OH stretching – 2982 cm^{-1}, 1406 cm^{-1}), carbonyl compounds (C-H stretching – 2901 cm^{-1}, C=O stretching – 1668 cm^{-1}), water (2133 cm^{-1}), allenes (C=C=C bond -1923 cm^{-1}), aromatic ring (1454 cm^{-1}), alcohol (1323 cm^{-1}, 1260 cm^{-1}), aromatic hydrocarbons (880 cm^{-1}) and mineral components (539 cm^{-1}). The peaks at 1067 cm^{-1} and 1040 cm^{1} are attributed to characteristic functional groups of polyflavonoids and, respectively, –C-O- groups of the polyols such as flavones and terpenoids.

UV-VIS spectrum (Fig. 2) of the leaves extract (PML and PEL) seems to be a complex mixture of pigments: chlorophyll *a* – around 415 nm and 660-670 nm; chlorophyll *b* – 450 and 640 nm, and in less extent, carotenoids, while the rhizomes extracts (PMR and PER) contains traces of chlorophyll *a* and minor traces of chlorophyll *b.*

The total phenolic content and antioxidant activity of the extracts (Table 1) shows a direct correlation between the phenolic content and the antioxidant potential.

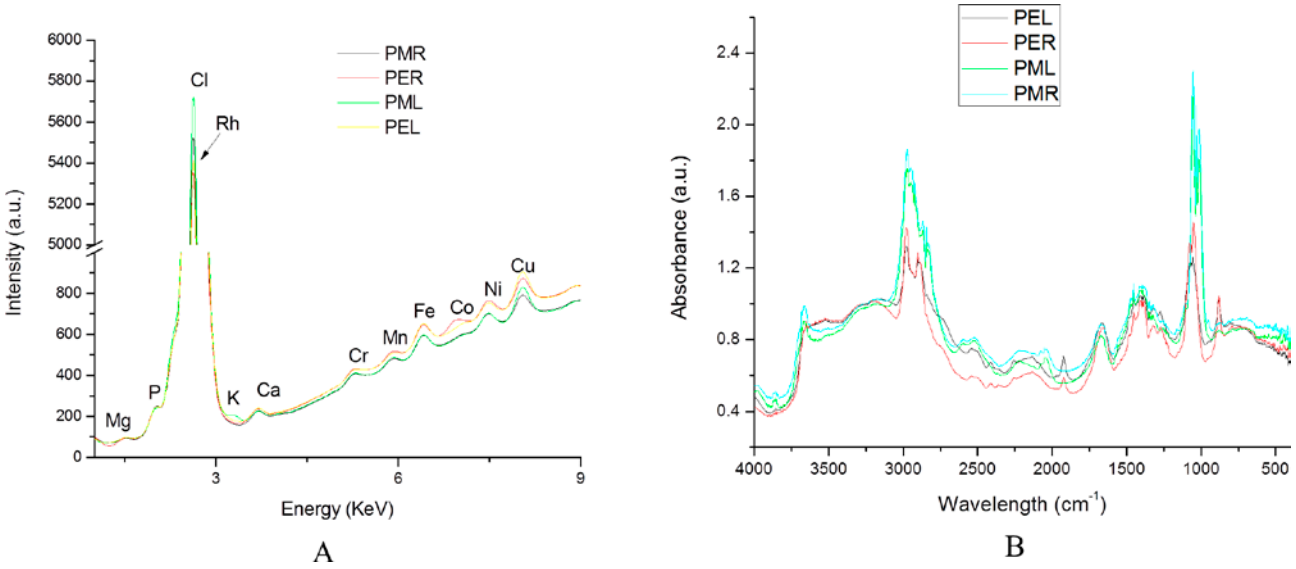

Fig. 1. EDXRF spectra (A) and FTIR spectra (B) of the ethanol and methanol extracts of *Polystichum setiferum* (Forssk.) Moore ex Woyn.

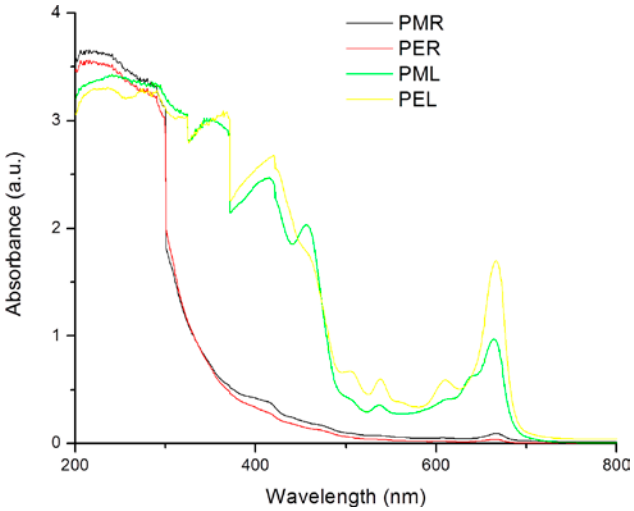

Fig. 2. UV-Vis spectra of the ethanol and methanol extracts of *Polystichum setiferum* (Forssk.) Moore ex Woyn.

Table 1. Total phenolic content and antioxidant activity of the ethanol and methanol extracts of *Polystichum setiferum* (Forssk.) Moore ex Woyn.

Extract	Total phenolic content (mg GAE/100 g dry mass)	Antioxidant activity (%)
PMR	187.25±0.78	95.58±0.95
PML	44.64±0.16	74.32±0.62
PER	161.24±0.65	92.55±0.68
PEL	23.57±0.12	90.38±0.55

Antimicrobial activity

Antimicrobial activity of fern extracts is illustrated in Table 2. Statistical analysis of experimental data shows that the highest value for inhibition zone (9.5±0.28 mm) was determined for PEL against *Elizabethkingia meningoseptica*. Except *Citrobacter freundii,* the microorganisms being tested displayed significant differences of ≤2 mm between inhibition zone induced by PEL and corresponding concentration of ethanol. In comparison, the smallest inhibition zone was noted for the methanol extracts, irrespective of the part of the plant material used in extraction or the type of microorganisms tested.

Mitotic index variation

The effect of *Polystichum setiferum* (Forssk.) Moore ex Woyn. extracts is relevant, but there is not data about their effect on MI, so the MI of root tips cells to leaves and rhizome extracts was evaluated (Fig. 3). The highest frequency of cells undergoing mitosis was noted in control samples. The MI in meristematic root cells of *Allium cepa* L. treated with *Polystichum setiferum* (Forssk.) Moore ex Woyn. methanol and ethanol extracts of leaves follow similar trends: decreased at the minimum of 6h treatment and rise progressively with increasing of time exposure to 12 and 24h. The MI values ascertained for PEL were slightly lower, when comparing with PML, that may be the consequence of higher concentration of metals in ethanol extracts, as EDXRF analysis demonstrates.

Table 2. Antimicrobial activity of the extracts of leaves and rhizomes of *Polystichum setiferum* (Forssk.) Moore ex Woyn. (inhibition zone – in mm).

Extracts/ Control	Tested microorganisms				
	Escherichia coli ATCC 25922	*Staphylococcus aureus* ATCC 25923	*Enterobacter cloacae*	*Citrobacter freundii*	*Elizabethkingia meningoseptica*
	IZ	IZ	IZ	IZ	IZ
PMR	7.00±0.28 fghi	R	6.16±0.16 hi	6.16±0.16 hi	R
PML	7.00±0.00 fghi	R	6.5±0.18 hi	6.83±0.16 ghi	R
PER	8.00±0.00 f	R	7.33±0.33 fgh	9.16±0.16 e	6.66±0.33 ghi
PEL	9.33±0.33 e	8.00±0.00 f	7.66±0.33 fg	7.33±0.33 fgh	9.5±0.28 e
Ampicillin	14±0.00 d	25.66±0.33 c	30.33±0.33 a	9.33±0.33 e	29±1.00 b
Ethanol	7.33±0.33 fgh	6.16±0.16 hi	6.66±0.33 hi	7.66±0.33 fg	7.33±0.88 fgh
Methanol	7.00±0.57 fghi	6±0.00 i	6.66±0.57 hi	6.33±0.57 hi	6.33±0.57 hi

*Means with the same letter are not significantly different from each other (Tukey test, P>0.05)
* R – resistant

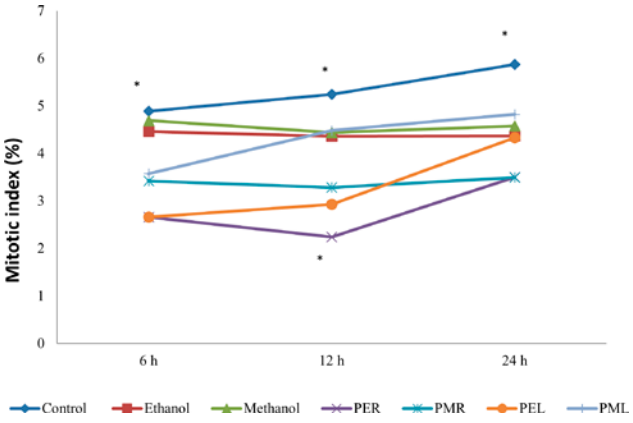

Fig. 3. The influence of the extracts of leaves and rhizomes of *Polystichum setiferum* (Forssk.) Moore ex Woyn. on the mitotic index in meristematic root cells of *Allium cepa* L. (*the interpretation of the significance of the differences by means of the Tukey test, p<0.05).

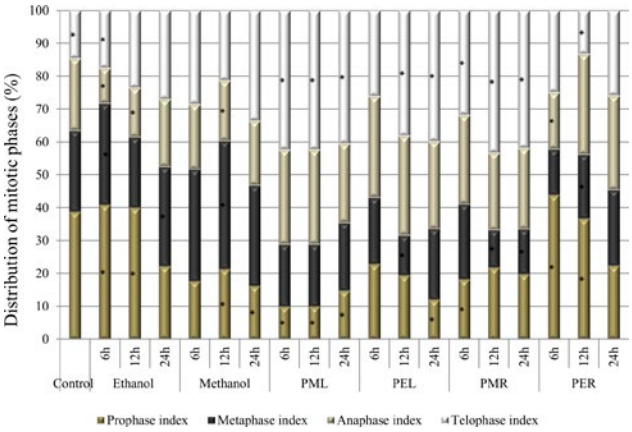

Fig. 4. The influence of the alcoholic extract of the rhizome and leaves of *Polystichum setiferum* (Forssk.) Moore ex Woyn. on the distribution of the mitotic phases in the meristematic root cells of *Allium cepa* L. (*interpretation of the significance of the differences, by means of the Tukey test, p<0.05).

Distribution of mitotic phases

Ethanol and methanol extracts affected the percentage of mitotic phases for all tested times (Fig. 4). We showed here that treatments with methanol extracts of leaves and rizomes of *Polystichum setiferum* (Forssk.) Moore ex Woyn., except PML-24h, had caused mitotic arrest in meristematic root cells of *Allium cepa* L., accumulating telophase cells. Prophase cells frequency decreased significantly in these experimental conditions. In contrast, the frequency of telophase cells decreased in root tips treated with ethanol extracts, except PEL-12h and PEL-24h.

DISCUSSION

As a general remark, the ethanol seems to extract with higher efficiency the metals from the samples, as all the metals are in higher concentration in the ethanol extracts, while P has the same concentration in all the samples. It can be observed that the methanol extracts have higher intensity of the absorbance bands, which can be correlated with the results obtained for the total phenolic content and with the UV-VIS analysis.

It can be noticed that all extracts presents strong absorption bands corresponding to phenolic acids (more intense for the rhizomes extracts). Also, even if the methanol seems to be a more efficient solvent for the extraction of the phenolic compounds, the ethanol seems to be more efficient for the extraction of pigments.

Antioxidant activity has been noticed for other species of *Polystichum* genera, such as *Polystichum lepidocaulon* (Hooker) J. Smith, *Polystichum polyblepharum* (Roem ex. Kunze) C. Presl (Shin 2010) and *Polystichum semifertile* (C.B. Clarke) Ching (Ding et al. 2008). According to Shin (2010) the crude extracts obtained from some ferns, such as those of the genera *Davallia*, *Hypolepis*, *Pteridium*, *Cyrtomium*, *Dryopteris*, *Polystichum*, *Dicranopteris*, *Lycopodium*, *Osmunda*, *Adiantum*, *Coniogramme*, *Polypodium*, *Pyrrosia*, *Pteris*, *Lygodium*, *Selaginella*, *Thelypteris*, *Athyrium*, *Matteuccia*, *Onoclea* şi *Woodsia* have strong antioxidant properties, sometimes substantially more effective than other natural or synthetic antioxidants.

Statistical analysis of experimental data indicates that PEL had a significant antimicrobial activity against gram negative bacteria, *Escherichia coli* and *Elizabethkingia meningoseptica;* furthermore, PEL was solely responsible for any antimicrobial activity noticed against *Staphylococcus aureus*, as comparing with PER, PML and PMR. Aerobic *Gram*-negative bacilli *Citrobacter freundii* showed statistic significant sensitivity to PER.

The antimicrobial assay shows no correlation between the phenolic content and the antimicrobial potential. Thus, the antimicrobial effect observed might be assigned to the other type of compounds identified by FTIR, as well as to the metals identified by X-ray fluorescence in higher concentration in the ethanol extracts. Recent studies indicate that different metals cause various types of injuries to microbial cells as a result of generation of reactive oxygen species (ROS), membrane damage, interruption of electron transport, protein dysfunction or DNA damage and inhibition of DNA replication (Lemire et al. 2013; Dizaj et al. 2014).

Antibacterial properties of extracts obtained from leaves of a various fern species, such as *Asplenium nidus*,

Blechnum orientale, C*ibotium barometz*, *Dicranopteris linearis* var. *linearis*, against Gram positive bacteria (e.g. *Bacillus cereus*, *Micrococcus luteus*, *Staphylococcus aureus*, as well as Gram negative bacteria (e.g. *Escherichia coli*, *Pseudomonas aeruginosa*, *Salmonella enterica* (formely *Salmonella choleraesuis*), *Enterobacter aerogenes*, *Klebsiella pneumoniae*) have been noticed by Lai et al. (2009). These results justify and certify the use of these species in traditional medicine.

The *Allium* root tip biossay was widely applied as bioindicator of pesticides, fertilizers and heavy metals cytogenotoxic effects, but is especially relevant for evaluation of the bioactivity of plant extracts (Bonciu et al., 2018).

Taking a comparative approach to the cytogenetic effects of extracts of leaves and rhizome, respectivelly, methanol and ethanol extracts of rhizome have had a stronger mitodepressive effect over the meristematic root cells. The decrease of MI in the root tips of *A. cepa* L. has already been highlighted as indicator of the antiproliferative activity of different extracts, such as Frescura et al. (2012) evaluating the *Luehea divaricata* extracts, Kuhn et al. (2015) who studied the leaves and fruits of *Eugenia uniflora* infusions, Sutan et al (2018) assessing the *Aconitum toxicum* Reichenb. rhizome extracts. The MI of samples that has been treated with PER for 12h was significantly lower than in the control.

The higher values of MI determined in the root meristems treated with methanol extracts may be directed related to the higher content of phenolic acids (fig. 1B). Due to their redox properties, which allow them to act as reducing agents or hydrogen-atom donors (Amarowicz et al. 2010), phenolic compounds exert protective effect against damaged mediated by ROS.

As the oxidative stress exerts its effect on the cell cycle shortly after the stress was imposed (Reichheld et al. 1999, cited by West et al. 2014), this variation may be the consequence of stress adaptation that prevents cell death or constitute a radical route to cell death. Results presented by West et al. (2014) regarding the response of primary root of *Arabidopsis* to salt stress suggested that plants have a general mechanism that rapidly blocks cell cycle progression under stress conditions, presumably to impede transition to a stage where the cells are susceptible to damage (e.g. M-phase), simultaneously the cellular defence system being activated. Stress-adapted cells undergo cell cycle stages at default rates.

The root tips incubated in alcoholic extracts of leaves and rhizome have revealed these variations of MI values, without showing any chromosome breaking action.

Comparing to ethanol and methanol effects on mitosis in onion root tips, mitotic inhibition induced by extracts of leaves and rhizomes of *Polystichum setiferum* (Forssk.) Moore ex Woyn. was more intense. Decreasing and significant decreasing of mitotic index in root meristems of *Allium cepa* L. suggest the mitodepressive potential of alcoholic extracts of *Polystichum setiferum* (Forssk.) Moore ex Woyn., although mitotic delay induced by low concentration of ethylic alcohol were previously noticed by Ancara and Nuti Ronchi (1967).

Increased frequency of telophase cells may be the consequence of high activity of Cdk/mitotic cyclin complex which inhibits the pathway that promotes exit from mitosis. Mitosis progress requires the ubiquitination of proteins whose proteolysis is necessary for chromatid separation and pre-replication complexes assembles, so that the cell is ready to begin DNA replication at the next S phase. When ubiquitination of proteins is inhibited, telophase arrest is induced (Searle and Sanchez 2007).

ROS interference with nuclear envelope dynamics was evidenced by the delayed breakdown of the nuclear envelope at late prophase and its delayed reconstitution at telophase (Livanos et al. 2012), which lead to delayed cell exit from telophase. This delay may be due to experimental disturbance of ROS homeostasis, thus affecting microtubule dynamics and organization (Livanos et al. 2012). It has also been suggested that arrested telophase cells perish by apoptosis (Swe and Sit 1997). Mitotic and chromosomal abnormalities were detected at insignificant levels comparing with controls.

CONCLUSION

The chemical analyses conducted showed a direct correlation between the solvent used for extraction and the total phenolic content. The rhizomes extracts showed a good antioxidant potential, also in good correlation with the total phenolic content.

The antibacterial effect of ethanol extract was stronger against bacteria from soil than clinical bacterial strains. Methanol extracts of fern demonstrated some effects on tested bacterial strains, just clinical ones were slight inhibited by these extracts.

Mitoinhibitory effect of leaves and rhizome extracts of *Polystichum setiferum* (Forssk.) Moore ex Woyn. without cytotoxic and clastogenic effects suggest its antimitotic drugs potential. Although this is an important advance in our understanding of extracts effects further researches must be done. Questions like what concentration of extract for what time of treatment repetition should be used for an excellent cellular response, in order to increase the apoptotic index and induce the cell death remained unanswered.

FUNDING

This work was supported by a grant of the Romanian Ministery of Research and Innovation, CCCDI-UEFISCDI, project number PN-III-P1-1.2-PCCDI-2017-0332/Project 3, contract 6PCCDI/2018, within PNCDI III.

REFERENCES

Amarowicz R, Pegg RB, Rahimi-Moghaddam P, Barl B, Weil JA. 2010. Free radical scavenging capacity and antioxidant activity of selected plant species from the Canadian prairies. Food Chem. 84: 551–562.

Ancara PG, Nuti Ronchi V. 1967. Effect of ethylic alcohol on the mitotic cycle of *Allium cepa* root meristems. Caryologia. 20(3): 229-232.

Atanasov AG, Waltenberger B, Pferschy-Wenzig E-M, Linder T, Wawrosch C, Uhrin P, Temml V, Wang L, Schwaiger S, Heiss EH, Rollinger JM, Schuster D, Breuss JM, Bochkov V, Mihovilovic MD, Kopp B, Bauer R, Dirsch VM, Stuppner H. 2015. Discovery and resupply of pharmacologically active plant-derived natural products: A review. Biotechnol Adv. 33(8): 1582-1614.

Bahadori MB, Mahmoudi KF, Ali Ahmadi A, Bahadori Sh, Valizadeh H. 2015. Antibacterial evaluation and preliminary phytochemical screening of selected ferns from Iran. Research Journal of Pharmacognosy. 2(2): 53-59.

Bonciu E, Firbas P, Fontanetti CS, Wusheng J, Karaismailoğlu MC, Liu D, Menicucci F, Pesnya DS, Popescu A, Romanovsky AV, Schiff S, Ślusarczyk J, de Souza CP, Srivastava A, Sutan A, Papini A. 2018. An evaluation for the standardization of the *Allium cepa* test as cytotoxicity and genotoxicity assay. Caryologia. 71(3): 191-209.

Chanda S, Rakholiya K, Nair R. 2011. Antimicrobial activity of *Terminalia catappa* L. leaf extracts against some clinically important pathogenic microbial strains. Chinese Med. 2: 171-177.

Chanda S, Rakholiya K, Parekh J. 2013. Indian medicinal herb: Antimicrobial efficacy of *Mesua ferrea* L. seed extracted in different solvents against infection causing pathogenic strains. J Acute Dis. 2(4): 277-281.

Chisembu KC. 2015. Plants and other natural products used in the management of oral infections and improvement of oral health. Acta Tropica. 154: 6-18.

Ding ZT, Fang YS, Tai ZG, Yang MH, Xu YQ, Li F, Cao QE. 2008. Phenolic content and radical scavenging capacity of 31 species of ferns. Fitoterapia. 79: 581-583.

Dizaj SM, Lotfipour F, Barzegar-Jalali M, Zarrintan MH, Adibkia K. 2014. Antimicrobial activity of the metals and metal oxide nanoparticles. Mat Sci Eng C. 44(1): 278–284.

Dubey D, Padhy RN. 2013. Antibacterial activity of *Lantana camara* L. against multidrug resistant pathogens from ICU patients of a teaching hospital. J Herb Med. 3(2): 65-75.

Fierascu I, Bunghez IR, Fierascu RC, Ion RM, Dinu-Pirvu CE, Nuta D. 2014. Characterization and antioxidant activity of phytosynthesised silver nanoparticles using *Calendula officinalis* extract. Farmacia. 62(1): 129-136.

Fierascu I, Ungureanu C, Avramescu SM, Fierascu RC, Ortan A, Soare LC, Paunescu A. 2015. *In vitro* antioxidant and antifungal properties of *Achillea millefolium* L. Rom Biotech Lett. 20(4): 10626-10636.

Frescura VDS, Laughinghouse IV HD, Tedesco SB. 2012. Antiproliferative effect of the tree and medicinal species *Luechea divaricate* on the *Allium cepa* cell cycle. Caryologia. 65(1): 27-33.

Georgiev MI. 2014. From plants to pharmacy shelf. Biotechnol Adv. 32(6): 1051–1052.

Grierson DS, Afolayan AJ. 1999. Antibacterial activity of some indigenous plants used for the treatment of wounds in the Eastern Cape, South Africa. J Ethnopharmacol. 66(1): 103-106.

Gyawali R, Ibrahim SA. 2014. Natural products as antimicrobial agents. Food Control. 46: 412-429.

Jeyaseelan EC, Jenothiny S, Pathmanathan MK, Jeyadevan JP. 2012. Antibacterial activity of sequentially extracted organic solvent extracts of fruits, flowers and leaves of *Lawsonia inermis* L. from Jaffna. Asian Pac J Trop Biomed. 2: 798-802.

Kirtikar KR, Basu BD. 1999. Indian medicinal plants, Vol 4, Dehradun: National Book Distributions, pp. 2748-2749.

Kuhn AW, Tedesco M, Laughinghouse IV HD, Flores FC, da Silva CB, do Canto-Dorow TS, Tedesco SB. 2015. Mutagenic and antimutagenic effects of *Eugenia uniflora* L. by the *Allium cepa* L. test. Caryologia. 68(1): 25-30.

Kumar S, Chand G, Sankhyan P. 2013. Herbal folk remedies for curing various ailments in Lug Valley of District Kullu, Himachal Pradesh (N.W. Himalaya). Int J Ayu Herb Med. 3(5): 1308-1314.

Lai HY, Lim YY, Tan SP. 2009. Antioxidative, tyrosinase inhibiting and antibacterial activities of leaf extract from medicinal ferns. Biosci Biotechnol Biochem. 73(6): 1362-1366.

Lall N, Kishore N. 2014. Are plants used for skin care in South Africa fully explored? J Ethnopharmacol. 153: 61-84.

Lans C, Turner N, Khan T, Brauer G, Boepple W, 2007. Ethnoveterinary medicines used for ruminants in British Columbia, Canada. J Ethnobiol Ethnomed. 3: 11.

Lemire JA, Harrison JJ, Turner RJ. 2013. Antimicrobial activity of metals: mechanisms, molecular targets and applications. Nat Rev Microbiol. 11: 371–384.

Livanos P, Galatis B, Quader H, Apostolakos P. 2012. Disturbance of reactive oxygen species homeostasis induced atypical tubulin polymer formation and affects mitosis in root-tip cels of *Triticum turgidum* and *Arabidopsis thaliana*. Cytoskeleton (Hoboken). 69: 1-21.

Morero RE, Chiarini FE, Urdampilleta J, Barboza GE, Barrington DS. 2015. Cytological study of *Polystichum* (Dryopteridaceae) species from southern South America. Austral J Bot. 63(5): 403-414.

Mundy L, Pendry B, Rahman M. 2016. Antimicrobial resistance and synergy in herbal medicine. J Herb Med. 6: 53-58.

Panahi Y, Akhavan A, Sahebkar A, Hosseini SM, Taghizadeh M, Akbari H, Sharif MR, Imani S. 2014. Investigation of the effectiveness of *Syzygium aromaticum*, *Lavandula angustifolia* and *Geranium robertianum* essential oils in the treatment of acute external otitis: A comparative trial with ciprofloxacin. J Microbiol Immunol Infect. 47(3): 211-216.

Reichheld JP, Vernoux T, Lardon F, Van Montagu M, Inzé D. 1999. Specific checkpoints regulate plant cell cycle progression in response to oxidative stress. Plant J. 17: 647–656.

Santos MG, Kelecom A, Paiva SR, Moraes MG, Rocha L, Garrett R. 2010. Phytochemical studies in Pteridophytes growing in Brazil: a review. Am J Plant Sci Biotechnol. 4(Special Issue 1): 113–125.

Sârbu I, Ştefan N, Oprea A. 2013. *Plante vasculare din România. Determinator ilustrat de teren*. Editura VictorBVictor, Bucuresti (In Romanian).

Shin SL. 2010. Functional components and biological activities of Pteridophytes as healthy biomaterials. Ph.D. Dissertation, Chungbuk National University, Cheongju, Korea.

Schnekenburger M, Dicato M, Diederich M. 2014. Plant-derived epigenetic modulators for cancer treatment and prevention. Biotechnol Adv. 32(6): 1123–1132.

Searle JS, Sanchez Y. 2007. The many layers of cell cycle regulation. In: Nitiss JL, Heitman J, editors. *Yeast as a tool in cancer research*. Springer Netherlands, pp. 42-46.

Serban C, Mitrea N, Ordeanu V. 2012. Research on bacterial resistance to antibiotics, in suspicion of nosocomial infections, in major hospitals in Bucharest, Farmacia. 60(3): 350-357.

Singh HB. 1999. Potential medicinal pteridophytes of India and their chemical constituents. J Econ Tax Bot. 23(1): 63-78.

Soare LC, Sutan NA. 2018. Current Trends in Pteridophyte Extracts: From Plant to Nanoparticles. In: Fernández H, editor. *Current advances in fern research*. Springer International Publishing AG, part of Springer Nature, Switzerland, pp. 329-357.

Sutan NA, Fierascu I, Fierascu RC, Manolescu DS, Soare LC. 2016. Comparative analytical characterization and *in vitro* cytogenotoxic activity evaluation of *Asplenium scolopendrium* L. leaves and rhizome extracts prior to and after Ag nanoparticles phytosynthesis. Ind Crops Prod. 83: 379-386.

Sutan NA, Manolescu DS, Fierascu I, Neblea AM, Sutan C, Ducu C, Soare LC, Negrea D, Avramescu SM, Fierascu RC. 2018. Phytosynthesis of gold and silver nanoparticles enhance *in vitro* antioxidant and mitostimulatory activity of *Aconitum toxicum* Reichenb. rhizomes alcoholic extracts. Mater Sci Eng C. 93: 746-758.

Swe M, Sit KH. 1997. Staurosporine induces telophase arrest and apoptosis blocking mitosis exit in human Chang liver cells. Biochem Biophys Res Commun. 236(3): 594-598.

Tedesco SB, Laughinghouse IV HD. 2012. Bioindicator of genotoxicity: the *Allium cepa* test. In: Srivastava JK, editor. *Environmental Contamination*. In: Tech Publisher, Rijeka. p. 137–156.

Thakar SB, Ghorpade PN, Kale MV, Sonawane KD. 2015. Fern ethnomedicinal plant database: Exploring fern ethnomedicinal plants knowledge for computational drug discovery. Curr Comput Aided Drug Des. 11(3): 266-271.

West G, Inzé D, Beemster GTS. 2004. Cell cycle modulation in the response of the primary root of *Arabidopsis* to salt stress. Plant Physiol. 135: 1050-1058.

Xia X, Cao JG, Dai XL, Wang QX, Xiao JB. 2014. Flavonoids contents and bioactivities of 19 species of ferns from China. Ind Crops Prod. 58: 91–98.

Caryologia
International Journal of Cytology, Cytosystematics and Cytogenetics

Firenze University Press
www.fupress.com/caryologia

Citation: A.-M. Dutrillaux, B. Dutrillaux (2019) Telomeric heterochromatin and meiotic recombination in three species of Coleoptera (*Dorcadion olympicum* Ganglebauer, *Stephanorrhina princeps* Oberthür and *Macraspis tristis* Laporte). *Caryologia* 72(2): 63-68. doi: 10.13128/cayologia-194

Published: December 5, 2019

Data Availability Statement: All relevant data are within the paper and its Supporting Information files.

Competing Interests: The Author(s) declare(s) no conflict of interest.

Telomeric heterochromatin and meiotic recombination in three species of Coleoptera (*Dorcadion olympicum* Ganglebauer, *Stephanorrhina princeps* Oberthür and *Macraspis tristis* Laporte)

Anne-Marie Dutrillaux, Bernard Dutrillaux*

Systématique, Évolution, Biodiversité, ISYEB - UMR 7205 – CNRS MNHN UPMC EPHE, Muséum National d'Histoire Naturelle, Sorbonne Universités, 57 rue Cuvier CP50 F-75005, Paris, France
*Corresponding author: bdutrill@mnhn.fr

Abstract. Centromeres are generally embedded in heterochromatin, which is assumed to have a negative impact on meiotic recombination in adjacent regions, a condition required for the correct segregation of chromosomes at anaphase I. At difference, telomeric and interstitial regions rarely harbour large heterochromatic fragments. We observed the presence at the heterozygote status of heterochromatin in telomere region of some chromosomes in 3 species of Coleoptera: *Dorcadion olympicum; Stephanorrhina princeps* and *Macraspis tristis.* This provided us with the opportunity to study the relationship between heterochromatin, chiasma location and meiotic recombination independently from the proximity of centromeres in this order of insects. In acrocentric chromosomes, the presence of heterochromatin in telomere region of the long arm displaces recombination near the centromere. In sub-metacentrics, recombination is almost always restricted to the other arm. This at distance effect of heterochromatin may deeply influence genetic drift.

Keywords. C-banded, telomeric heterochromatin, meiosis, recombination, Coleoptera.

INTRODUCTION

In almost all living organisms, centromeres are surrounded by heterochromatin, which harbours repetitive DNA (Nakaseko et al. 1986), whose function is not yet completely understood. In cells in mitotic growth, heterochromatin represses transcription and expression of genes located into it (Grewal and Jia 2007). During meiosis of most living organisms, recombination is necessary for the correct chromosome segregation at anaphase I, but it does not occur in heterochromatin. Consequently, recombination is repressed in centromeric regions, which harbour heterochromatin. In *Schizosaccharomyces pombe*, it was found to be approximately 200 times less in het-

erochromatin than in the genome-wide average (Ellermeier et al. 2010). A current interpretation is that recombination, thus chiasma formation in centromeric region, would lead to abnormal chromosome segregation (Lynn et al. 2004). Thus, a function of centromeric heterochromatin would be to displace recombination far from the centromeres and allow the correct chromosome segregation. Large and variable amounts of heterochromatin are present in the karyotype of many animals belonging to various taxonomic groups, but their position is not at random: frequently juxta-centromeric and rarely interstitial or terminal. In mammals, a wellknown example of terminal heterochromatin is that of the Hedgehog (Insectivora) in the karyotype of which 2 to 4 chromosome pairs are involved. However, the heterochromatic blocks are not strictly terminal because NORs (Nucleolar Organizer Regions) are located at their extremity (Mandhal 1979). It was noticed that no meiotic recombination occurred in and at proximity of heterochromatin (Natarajan and Gropp 1971). The same particularities were observed in the Primate *Cebus capucinus* (Dutrillaux 1979) but such examples remain rare. In insects, terminal heterochromatin was observed in acrocentric chromosomes of several species of grasshoppers (John and King 1982, 1985, Torre et al. 1985). These authors attributed the displacement of chiasmata to proximal position to the presence of terminal heterochromatin. In Coleoptera, large heterochromatic fragments are commonly seen in most families (Juan and Petitpierre, 1989, Correa et al., 2008, Dutrillaux and Dutrillaux, 2016), but almost always in the centromere region, as in other taxonomic groups. This preferential location may result from the amplification of DNA repeated sequence surrounding centromeres, as shown for α satellite sequences (Rudd et al. 2006, Shepelev et al. 2009). As it will be discussed, the correct segregation of chromosomes at meiosis may also depend on the embedding of centromeres in heterochromatin. Displacement of heterochromatin from centromere regions to intercalary or terminal regions would necessitate secondary events, but terminal heterochromatin may have other origins. It will be also discussed that the presence of heterochromatin in telomeric position may not confer a selective advantage, by imposing meiotic constraints. Among hundreds of species of Coleoptera we studied, karyotypes with large amounts of heterochromatin in terminal position were rarely observed. We confirm that heterochromatin terminally located on the long arm of acrocentrics may not decrease recombination, but simply displaces it near to the centromere, usually considered as a cold region (Mahtani and Willard 1998). In addition, we show that in non-acrocentric chromosomes, heterochromatin terminally located on one arm displaces recombination to the other arm. Thus, heterochromatin can suppress recombination on a whole arm and influence meiotic recombination at much larger distance than it was generally thought.

MATERIAL AND METHODS

Three examples belonging to three different families or sub-families were found among about 400 species of Polyphagan beetles:

Dorcadion olympicum Ganglebauer 1882 (Cerambycidae: Lamiinae: Dorcadionini). Two specimens were captured in May 2014 in Eastern Greece, near Alexandroupolis (40° 50'57"N and 25°52'46"E).

Stephanorrhina princeps Oberthür 1880 (Scarabaeidae: Cetoninae: Goliathini). Two specimens of African origin (Malawi) were obtained in September2007 from a private breeding.

Macraspis tristis Laporte 1840 (Scarabaeidae: Rutelinae: Rutelini). Eight adult specimenswere obtained in March 2008 from grubs captured in Guadeloupe (Basse-Terre, near Deshayes 16°18'00"N and 61°47'00"W) in December 2006.

Chromosome preparations of cells at various stages of meiosis were obtained as described (Dutrillaux and Dutrillaux 2009, Dutrillaux et al. 2010). Proliferating cells obtained from either eggs, testes or mid gut were processed as described. Chromosomes were Giemsa stained and further silver stained for localization of the Nucleolus Organizer Region (NOR) and/or C-banded for localization of heterochromatin. Image capture and karyotyping were performed using IKAROS software (Metasystems, Germany). Chromosome nomenclature: to avoid ambiguous interpretations, we will call acrocentric all chromosomes with a single euchromatic arm, whatever the size of the heterochromatin (generally C-banded) forming the other arm. Chromosomes with euchromatin (not C-banded) on both arms are either metacentric or sub-metacentric. We will focus on chromosomes with large heterochromatic blocks distally attached to euchromatic arms.

RESULTS

Dorcadion olympicum

The mitotic male karyotype is composed of 24 chromosomes. Pairs 3 and 5 are sub-metacentric and all other autosomes are acrocentric. The X chromosome is sub-metacentric and the Y is punctiform (24,XY). In one of the two specimens studied, the length of one chromo-

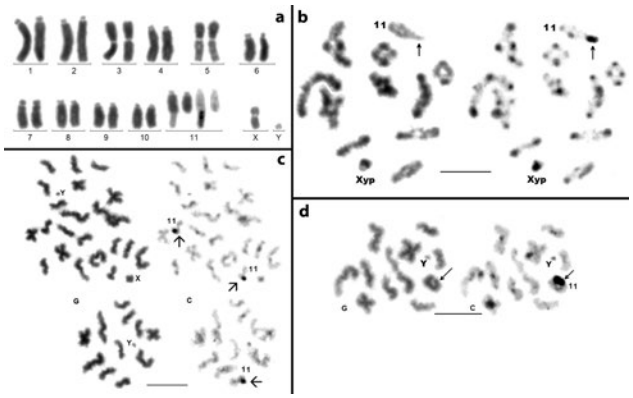

Fig. 1. Chromosomes of *Dorcadion olympicum* **:** a) Giemsa-stained karyotype and C-banded chromosomes 11 exhibiting additional heterochromatin in one homologue. b) Giemsa stained (left) and C-banded (right) spermatocyte I at diakinesis/metaphase with bivalent 11 carrying heterochromatin at one side (arrow). X and Y form a parachute bivalent (Xyp). Barr= 10 mm, as in other figures. c) Group of 3 spermatocytes II at metaphase, sequentially Giemsa stained (G) and C-banded (c). As in most other metaphases II, centromeric heterochromatin is poorly C-banded and chromosome 11 is asymmetrical, with compacted heterochromatin at the tip of a single chromatid (arrows). d) 12,Y spermatocyte II in which the 2 heterochromatin carrier chromatids of chromosome 11 remain cohesive, whereas all other chromosomes have clearly non-cohesive chromatids.

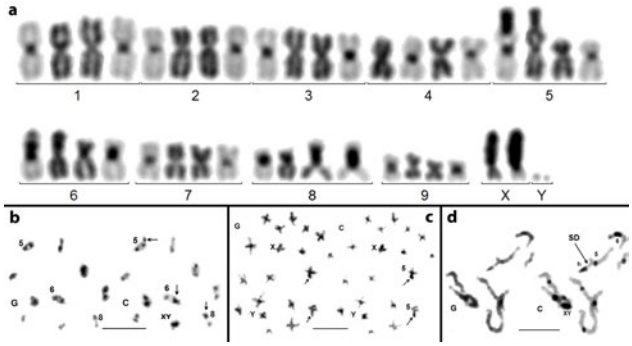

Fig. 2. Sequentially Giemsa stained (G) and C-banded (C) chromosomes of *Stephanorrhina princeps* a) Giemsa stained (center) and C-banded karyotype of a spermatogonium exhibiting additional heterochromatin on one chromosome of pairs 5, 6, 8 and on the X. Only heterochromatin of chromosome 5 is clearly separated from the centromere region. b) Diakinesis/metaphase I: heterochromatin (arrows) remains opposite to chiasmata. c) Exceptionally, in each of these 2 brother spermatocytes II, chromosome 5 is asymmetrically carrier of heterochromatin. d) Spermatocyte I at pachynema: synapsis defect (SD) of the proximal (euchromatic) part of the short arm of bivalent 5.

some 11 is enlarged by the addition of a large amount of C-banded heterochomatin at the telomeric region of the long arm. (Fig. 1a). Following a simple Giemsa staining, the chromatids of this fragment look hyper-cohesive, thin and pale. Centromeric regions are faintly C-banded, as it frequently occurs in the genus Dorcadion (personal data). At diakinesis/metaphase I of meiosis, the sex bivalent has the parachute configuration, usually found in Polyphagan Coleoptera. The compaction of the additional heterochromatin of bivalent 11 is much variable: quite elongated at early diakinesis, it becomes highly compacted at late metaphase I. Bivalent 11 remains easily identified by C-banding (Fig. 1b). The euchromatic component of bivalent 11 has the same aspect in the 131 analysed metaphases I: a cross with very uneven branches. The block of heterochromatin is always located at the tip of the longest branch. This indicates that chiasmata are systematically located near the centromere. In 90/95 spermatocytes II at metaphases, the heterochromatic block is located on a single chromatid of chromosome 11, demonstrating that one crossing-over had occurred in its long arm (Fig. 1c). In 5 instances only, the heterochromatin is present on both chromatids, which may be interpreted as either a lack of recombination in the long arm or the result of a double recombination between the centromere and the heterochromatin. Interestingly, in these chromosomes, the heterochromatin blocks remain cohesive, while euchromatic arms are well separated, as usual at this stage. This gives it a ring appearance (Fig.I d). Finally, in 4 additional pairs of sister spermatocytes II (or diploid ones), the heterochromatin carrier chromosomes remain close to each other suggesting heterochromatin remained associated at anaphase, inducing chromosome lagging.

Stephanorrhina princeps

The mitotic karyotype is composed of 18 meta- or sub-metacentric autosomes, one large X, and one punctiform Y (20, XY). Large and variable fragments of heterochromatin are C-banded on one chromosome of pairs N°5, 6, 8 and on the X. In pair N°5, the heterochromatin is distally located on the short arm (Fig. 2a). We will focus on the meiotic behaviour of the heterozygote chromosomes 5. As in the previous species, the chromatids are hyper-cohesive in their heterochromatic portion. At diakinesis/metaphase I, the heterochromatin is fuzzy and hardly detectable without C-banding. In 37/40 instances, the heterochromatin is located at one extremity of bivalent 5, which looks asymmetrical after C-banding (Fig. 2b). In 3 instances, heterochromatin is in the centre of the bivalent, which has a symmetrical appearance. Amongst 23 spermatocytes II at metaphase, chromosomes 5 have a C-band on either both chromatids (12 times), or a single chromatid (twice, fig.

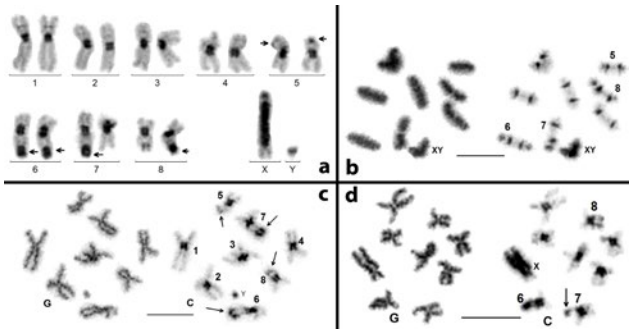

Fig. 3. Giemsa (G) stained and C-banded (C) chromosomes of *Macraspis tristis*. a) C-banded karyotype of a spermatogonium exhibiting heterozygosity for heterochromatin of pairs 7 and 8 and homozygosity for pairs 5 and 6. b) Sequentially Giemsa stained and C-banded spermatocyte I at metaphase with asymmetric bivalents 7 and 8. Heterochromatin of bivalents 5, 6, 7 and 8 is always external, opposite to chiasmata or terminal association. c) Spermatocyte II: all heterochromatin fragments (arrows)are symmetrically distributed on both chromatids. d) Unique spermatocyte II with asymmetrical chromosome 7.

2C), or had no C-band (9 times). Thus, recombination rarely occurred in the heterochromatin carrier arm. At pachynema, the bivalents with enlarged heterochromatin tend to remain close to each other, in spite of the drastic hypotonic shock to which they had been submitted. A synapsis defect of the euchromatic fragment comprised between the telomeric and centromeric heterochromatin was recurrently observed (Fig. 2d).

Macraspis tristis

The karyotype, composed of 18 chromosomes, is characterized by the frequent presence of large and variable heterochromatic fragments at telomeric regions of one arm of 3 pairs of sub-metacentrics (N°6, 7 and 8) and on the X (Fig. 3a). In all diakineses/metaphases I examined from all the specimens, the heterochromatin carrier bivalents have the same configuration: chiasma or terminal association in the euchromatic arms and opposite position of the heterochromatin (Fig.3b). This suggests that no recombination occurred in the heterochromatin carrier arms. In the specimen considered here, pairs N°7 and 8 were heterozygote for the presence or absence of a large heterochromatin fragment. Among 11/12 spermatocytes II, all carrier chromosomes had similarly heterochromatin in both chromatids (Fig. 3c). In a single one, one chromosome was asymmetrical, with heterochromatin on a single arm, indicating that recombination took place between the centromere and the heterochromatin (Fig. 3d). In a second specimen, only pair N° 8 was heterozygote for the presence of heterochromatin. No asymmetry was observed on chromosomes from 28 spermatocytes II. Finally, in a third specimen, both pairs N° 7 and 8 were heterozygote, and no asymmetry was detected among 8 spermatocytes II. Thus, in 65 analysed sub-metacentrics, recombination was almost always suppressed between the distally located heterochromatin and the centromere, and occurred in the other arm (64/65 times). As in *S. princeps*, the bivalents with enlarged heterochromatin tended to associate at pachynema.

DISCUSSION

Recombination and heterochromatin

Only few data exist on meiotic recombination and chromosome segregation in beetles, and most of them were obtain before the heterochromatin detection was possible (Smith and Virkki 1978). In both literature and our own data, a general observation is that most bivalents exhibit a single chiasma in a fairly distal, if not terminal, position at diakinesis/metaphase I. This is in agreement with the findings, in other organisms, that repression of recombination occurs not only in juxta-centromeric heterochromatin, but also in adjacent regions. Thus, recombination hot spots are rarely located near to the centromeres, but most frequently in intercalary and near telomeric regions (Lichten and Goldman, 1995). The presence of large heterochromatin fragments in chromosomes is not exceptional. They generally occur in centromeric regions, where recombination rarely occurs (Ellermeier et al., 2010). Their more exceptional occurrence at telomeric regions offers the possibility to look for the possible influence of heterochromatin on meiotic recombination and chromosome segregation, independently from the proximity of the centromere and associated repetitive DNA. Such analysis was already performed in grasshoppers, in which some species have terminal heterochromatin in acrocentric chromosomes. It showed the displacement of chiasmata to a proximal position in heterochromatin carrier, compared to other chromosomes (John and King, 1982, 1985, de la Torre et al., 1986).

Our observations in *D. olympicum* confirm these findings: at metaphase I, the heterochromatic block of chromosome 11 is almost always at distance from the chiasma. In addition, we could quantify recombination through the analysis of 95 spermatocytes at metaphase II: 90/95 chromosomes 11 carry heterochromatin on a single chromatid, which formally demonstrates an almost systematic occurrence of crossing over between the centromere and the heterochromatic block. Thus, there was

no crossing-over suppression but a displacement towards proximal regions. The 5 metaphases II with symmetrical chromosomes 11 cannot be interpreted univocally: either 2 or no crossing-over occurred or crossing-over occurred in the short (heterochromatic) arm. As discussed below, these few cells provide us with interesting information about chromosome cohesion and segregation.

In *M. tristis* and *S. princeps*, all autosomes are submetacentric, and the analysis of spermatocytes I at metaphase indicates that most bivalents form a single chiasma. For chromosomes with one heterochromatin carrier arm, chiasmata are almost systematically located on the other arm. This absence of recombination in the heterochromatin carrier arm is confirmed by the analysis of spermatocytes II in metaphase: at difference with the acrocentric of *Dorcadion*, heterochromatin is almost always either present or absent on both arms. This suggests a "choice" between the two arms, by suppression of recombination in the whole heterochromatin carrier arm. As observed in a proportion of pachytene cells of *S. princeps*, there is an asynapsis of the whole euchromatic fragment located between centromeric and telomeric heterochromatin, which may be related to the lack of recombination. These 3 examples show that large telomeric heterochromatin fragments can drastically influence meiotic recombination in euchromatin, with an effect at a long distance. It may create a hot spot of recombination fairly close to the centromere, which is quite unusual, as in *D. olympicum*. It may also generate a cold and a hot arm, as in the two other species. This effect is probably not due to the heterozygote status, because when both arms are carrier, they are generally not involved in chiasmata at diakinesis. By altering meiotic recombination, these occasional heterochromatic fragments alter the gene linkage between all the genes of the chromosome and influence genetic drift.

Cohesion, compaction and heterochromatin

At metaphase I, sister chromatids are maintained together by cohesins, a ring-shaped protein complex formed by 4 sub-units: Scc1 (Rec8), Scc3, Smc1 and Smc3. At anaphase I, cohesins are cleaved by separase all along chromatids, except in centromere regions where the sub-unit Rec8 is protected from cleavage by the protein complex Shugoshin/protein phosphatase PP2A, which counteracts its phosphorylation (Riedel et al. 2006). This permits the resolution of chiasmata, which occur in euchromatic fragments. At the following metaphase II, cohesins are no more efficient. Chromatids are well separated and chromosome cohesion is maintained at the centromere regions only. Finally, after inactivation of PP2A, centromere cleavage occurs at anaphase II, enabling the segregation of monochromatidic chromosomes. Why and how Shugoshin/PP2A complex is located in centromere regions remains unknown. Our observation may provide some information. In spermatocytes II, all chromosomes have well separated chromatid, with the exception of chromosomes 11 of *D. olympicum,* which are ring shaped when they are symmetrically carrier of terminal heterochomatin. It means that cohesin was not cleaved both at centromere and telomere, the two heterochromatic regions. Thus, Rec8 seems to be protected from cleavage by heterochromatin. This protection, necessary for the correct chromosome segregation at anaphase I, may be one of the reasons why centromeres are systematically embedded in heterochromatin.

It is commonly observed that in metaphases of mitotic cells also, heterochromatic fragments are more cohesive than euchromatin. At the molecular level, the search of a particular relationship between the protein complexes involved in cohesion and heterochromatin components could be of interest. The DNA methylation status may play a role in this context. In human cells, although juxta-centromeric heterochromatin of chromosomes 1, 9 and 16 is not G-C rich, it is strongly labelled by antibodies to 5-MdC (5-methyldeocycytidine), indicating its strong methylation status (Miller et al., 1974; Montpellier et al., 1994). In mouse germ cells, large variations of DNA methylation were reported during the progression of gametogenesis (Coffigny et al. 1999; Bernardino-Sgherri et al. 2002; Marchal et al. 2004). Drastic changes from hypo- to hyper-methylation occur in heterochromatin and euchromatin in an opposite way. For example, in early spermatogonia, hypo-methylated and elongated centromeric heterochromatin displays premature cleavage, while chromosomes remain cohesive at hyper-methylated chromatids. On the opposite, euchromatic chromatids are cleaved in spermatocytes II, when they are poorly methylated while chromosomes remain cohesive at their methylated and compacted centromere regions. Unfortunately, we could not study the methylation status of beetle chromosomes during gametogenesis, but the high similitude of variations of chromosome compaction and cohesion suggests they might correlate with DNA methylation changes.

In conclusion, the presence of large fragments of heterochromatin at telomere regions deeply alters meiotic recombination in beetles, as in other animals. Large terminal heterochromatic fragments have a suppressive effect on recombination, which seems to spreads to a much larger distance than that of centromeric heterochromatin and may depend on a different mechanism. It should have some consequences on the transmission

of genetic characters, by altering gene linkage. The variations of compaction/cohesion/recombination, opposite in euchromatin and heterochromatin during meiosis progression, suggest that the activities of the protein complexes involved are highly dependant on chromatid structure and composition.

REFERENCES

Bernardino-Sgherri J, Chicheportiche A, Niveleau A, Dutrillaux B. 2002. Unusual chromosome cleavage dynamic in rodent neonatal germ cells. Chromosoma. 111: 341-347.

Coffigny H, Bourgeois C, Ricoul M, Bernardino J, Vilain A, niveleau A, Malfoy B, Dutrillaux B. 1999 Alteration of DNA methylation patterns in germ cells and Sertoli cells from developing mouse testis. Cytogenet Cell Genet. 87: 175-181.

Corréa RX, Pompolo SG, Santos IS, Silva JG, Costa MA. 2008. Karyotype, heterochromatin distribution in meiosis of *Zabrotes subfasciatus* (Bohemann) (Coleoptera: Chrysomelidae, Bruchinae). Neotropical Entomol. 37: 546-551.

Dutrillaux B. 1979. Chromosome evolution in Primates: tentative phylogeny from Microcebus murinus (Prosimian) to man. Hum Genet. 48: 251-314.

Dutrillaux A-M, Dutrillaux B. 2009. Chromosome polymorphism and Fanconi-like instability in the scarabaeid beetle Macraspis tristis from Guadeloupe. Cytogenet Genome Res. 125: 142-148.

Dutrillaux A-M, Dutrillaux B. 2016. Chromosome comparison of 17 species/sub-species of African Goliathini (Coleoptera, Scarabaeidae, Cetoniinae). CompCytogen. 10: 269-282. doi: 10.3897/CompCytogen.v10i2.8003

Dutrillaux A-M, Pluot-Sigwalt D, Dutrillaux B. 2010. (Ovo-)viviparity in the darkling beetle, *Alegoria castelnaui* (Tenebrionidae : Ulomini), from Guadeloupe. European J Entomol. 107: 481-485.

Ellermeier C, Higuchi EC, Phadnis N, Holm L, Geelhood JL, Thon G, Smith GR. 2010. RNAi and heterochromatin repress centromeric meiotic recombination. www.pnas.org/cgi/doi/10.1073/pnas.0914160107

Grewal SI, Jia S. 2007. Heterochromatin revisited. Nat Rev Genet. 8:35-46.

John B, King M. 1982. Meiotic effects of supernumerary heterochromatin in heteropteris obscurella. Chromosoma. 85: 39-65.

Juan C, Petitpierre E 1989. C-banding and DNA content in seven species of Tenebrionidae. Genome. 32: 834-839.

Lichten M, Goldman ASH. 1995. Meiotic recombination hot spots. Ann Rev genet. 29: 423-444.

Lynn A, Ashley T, Hassold T. 2004. Variation in human meiotic recombination. Ann Rev Genomics Hum Genet. 5: 317-349.

Mahtani MM, Willard HF. 1998. Physical and genetic mapping of the human X chromosome centromere: repression of recombination. Genome Res. 8: 100-110.

Mandahl N. 1978. Variation in C-stained chromosome regions in European hedgehogs (Insectivora, Mammalia). Hereditas. 89: 107-128.

Marchal R, Chicheportiche A, Dutrillaux B, Bernardino-Sgherri J. 2004. DNA methylation in mouse gametogenesis. Cytogenet Genome Res. 105: 316-324.

Montpellier C, Bourgeois C, Kokalj-Vokac N, Muleris M, Niveleau A, Reynaud C, Gibaud A, Malfoy B, Dutrillaux B. 1994. Detection of methylcytosine-rich heterochromatin on banded chromosomes. Application to cells with various status of DNA methylation. Cancer genet Cytogenet. 78: 87-93.

Miller OJ, Schnedl W, Allen j, Erlanger BF. 1974. 5-methylcytosine localised in mammalian constitutive heterochomatin. Nature. 251: 636-637

Nakaseko Y, Adachi Y, Funahashi S, Niwa O, Yanagida M. 1986. Chromosome walking shows a highly homologous repetitive sequence present in all the centromeres regions of fission yeast. EMBO J. 5: 1011-1021.

Natarajan AT , Gropp A. 1971. The meiotic behaviour of autosomal heterochromatic segments in hedgehogs. Chromosoma. 35: 143-152.

Riedel CG, Katis VL, Katou Y, Mori S, Itoh T, Helmart W, Galova M, Petronczki M Gregan J, Cetin B et al. 2006. Protein phosphatase 2A protects centromeric sister chromatid cohesion during meiosis. Nature. 441: 53-61.

Rudd MK, Wray GA, Willard HF. 2006. The evolutionary dynamics of α-satellite. Genome Research. 16:88-96. doi:10.1101/gr.3810906.

Shepelev VA Alexandrov, AA, Yurov, YB, Alexandrov, IA. 2009. The evolutionary origin of man can be traced in the layers of defunct ancestral alpha satellites flanking the active centromeres of human chromosomes. PLoS Genet, *5*(9), e1000641.

Smith SG, Virkki N. 1978. Animal Cytogenetics,vol 3: Inseta 5: Coleoptera (Gebrüder Borntraeger, Berlin.

Torre de la J, Lopez-Fernandez C, Nichols R, Gonsalvez J. 1986. Heterochromatin readjusting chiasma distribution in two species of the genus Arcyptera: the effect among individuals and populations. Heredity 56: 177-184.

Caryologia
International Journal of Cytology, Cytosystematics and Cytogenetics

Firenze University Press
www.fupress.com/caryologia

OPEN ACCESS

Citation: A. Vangelisti, G. Usai, F. Mascagni, L. Natali, T. Giordani, A. Cavallini (2019) A whole genome analysis of long-terminal-repeat retrotransposon transcription in leaves of *Populus trichocarpa* L. subjected to different stresses. *Caryologia* 72(2): 69-79. doi: 10.13128/cayologia-232

Published: December 5, 2019

Data Availability Statement: All relevant data are within the paper and its Supporting Information files.

Competing Interests: The Author(s) declare(s) no conflict of interest.

A whole genome analysis of long-terminal-repeat retrotransposon transcription in leaves of *Populus trichocarpa* L. subjected to different stresses

Alberto Vangelisti[#], Gabriele Usai[#], Flavia Mascagni[#], Lucia Natali, Tommaso Giordani[*], Andrea Cavallini

Department of Agriculture, Food and Environment, University of Pisa, Via del Borghetto 80, I-56124 Pisa, Italy

[#] These authors contributed equally to this study

[*] Corresponding author: tommaso.giordani@unipi.it

Abstract. Long terminal repeat retrotransposons have a main role in shaping the structure of plant genomes. We used available genomic resources to study as several factors affect the expression of long terminal repeat retrotransposons in *Populus trichocarpa*. Such factors included redundancy of a retrotransposon in the genome, chromosomal localization, "genotype" of the retrotransposon, and changes in the environment. Overall, we identified and annotated 828 full-length retrotransposons, and analyzed their abundance in the genome. Then, we measured their expression in leaves of plants subjected to several stresses (drought, cold, heat, and salt) as well as in control plants. Our analyses showed that the expression of retrotransposons was generally low, especially that of abundant elements. The transcription of an element was found to be only slightly dependent on its chromosomal localization, rather it depended on the superfamily and the lineage to which the retrotransposon belonged. Finally, some retrotransposons were specifically activated by different environmental stresses.

Keywords. LTR-retrotransposons, retrotransposon expression, retrotransposon abundance, Illumina cDNA libraries, *Populus trichocarpa*.

INTRODUCTION

Transposable elements are mobile DNA sequences, which are abundant and widespread in all eukaryotic genomes. They can change their position on chromosomes by a mechanism, called transposition, driven by enzymes encoded by the element itself. Transposable elements can be divided between retrotransposons (REs, Class I) and DNA transposons (Class II), according to their transposition mechanism (Wicker et al. 2007).

The transposition of REs occurs through a "copy and paste" replicative mechanism that includes the transcription of an RNA intermediate followed by its retro-transcription and insertion into the genome (Wicker et al.

2007). This transposition mechanism has allowed REs to become the largest portion of most eukaryotic genomes, often represented by many thousands of copies (San-Miguel et al. 1998; Vicient et al. 1999).

A retrotransposon can be classified as LTR- or not LTR-RE, according to the presence of long terminal repeats (LTRs) at its ends. As for the LTR-REs, the promoter elements, the polyadenylation signals and the expression enhancers are found in the LTRs. These domains regulate the transcription of the element (Bennetzen 2000). In the coding portion of the LTR-REs, Gag and Pol domains can be found. Gag encodes virus-like particles, Pol encodes the enzymes necessary to produce new cDNA molecules from the RE transcripts and to integrate them into new sites in the host genome (Bennetzen 2000). Other structural features involved in the RE replication process include a primer binding site and a poly-purine tract (Bennetzen 2000).

The LTR-REs are essentially subdivided into two superfamilies, *Gypsy* and *Copia* (Wicker et al. 2007), according to the order of gene sequences within the Pol domain. Superfamilies, in turn, are distinguished into several lineages in relation to sequence conservation and structure (Barghini et al. 2015a; Usai et al. 2017; Buti et al. 2018; Mascagni et al. 2017; 2018a).

The replicative activity of LTR-REs can determine large variations in the genome structureof eukaryotic species (Springer et al. 2009; Vitte et al. 2014). Among the effects of retrotransposition, besides determining changes in genome size, RE-related structural variations can modify the regulation patterns of protein-encoding genes and, consequently, their activity, influencing the phenotype (Slotkin and Martienssen 2007; Butelli et al. 2012; Falchi et al. 2013; Lisch 2013).

The first phase of retrotransposition is represented by the transcription of the element. The RE transcripts can be capped and polyadenylated or not. In the former case, transcripts should be destined to be translated into the enzymes for retrotransposition, in the latter case, transcripts should be reverse-transcribed (Chang et al. 2013; Meignin et al. 2003).

Transcription of REs has been described in several plant species (Grandbastien 2015). In some grass species LTR-REs are poorly constitutively transcribed (Vicient et al. 2001; Ishiguro et al. 2014). In other species, for example in *Populus* x *canadensis*, certain LTR-REs are expressed constitutively, without apparent induction conditions (Giordani et al. 2016). Retrotransposition is completed when a new copy of the element is inserted into the genome. This has been reported for *Tnt1* and *Tto1* elements of *Nicotiana* and for *Tos17* of rice, induced by tissue culture (Grandbastien 1998). Complete retrotransposition of a *Copia* RE has been described also in sunflower seedlings, grown under standard conditions (Vukich et al. 2009).

Retrotransposition is generally limited by the host genome due to its potentially mutagenic action. A major mechanism to inactivate mobile elements involves the methylation of histones and cytosine residues with consequent silencing of chromatin (Dieguez et al. 1998). Post-transcriptional silencing by RNA degradation also plays an important role in the epigenetic control of RE activity (Slotkin and Martienssen 2007; Lisch 2013; Ito 2013).

In recent years, many studies have been carried on the LTR-REs of the genus *Populus* and in particular on *P. trichocarpa*, which is considered a model species for forest trees. The *P. trichocarpa* genome was the first genome to have been sequenced for a forest species (Tuskan et al. 2006) and has been recently updated (Zeng et al. 2017). This species has a relatively small genome (550 Mbp) and REs cover approximately 176 Mbp (32% of the genome), with a prevalence of *Gypsy* over *Copia* RE sequences (Tuskan et al. 2006). *Populus trichocarpa* REs have been identified and annotated according to their superfamily and lineage, and LTR-RE genomic abundance and age of insertion were analyzed as well (Natali et al. 2015; Mascagni et al. 2018b). *P. trichocarpa* LTR-REs have been also used as a reference for several analyses related to the repetitive component in other species of the genus *Populus* (Giordani et al. 2016; Usai et al. 2017).

The transcription of REs is only the first step for retrotransposition and insertion of new copies of the element in the genome. For this reason, analyses on LTR-RE activity should include searching for new insertion events. However, an overall study of factors potentially able to influence the transcription of these elements is not yet available for poplar. We therefore decided to perform a meta-analysis of LTR-RE expression by using publicly available genomic DNA and cDNA libraries obtained from leaves of plants cultivated under standard conditions or subjected to four types of abiotic stress (cold, drought, heat, and salt). The objectives of this work were to evaluate i) the expression level of REs under standard and stress conditions; ii) the correlation between abundance of REs and their expression level; iii) the possibility that different LTR-REs are induced by different (and specific) stresses; iv) the possibility that the expression of a RE is related to the "genotype" of the RE itself, i.e., to the lineage to which it belongs; v) the possibility that the chromosomal localization of a RE can influence its expression.

METHODS

Isolation of full-length LTR-REs of P. trichocarpa

Putative full-length LTR-REs were isolated from the GCA_000002775.3 version (Zeng et al. 2017) of the *P. trichocarpa* genome sequence (Tuskan et al. 2006; Slavov et al. 2012), deposited at the NCBI site (WGS project number AARH02, http://www.ncbi.nlm.nih.gov/assembly/GCF_000002775.3). Full-length LTR-REs were isolated by using: i) LTRharvest (Ellinghaus et al. 2008) with the following parameters: minlenltr=100, maxlenltr=6000, mindistltr=1500, maxdistltr=25000, mintsd=5, maxtsd=5, similar=85, vic=10, including the presence of TG and CA dinucleotides at 5' and 3'-ends, respectively; ii) LTR-FINDER (Xu et al. 2007), under default.

A random sample of putative LTR-REs (around 20% of the isolated elements) were manually validated using DOTTER (Sonnhammer and Durbin 1995) to verify the occurrence of the two LTRs, of dinucleotides TG and CA at the respective 5' and 3' ends, and of the tandem site duplications. All LTR-REs were annotated by using BLASTN search against plant RE datasets (Barghini et al. 2015b; Natali et al. 2015; Usai et al. 2017; Buti et al. 2018) and by using the Domain Search tool of RepeatExplorer (Novak et al. 2013). Whenever possible, the full-length LTR-REs were identified as belonging to *Gypsy* or *Copia* superfamilies and to the respective lineages.

A multi-FASTA file with the sequences of identified full-length LTR-REs is available at the sequence repository site of the Department of Agriculture, Food and Environment of the University of Pisa (http://pgagl.agr.unipi.it/sequence-repository/).

Illumina cDNA libraries collection

The expression of LTR-REs was analyzed using Illumina cDNA paired-end libraries publicly available at the NCBI SRA (https://www.ncbi.nlm.nih.gov/sra/, BioProject accession PRJEB19784) (Filichkin et al. 2018). Such cDNA libraries were obtained from RNAs from leaves of *P. trichocarpa* (clone Nisqually 1) plants exposed to different stresses, i.e., heat, cold, drought, and salt. All cultivation conditions are described by Filichkin et al. (2018). In brief, for heat stress, plants were treated at 39°C for 12 h (short treatment) or 7 days (prolonged treatment). For cold stress, plants were exposed to cycles of 4°C (night)/12°C (day) for 24 h (short treatment) or 7 days (prolonged treatment). For drought treatment, watering was withheld until soil moisture reached 0.1 m^3/m^3 and maintained at the level of 0.06 –0.1 m^3/m^3 for 5 days (short treatment) or for 12 days after water withholding (prolonged treatment). For salt stress, plants were irrigated with 100 mM NaCl solution for 24 h (short treatment) or for 7 days (prolonged treatment). Three replicate libraries were downloaded for each stress and control plants.

Illumina genomic DNA sequences of the same clone of *P. trichocarpa* were retrieved from the NCBI Sequence Read Archive (NCBI, Washington, USA, https://www.ncbi.nlm.nih.gov/sra, SRA ID SRR1801106).

The quality of the cDNA and genomic DNA reads was checked using FastQC (v. 0.11.3) (http://www.bioinformatics.babraham.ac.uk/projects/fastqc/), and the overall quality was improved by removing Illumina adapters and trimming the reads using Trimmomatic (v. 0.38) (Bolger et al., 2014) with different parameters for cDNA (ILLUMINACLIP:2:30:10, SLIDINGWINDOW:4:20, CROP:96, HEADCROP:12 and MINLEN:90) and genomic DNA (ILLUMINACLIP:2:30:10, SLIDINGWINDOW:4:15, CROP:85, MINLEN:85). Organellar sequences were removed from the Illumina libraries by mapping against a database of chloroplast genomes of poplar species (Usai et al. 2017) using CLC-BIO GenomicWorkbench (v. 9.5.3, CLC-BIO, Aarhus, Denmark) with the following parameters: mismatch cost 2, insertion cost 3, deletion cost 3, length fraction 0.5, similarity fraction 0.8. All matching reads were considered putatively belonging to organellar genomes and removed.

Estimation of retrotransposon expression and abundance in the genome

The expression of LTR-REs was measured mapping cDNA sequence reads of control and cold-, drought-, heat-, or salt-exposed leaves onto the library of *P. trichocarpa* full-length LTR-REs, using CLC-BIO Genomic Workbench with the following parameters: mismatch cost 1, deletion cost 1, insertion cost 1, similarity 0.9 and length fraction 0.9. The expression level of each sequence was calculated and converted both to mapped reads per million (MRpM) and to RPKM (Mortazavi et al. 2008). LTR-REs mapped by 1 to 10 reads per million of reads in at least one sample were considered as expressed (Lu et al. 2013), those mapped by at least 10 reads per million were considered as highly expressed.

Expression values were compared, using Baggerley's test (Baggerley et al. 2003), considering RPKM values in the short and prolonged stage of each treatment in comparison to control leaves. The weighted proportion fold changes between a treatment and controls were considered significant when the weight of a sample was at least two-fold higher or lower than another, with a false dis-

covery rate (FDR; Benjamini and Hochberg, 1995) corrected p-value ≤ 0.05.

In order to assess genomic abundance of REs, genomic DNA reads of *P. trichocarpa* were mapped onto reference retrotransposon domains library using CLC-BIO Genomics Workbench with the same parameters described above. For each LTR-RE the average coverage was calculated. The average coverage is the sum of the bases of the aligned parts of all the reads divided by the length of the reference sequence.

Localization of expressed REs along the poplar genome

Each of the 19 linkage groups (LGs) of the currently available *P. trichocarpa* genome sequence (version GCA_000002775.3, Zeng et al. 2017) were subdivided into 3-Mbp-long genome regions. Then, in order to localize LTR-RE sequences in the genome, the LTR-REs were used for masking the 3-Mbp-long fragments of the poplar genome using RepeatMasker (http://www.repeatmasker.org) with the following parameters: s, no-is, no-low. Masking was performed using i) all isolated full-length elements; ii) all *Chromovirus* LTR-REs; iii) a putative poplar centromeric sequence (Islam-Faridi et al. 2009; Cossu et al. 2012); iv) all LTR-REs expressed in control leaves (mapped by more than ten reads per million). The number of masked bases was then counted for each of the 3 Mbp fragment using an in-house perl script.

RESULTS

Identification of full-length LTR-REs of P. trichocarpa

The full-length LTR-REs used in this study were isolated from the updated genome sequence of *P. trichocarpa* (Zeng et al. 2017), by performing a complete genome scan with LTRharvest and LTRFinder. Besides using these tools with stringent parameters, a sample of isolated elements were manually validated at structural level and all were confirmed as LTR-REs.

The dataset includes 828 full-length LTR-REs. Table 1 reports the number of LTR-REs belonging to the *Gypsy* and *Copia* superfamilies, subdivided according to the lineage to which they belong, i.e. *Athila*, *Ogre* and *Chromovirus* for *Gypsy* elements and *Ale* (distinguished into *AleI* and *AleII*), *Angela*, *Bianca*, *Ivana/Oryco*, *SIRE* and *TAR/Tork* for *Copia* elements. For each lineage the mean average coverage is also reported, calculated after mapping elements with Illumina gDNA reads, which represents the mean abundance of that lineage in the *P. trichocarpa* genome.

Transcription of LTR-REs

The expression of 828 full-length LTR-REs was measured by mapping the elements with Illumina cDNA reads obtained from leaves of plants of *P. trichocarpa* cultivated in standard conditions (controls) and under different stress (drought, heat, cold, or salt). In the control leaves, only 0.47% of the cDNA reads mapped the library, hence, in general, LTR-REs are barely expressed (Fig. 1).

The expression level of LTR-REs decreased with stress, in the decreasing order drought-cold-heat-salt (Fig. 1). No significant difference was observed between short and prolonged treatments, with the exception of cold treatment, where expression decreased reduced in prolonged exposition.

According to Lu et al. (2013), we considered as expressed those LTR-REs mapped by more than one read per million. The number of expressed LTR-REs in controls and in drought-, cold-, heat- and salt-exposed leaves is reported in Fig. 2. The number of LTR-REs expressed in drought-treated leaves is similar to that of control leaves. On the contrary, this number is strongly reduced after the other treatments (Fig. 2). However, the

Table 1. Number and mean average coverage of full-length LTR-REs collected in the *P. trichocarpa* genome (version GCA_000002775.3) and separated according to their superfamily and lineage.

Super-family	Lineage	Nr. of elements	Mean average coverage
Copia	*AleI*	42	14.04
	AleII	122	22.33
	Angela	2	64.13
	Bianca	1	28.24
	Ivana/Oryco	104	19.06
	SIRE	7	42.11
	TAR/Tork	90	17.45
	Total	368	19.89
Gypsy	*Athila*	126	57.37
	Chromovirus	174	40.20
	Ogre	67	41.16
	Unknown	50	13.46
	Total	417	42.34
Unknown		43	22.65
Total		828	31.34

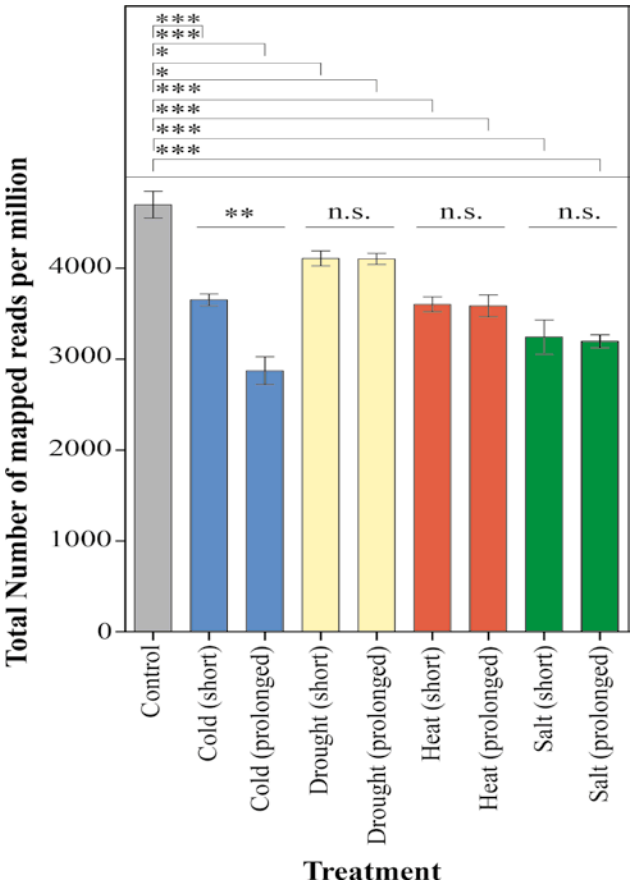

Fig. 1. Total number of mapped reads (per million of reads) on the 828 full-length LTR-REs of *P. trichocarpa*, in leaves of control and stress-exposed plants. Stresses included cold, drought, heat and salt treatments, for short and prolonged times. The differences between control and each treatment and between short and prolonged stress treatments were significant at $p<0.001$ (***), $p<0.01$ (**), $p<0.05$ (*), or not significant (n.s.) according to Tukey's test.

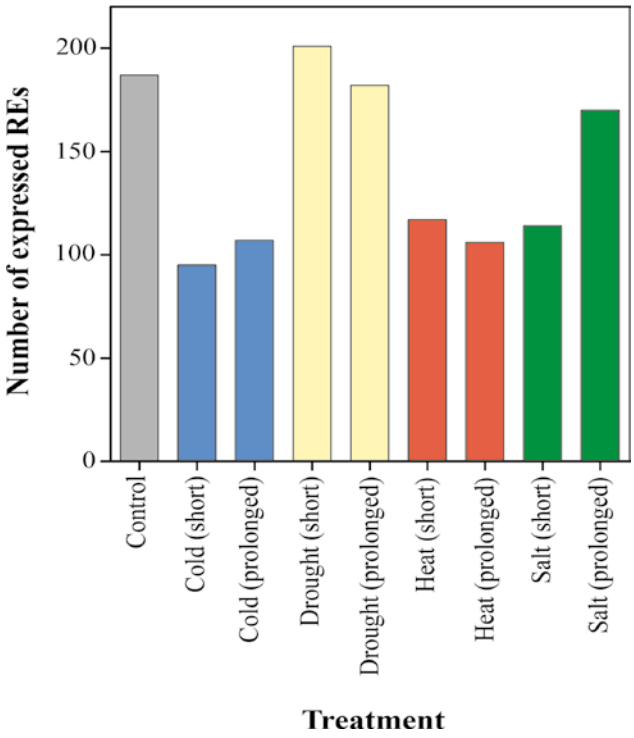

Fig. 2. Number of expressed (MRpM > 1) LTR-REs in leaves of control and stress-exposed plants. Stresses included cold, drought, heat and salt treatments, for short and prolonged times.

number of expressed LTR-REs increased after prolonged salt treatment.

The relationship between the abundance of a retrotransposon in the genome and its expression

In another analysis we measured the relationship between the abundance of a LTR-RE in the genome and the corresponding expression level. Such data are reported for control leaves in Fig. 3. It can be observed that abundant LTR-REs (average coverage > 100) are lowly expressed. Similar results were also found in leaves of plants exposed to different stresses (not reported).

Since assessing the expression of a LTR-RE is based on the occurrence of LTR-RE sequences in cDNA libraries, one might ascribe such occurrence to genomic DNA contamination. Actually, since the most abundant LTR-REs resulted slightly or even not expressed, contamination by genomic DNA in the cDNA libraries can be largely ruled out.

Influence of chromosomal localization on retrotransposons expression

In order to verify whether active LTR-REs were localized at specific chromosomal sites, we aligned LTR-RE sequences, highly expressed (MRpM > 10) in the control leaves, to the genome of *P. trichocarpa* (Fig. 4). For comparison, we separately aligned the genome with all the 828 LTR-REs; furthermore we determined the putative position of the centromere on each linkage group (LG) by aligning a tandemly repeated centromeric sequence of *P. trichocarpa* (Islam-Faridi et al. 2009) and *Chromovirus* elements (which preferentially localize at centromeres, Neumann et al. 2011). The chromosomal profiles of all the LTR-REs and highly expressed LTR-REs were substantially similar (Fig. 4). In some cases, minor peaks in the general LTR-REs profiles were apparently absent in the expressed LTR-REs profiles, suggesting that elements at those loci were generally inactive.

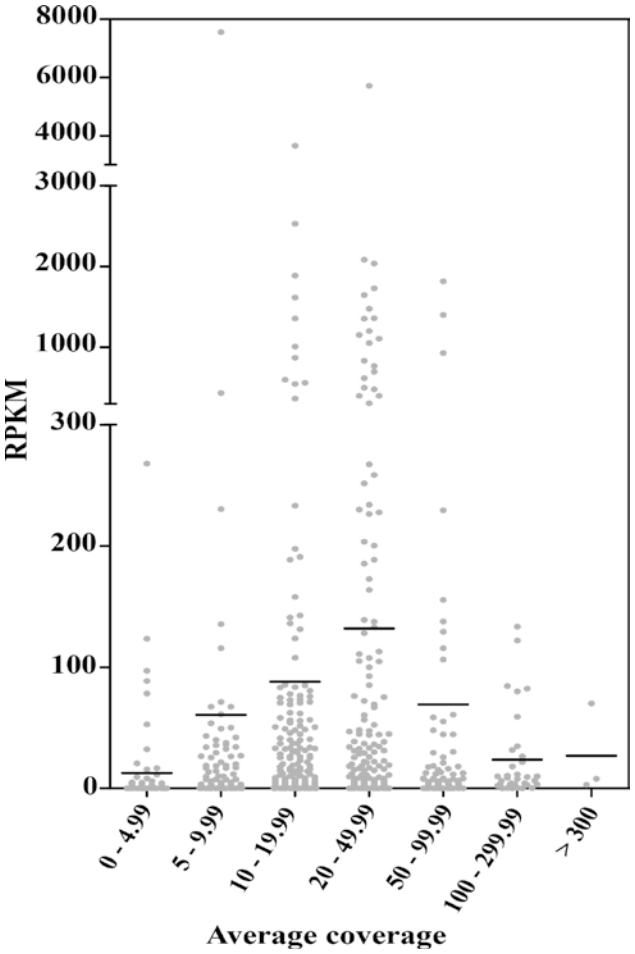

Fig. 3. Relationship between average coverage and RPKM for each of 828 full-length LTR-REs of *P. trichocarpa*.

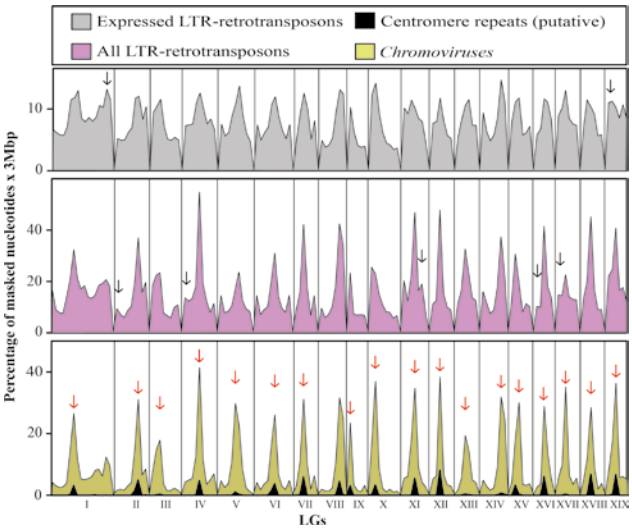

Fig. 4. Percentage of aligned nucleotides along *P. trichocarpa* LGs using all the full-length LTR-REs expressed in control leaves, all isolated full-length LTR-REs, all isolated *Chromovirus* REs and a putative centromeric sequence (in black). Red arrows indicate the putative position of the centromeres. Black arrows indicate minor peaks which are especially evident in the expressed LTR-REs profiles or in the profiles of all LTR-REs.

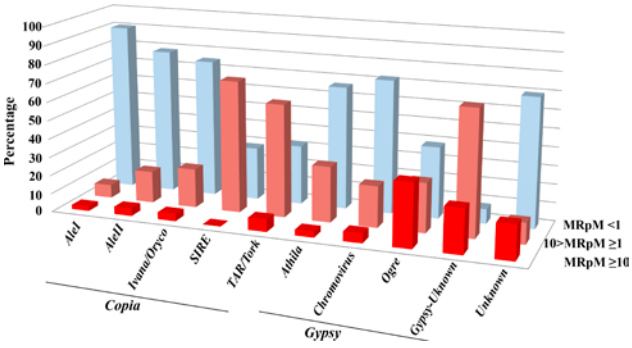

Fig. 5. Percentages of highly expressed (MRpM ≥ 10), expressed (MRpM ranging from 1 to 10) and unexpressed (MRpM < 1) LTR-REs, distinguished among LTR-RE superfamilies and lineages.

Only two peaks (within LG I and LG XIX) were apparently more evident in the expressed LTR-REs profiles, indicating that REs at these loci were particularly active. In general, it can be observed that peaks in putative centromere positions were less evident in the expressed LTR-RE profiles, suggesting that centromere LTR-REs were less active than elements lying at other loci (Fig. 4).

Influence of the superfamily/lineage of the retrotransposon on its expression

In order to assess whether the expression of LTR-REs was related to the superfamily/lineage to which the element belonged, LTR-REs were subdivided into lineages and separated among highly expressed (i.e., mapped by more than 10 reads per million), expressed (1-10 mapped reads per million) and not expressed (less than 1 mapped read per million). *Gypsy* elements resulted more expressed than *Copia*, in fact 48 out of 417 *Gypsy* REs (11.5%) were expressed, compared to 16 out of 368 *Copia* REs (4.4%). In general, most lineages showed low percentages of highly expressed or expressed LTR-REs (Fig. 5). However, for two *Copia* lineages (*SIRE* and *TAR/Tork*) and one *Gypsy* lineage (*Ogre*) the majority of LTR-REs resulted highly expressed or expressed (Fig. 5). In particular, the *Ogre* lineage showed the highest percentage of expressed elements. Diffused LTR-RE expression was also observed for those elements belonging to the *Gypsy* superfamily, but for which the lineage could not be determined.

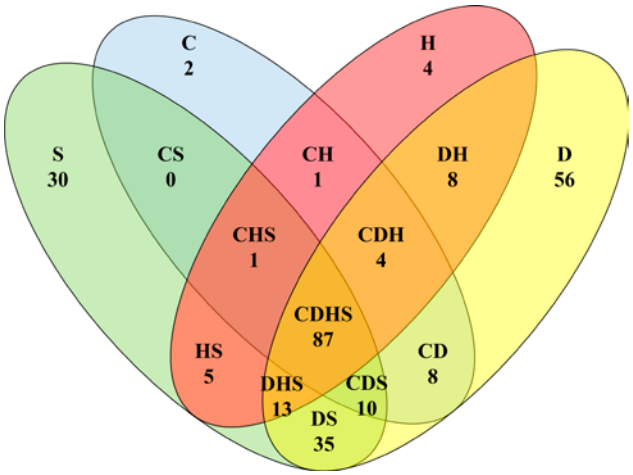

Fig. 6. Venn diagram of expressed (MRpM > 1) LTR-REs in the four stresses used in these experiments (D = drought; H = heat; C = cold; S = salt). Results of short and prolonged treatments were cumulated for each stress.

Stress-specific induction of retrotransposons expression

Most LTR-REs which were expressed in control leaves were also expressed in leaves of stress exposed plants. Of 313 LTR-REs expressed (MRpM > 1) in controls and/or in different stresses, only 4 (1.3%) were expressed only in controls and 81 (25.9%) were specifically activated by one or more stresses. Figure 6 reports the number of LTR-REs expressed (i.e. with more than one mapped read per million) after different stresses (in both short and prolonged treatments). Of 264 LTR-REs expressed during one or more stresses, 87 (33.0%) were active under each stress. Fifty-six elements (21.2%) were specifically active during drought treatments, 30 (11.4%) during salt treatments and 35 (13.3%) during both drought and salt stresses, indicating that these treatments were the most effective in inducing LTR-RE expression. On the contrary, cold and heat stresses induced only a limited number of LTR-REs (Fig. 6).

We also analysed differential expression of LTR-REs during the different stresses compared to the controls. Considering only the 72 highly expressed elements (MRpM > 10), 70 showed differential expression (fold change > 2, FDR-corrected $p < 0.05$) in at least one treatment (Fig. 7). No elements were differentially expressed along all treatments. In most cases, the same LTR-RE was under-expressed (blue in Fig. 7) or unaffected (white in Fig. 7) during the different stresses. Only 7 LTR-REs were induced (red in Fig. 7) or unaffected. Thirteen elements were repressed by certain treatments, activated by other, or unaffected (blue, red, or white in Fig. 7).

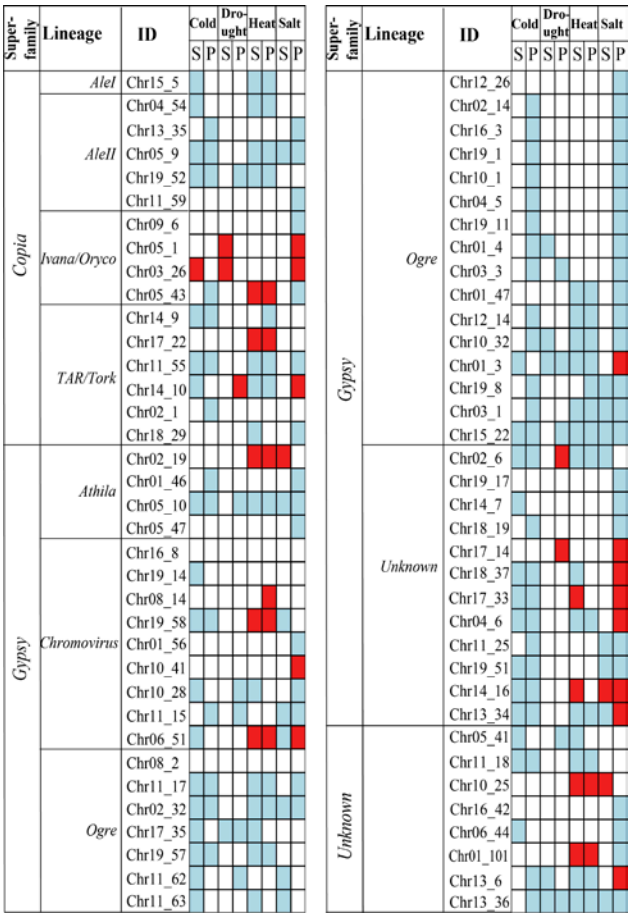

Fig. 7. Differential expression (fold change > 2, FDR-corrected $p < 0.05$) of LTR-REs after short (S) or prolonged (P) treatments with different stresses compared to controls. Blue cells refer to under-expression, red cells to over-expression, white cells indicate no effect of the treatment in comparison to control.

DISCUSSION

Availability of the updated sequence of the *P. trichocarpa* genome and of genomic DNA and cDNA libraries obtained from plants of the same genotype and subjected to different treatments, allowed us to evaluate several factors which can influence the expression of LTR-REs in this species.

In general, our data confirmed that the expression of retrotransposons is generally limited: only 72 out of 828 LTR-REs were mapped by more than ten reads per million. The transcription of REs have been reported in tissues and organs of many plant species (Grandbastien 2015), related to biotic and abiotic stresses or even without apparent induction. In rice, sunflower, *Citrus sinensis*, and even in poplars certain LTR-REs are actively transcribed (Rico-Cabanas and Martínez-Izquierdo

2007; Vukich et al. 2009; Gao et al. 2015; Giordani et al. 2016). However, the majority of LTR-REs are barely expressed (Vicient et al. 2001; Ishiguro et al. 2014; Vangelisti et al. 2019).

In some cases, specific LTR-RE sublineages have been shown to be activated and possibly over-expressed by different culture conditions, as tissue culture (Kashkush et al. 2003; Liu et al. 2004), wounding, methyl jasmonate and fungal elicitors (Takeda et al. 1999), various phytohormones and cold stress (He et al. 2010, 2012), heat stress (Ito et al. 2013). Hormones, and biotic/abiotic stresses induced a general LTR-RE activation in pine (Voronova et al. 2014; Fan et al. 2014) and in sunflower (Vangelisti et al. 2019). In the present study, as in all previous works, the same treatment up-regulated certain LTR-REs and repressed or unaffected other elements.

In *P. trichocarpa*, the overall RE expression level was higher in leaves of control plants than in those of plants exposed to different stresses, suggesting that plants responded to stresses increasing defence mechanisms related to REs. This is different from what found by Vangelisti et al (2019) in roots of sunflower: in this species, the expression level of LTR-REs remained substantially very low but it slightly increased after different stresses. Although the generally low level of LTR-REs expression, more than 40 elements showed a significant activity (more than 10 mapped reads x million), either in controls and stressed plants, suggesting that they are not silenced and hence may still have mutagenic potential, if retrotranscription and insertion in new sites would occur after expression.

The comparison, for each LTR-RE, of the abundance in the genome and its expression in leaves of control or stressed plants, showed that most expressed elements are generally lowly abundant. Such lack of correlation between LTR-RE abundance and transcription is not surprising: other studies showed that the more an element is repeated the more it is recognized by the RNA silencing machinery (Meyers et al. 2001; Yamazaki et al. 2001; Lisch 2009).

Low levels of transcription of repeated sequences are often attributed to DNA contamination of RNA samples. The low expression level of most abundant LTR-REs suggested also that the occurrence of retrotransposon-related reads in the cDNA libraries was not due to DNA contamination.

Genome localization of highly expressed (MRpM > 10) LTR-REs indicated that, in poplar, the expression of an element is only slightly related to its chromosomal localization, because the profiles of expressed LTR-REs parallels those of all LTR-REs. However, we observed a few specific chromosome regions showing differences between profiles of all the LTR-REs and expressed LTR-REs, suggesting that some regions are specifically activated or repressed. In species with much larger genomes than poplar, as the sunflower, LTR-RE expression was observed in specific genomic regions, relatively distant from putative centromeres, and preferentially located at chromosome ends (Mascagni et al. 2019).

Concerning the relationship between expression and superfamily/lineage of the elements, our results showed that expression of *Gypsy* REs was higher than expression of *Copia* elements. At lineage level, *Ogre* LTR-REs were by far the most transcribed elements. Among *Copia* lineages, the most expressed were *SIRE* and *TAR/Tork*, indicating that, besides chromosomal localization and genome abundance, also the "genotype" of the LTR-RE may play a role in its activation. Our results confirmed what previously shown in other studies, since many of the LTR-REs expressed in other species are actually of the *Copia* superfamily (Ma et al. 2008). In the case of tobacco, both *Tnt1* and *Tto1* (which are induced by tissue culture) belong to the *TAR/Tork* lineage (Neumann et al. 2019). *Gypsy* LTR-RE induction was reported in cotton (Hawkins et al. 2006), one of the families analyzed in that study belonged to the *Ogre* lineage. It can be concluded that, probably, different LTR-RE lineages are specifically activated in different species.

It can be assumed that young LTR-REs are more prone to be expressed than older elements, probably because the host needs time to develop defence mechanisms against new elements. *Ogre* and *TAR/Tork* elements are the youngest LTR-REs in *P. trichocarpa* (Mascagni et al. 2018b): this could explain why these two lineages showed the highest percentages of expressed elements.

Although most LTR-REs were expressed at the same level in plants subjected to different treatments, two stresses (salt and drought) specifically induced a number of LTR-REs. No elements were always induced or always repressed by every stress. In some cases, the same element was up-regulated by one stress and repressed by another, probably because of the occurrence, within the LTRs, of *cis*-regulatory motifs recognized in specific stresses, as those identified in the LTR of the *Ha*CRE1 element of sunflower (Buti et al. 2009).

In conclusion, this study outlines a general picture of LTR-RE activity in leaves of poplar plants treated with different stresses. Results allowed us to have a global insight on the features that affect LTR-RE expression. Since LTR-RE expression is just the first stage of retrotransposition, further studies are necessary to estimate subsequent stages of retrotransposition, including the

insertion of new elements in the genome, in order to clarify the biological significance of retrotransposon activity.

FUNDING

Research work funded by Department of Agriculture, Food, and Environment, University of Pisa, Italy, project PLANTOMICS.

DATA AVAILABILITY STATEMENT

The set of 828 full length LTR-REs of *P. trichocarpa* is available at the sequence repository of the Department of Agriculture, Food and Environment, University of Pisa (http://pgagl.agr.unipi.it/sequence-repository/).

REFERENCES

Baggerley KA, Deng L, Morris JS, Aldaz CM. 2003. Differential expression in SAGE: accounting for normal between-library variation. Bioinformatics. 19: 1477–1483.

Barghini E, Mascagni F, Natali L, Giordani T, Cavallini A. 2015a Analysis of the repetitive component and retrotransposon population in the genome of a marine angiosperm, *Posidonia oceanica* (L.) Delile. Mar Genomics. 24: 397–404.

Barghini E, Natali L, Giordani T, Cossu RM, Scalabrin S, Cattonaro F, Šimková H, Vrána J, Doležel J, Morgante M, Cavallini A. 2015b. LTR retrotransposon dynamics in the evolution of the olive (*Olea europaea*) genome. DNA Res. 22: 91-100.

Benjamini Y, Hochberg Y. 1995. Controlling the false discovery rate: a practical and powerful approach to multiple testing. J R Statistic Soc. 57: 289-300.

Bennetzen JL. 2000. Transposable elements contributions to plant gene and genome evolution. Plant Mol Biol. 42: 251–269.

Bolger AM, Lohse M, Usadel B. 2014. Trimmomatic: a flexible trimmer for Illumina sequence data. Bioinformatics. 30: 2114-2120.

Butelli E, Licciardello C, Zhang Y, Liu J, Mackay S, Bailey P. 2012. Retrotransposons control fruit-specific, cold-dependent accumulation of anthocyanins in blood oranges. Plant Cell. 24: 1242-1255.

Buti M, Giordani T, Vukich M, Gentzbittel L, Pistelli L, Cattonaro F, Morgante M, Cavallini A, Natali L. 2009. HACRE1, a recently inserted *Copia*-like retrotransposon of sunflower (*Helianthus annuus* L.). Genome. 52: 904-911.

Buti M, Moretto M, Barghini E, Mascagni F, Natali L, Brilli M, Lomsadze A, Sonego P, et al. 2018. The genome sequence and transcriptome of *Potentilla micrantha* and their comparison to *Fragaria vesca* (the woodland strawberry). GigaScience. 7: 1-14.

Chang W, Jääskeläinen M, Li S, Schulman AH. 2013. BARE retrotransposons are translated and replicated via distinct RNA pools. PLoS ONE. 8: e72270.

Cossu RM, Buti M, Giordani T, Natali L, Cavallini A. 2012. A computational study of the dynamics of LTR retrotransposons in the *Populus trichocarpa* genome. Tree Genet Genomes. 8: 61–75.

Dieguez MJ, Vaucheret H, Paszkowski J, Mittelsten Scheid O. 1998. Cytosine methylation at CG and CNG sites is not a prerequisite for the initiation of transcriptional gene silencing in plants, but it is required for its maintenance. Mol Gen Genet. 259: 207–215.

Ellinghaus D, Kurtz S, Willhoeft U. 2008. LTRharvest, an efficient and flexible software for *de novo* detection of LTR retrotransposons. BMC Bioinformatics. 9: 18.

Falchi R, Vendramin E, Zanon L, Scalabrin S, Cipriani G, Verde I, et al. 2013. Three distinct mutational mechanisms acting on a single gene underpin the origin of yellow flesh in peach. Plant J. 76: 175-187.

Fan FH, Cui BW, Zhang T, Ding GJ, Wen XP. 2014. LTR-retrotransposon activation, IRAP marker development and its potential in genetic diversity assessment of masson pine (*Pinus massoniana*). Tree Genet Genomes. 10: 213–222.

Filichkin SA, Hamilton M, Dharmawardhana PD, Singh SK, Sullivan C, Ben-Hur A, Reddy ASN, Jaiswal P. 2018. Abiotic stresses modulate landscape of poplar transcriptome via alternative splicing, differential intron retention, and isoform ratio switching. Front Plant Sci. 9: 5.

Gao X, Zhou J, Li J, Zou X, Zhao J, Li Q, et al. 2015. Efficient generation of marker-free transgenic rice plants using an improved transposon-mediated transgene reintegration strategy. Plant Physiol. 167: 11-24.

Giordani T, Cossu RM, Mascagni F, Marroni F, Morgante M, Cavallini A, Natali L. 2016. Genome-wide analysis of LTR-retrotransposon expression in leaves of Populus × canadensis water-deprived plants. Tree Genet Genomes. 12: 75.

Grandbastien MA. 1998. Activation of plant retrotransposons under stress conditions. Trends Plant Sci. 3: 181–189.

Grandbastien MA. 2015. LTR retrotransposons, handy hitchhikers of plant regulation and stress response. Biochim Biophys Acta. 1849: 403–416.

Hawkins JS, Kim HR, Nason JD, Wing RA, Wendel JF. 2006. Differential lineage-specific amplification of transposable elements is responsible for genome size variation in *Gossypium*. Genome Res. 16: 1252-1261.

He P, Ma Y, Dai HY, Li LG, Liu YX, Li H, Zhao GL, Zhang ZH. 2012. Characterization of the hormone and stress-induced expression of FaRE1 retrotransposon promoter in strawberry. J Plant Biol. 55: 1–7.

He P, Ma Y, Zhao G, Dai H, Li H, Chang L, Zhang ZH. 2010. FaRE1: a transcriptionally active *Ty1-copia* retrotransposon in strawberry. J Plant Res. 123: 707–714.

Ishiguro S, Ogasawara K, Fujino K, Sato Y, Kishima Y. 2014. Low temperature-responsive changes in the anther transcriptome's repeat sequences are indicative of stress sensitivity and pollen sterility in rice strains. Plant Physiol. 164: 671–682.

Islam-Faridi MN, Nelson CD, DiFazio SP, Gunter LE, Tuskan GA. 2009. Cytogenetic analysis of Populus trichocarpa - ribosomal DNA, telomere repeat sequence, and marker-selected BACs. Cytogenet Genome Res. 125: 74–80.

Ito H, Yoshida T, Tsukahara S, Kawabe A. 2013. Evolution of the ONSEN retrotransposon family activated upon heat stress in Brassicaceae. Gene. 518: 256–261.

Ito H. 2013. Small RNAs and regulation of transposons in plants. Genes Genet Syst. 88: 3–7.

Kashkush K, Feldman M, Levy AA. 2003. Transcriptional activation of retrotransposons alters the expression of adjacent genes in wheat. Nat Genet. 33: 102–106.

Lisch D. 2009. Epigenetic regulation of transposable elements in plants. Annu Rev Plant Biol. 60: 43–66.

Lisch D. 2013. How important are transposons for plant evolution? Nat Rev Genet. 14: 49-61.

Liu Z, Han PF, Tan M, Shan XH, Dong YZ, Wang XZ, Fedak G, Hao S, Liu B. 2004. Activation of a rice endogenous retrotransposon *Tos17* in tissue culture is accompanied by cytosine demethylation and causes heritable alteration in methylation pattern of flanking genomic regions. Theor Appl Genet. 109: 200–209.

Lu X, Chen D, Shu D, Zhang Z, Wang W, Klukas C, Chen L, Fan Y, Chen M, Zhang C. 2013. The differential transcription network between embryo and endosperm in the early developing maize seed. Plant Physiol. 162: 440–455.

Ma Y, Sun HY, Zhao GL, Dai HY, Gao XY, Li H, Zhang ZH. 2008. Isolation and characterization of genomic retrotransposon sequences from octoploid strawberry (*Fragaria* × *ananassa* Duch.). Plant Cell Rep. 27: 499–507.

Mascagni F, Cavallini A, Giordani T, Natali L. 2017. Different histories of two highly variable LTR retrotransposons in sunflower species. Gene. 634: 5-14.

Mascagni F, Vangelisti A, Giordani T, Cavallini A, Natali L. 2018a. Specific LTR-retrotransposons show copy number variations between wild and cultivated sunflowers. Genes. 9: 433.

Mascagni F, Usai G, Natali L, Cavallini A, Giordani T. 2018b. A comparison of methods for LTR-retrotransposon insertion time profiling in the *Populus trichocarpa* genome. Caryologia. 71: 85-92.

Mascagni F, Vangelisti A, Usai G, Giordani T, Cavallini A, Natali L. 2019. A computational genome-wide analysis of long terminal repeats retrotransposon expression in sunflower roots (*Helianthus annuus* L.). Submitted.

Meignin C, Bailly JL, Arnaud F, Dastugue B, Vaury C. 2003. The 5' untranslated region and gag product of Idefix, a long terminal repeat retrotransposon from *Drosophila melanogaster*, act together to initiate a switch between translated and untranslated states of the genomic mRNA. Mol Cell Biol. 23: 8246–8254.

Meyers BC, Tingey SV, Morgante M. 2001. Abundance, distribution, and transcriptional activity of repetitive elements in the maize genome. Genome Res. 11: 1660–1676.

Mortazavi A, Williams BA, McCue K, Schaeffer L, Wold B. 2008. Mapping and quantifying mammalian transcriptomes by RNA-seq. Nature Meth. 5: 621–628.

Natali L, Cossu RM, Mascagni F, Giordani T, Cavallini A. 2015. A survey of *Gypsy* and *Copia* LTR-retrotransposon superfamilies and lineages and their distinct dynamics in the *Populus trichocarpa* (L.) genome. Tree Genet. Genomes. 11: 107.

Neumann P, Navrátilová A, Koblížková A, Kejnovský E, Hřibová E, Hobza R, Widmer A, Doležel J, Macas J. 2011. Plant centromeric retrotransposons: a structural and cytogenetic perspective. Mob DNA. 2: 4.

Neumann P, Novák P, Hoštáková N, Macas J. 2019. Systematic survey of plant LTR retrotransposons elucidates phylogenetic relationships of their polyprotein domains and provides a reference for element classification. Mob DNA. 10: 1.

Novák P, Neumann P, Pech J, Steinhaisl J, Macas J. 2013. RepeatExplorer: a galaxy based web server for genome-wide characterization of eukaryotic repetitive elements from next generation sequence reads. Bioinformatics. 29: 792–793.

Rico-Cabanas L, Martínez-Izquierdo JA. 2007. CIRE1, a novel transcriptionally active *Ty1-copia* retrotransposon from *Citrus sinensis*. Mol Genet Genom. 277: 365.

SanMiguel P, Gaut BS, Tikhonov A, Nakajima Y, Bennetzen JL. 1998. The paleontology of intergene retrotransposons of maize. Nat Genet. 20: 43–45.

Slavov GT, DiFazio SP, Martin J, Schackwitz W, Muchero W, Rodgers-Melnick E, Lipphardt MF et al. 2012. Genome resequencing reveals multiscale geographic structure and extensive linkage disequilibrium in the forest tree Populus trichocarpa. New Phytol. 196: 713–725.

Slotkin RK, Martienssen R. 2007. Transposable elements and the epigenetic regulation of the genome. Nat Rev Genet. 8: 272–285.

Sonnhammer EL, Durbin R. 1995. A dot-matriprogram with dynamic threshold control suited for genomic DNA and protein sequence analysis. Gene. 167: GC1–GC10.

Springer NM, Ying K, Fu Y, Ji T, Yeh CT, Jia Y, et al. 2009. Maize inbreds exhibit high levels of copy number variation (CNV) and presence/absence variation (PAV) in genome content. PLoS Genet. 5: e1000734.

Takeda S, Sugimoto K, Otsuki H, Hirochika H. 1999. A 13-bp cis-regulatory element in the LTR promoter of the tobacco retrotransposon *Tto1* is involved in responsiveness to tissue culture, wounding, methyl jasmonate and fungal elicitors. Plant J. 18: 383–393.

Tuskan GA, DiFazio S, Jansson S, Bohlmann J, Grigoriev I, Hellsten U, Putnam N, Ralph S, Rombauts S, Salamov A, Schein J, Sterck L, Aerts A, Bhalerao RR, Bhalerao RP, Blaudez D, Boerjan W, Brun A, Brunner A, Busov V, Campbell M, Carlson J, Chalot M, Chapman J, Chen GL, Cooper D, Coutinho PM, Couturier J, Covert S, Cronk Q, Cunningham R, Davis J, Degroeve S, Déjardin A, dePamphilis C, Detter J, Dirks B, Dubchak I, Duplessis S, Ehlting J, Ellis B, Gendler K, Goodstein D, Gribskov M, Grimwood J, Groover A, Gunter L, Hamberger B, Heinze B, Helariutta Y, et al. 2006. The genome of black cottonwood, *Populus trichocarpa* (Torr. & Gray). Science. 313: 1596-1604.

Usai G, Mascagni F, Natali L, Giordani T, Cavallini A. 2017. Comparative genome-wide analysis of repetitive DNA in the genus *Populus* L. Tree Genet Genomes. 13: 96.

Vangelisti A, Mascagni F, Giordani T, Sbrana C, Turrini A, Cavallini A, Giovannetti M, Natali L. 2019. Arbuscular mycorrhizal fungi induce the expression of specific retrotransposons in roots of sunflower (*Helianthus annuus* L.). PLoS ONE. 14: e0212371.

Vicient CM, Suoniemi A, Anamthawat-Jonsson K, Tanskanen J, Beharav A, Nevo E, Schulman AH. 1999. Retrotransposon BARE-1 and its role in genome evolution in the genus *Hordeum*. Plant Cell. 11: 1769–1784.

Vicient CM, Jaaskelainen MJ, Kalendar R, Schulman AH. 2001. Active retrotransposons are a common feature of grass genomes. Plant Physiol. 125: 1283–1292.

Vitte C, Fustier MA, Alix K, Tenaillon MI. 2014. The bright side of transposons in crop evolution. Briefings Funct Genom. 13: 276-295.

Voronova A, Belevich V, Rungis D, Jansons A. 2014. Stress-induced transcriptional activation of retrotransposon-like sequences in the Scots pine (*Pinus sylvestris* L.) genome. Tree Genet Genomes. 10: 937–951.

Vukich M, Giordani T, Natali L, Cavallini A. 2009. *Copia* and *Gypsy* retrotransposons activity in sunflower (*Helianthus annuus* L.). BMC Plant Biol. 9: 150.

Wicker T, Sabot F, Hua-Van A, Bennetzen JL, Capy P, Chalhoub B, Flavell A, Leroy P, Morgante M, Panaud O, Paux E, SanMiguel P, Schulman AH. 2007. A unified classification systemfor eukaryotic transposable elements. Nature Rev Genet. 8: 973–982.

Xu Z, Wang H. 2007. LTR_FINDER: an efficient tool for the prediction of full-length LTR retrotransposons. Nucleic Acids Res. 35: W265–W268.

Yamazaki M, Tsugawa H, Miyao A, Yano M, Wu J, Yamamoto S, et al. 2001. The rice retrotransposon *Tos17* prefers low-copy-number sequences as integration targets. Mol Genet Genomics. 265: 336–344.

Zeng L, Zhang N, Zhang Q, Endress PK, Huang J, Ma H. 2017. Resolution of deep eudicot phylogeny and their temporal diversification using nuclear genes from transcriptomic and genomic datasets. New Phytol. 214: 1338-1354.

Caryologia
International Journal of Cytology, Cytosystematics and Cytogenetics

Firenze University Press
www.fupress.com/caryologia

OPEN ACCESS

Citation: H. Myoshu, M.A. Iwasa (2019) Differences in C-band patterns between the Japanese house mice (*Mus musculus*) in Hokkaido and eastern Honshu. *Caryologia* 72(2): 81-90. doi: 10.13128/cayologia-237

Published: December 5, 2019

Data Availability Statement: All relevant data are within the paper and its Supporting Information files.

Competing Interests: The Author(s) declare(s) no conflict of interest.

Differences in C-band patterns between the Japanese house mice (*Mus musculus*) in Hokkaido and eastern Honshu

Hikari Myoshu, Masahiro A. Iwasa*

Course in Natural Environment Studies, Graduate School of Bioresource Sciences, Nihon University, Kameino 1866, Fujisawa, Kanagawa 252-0880, Japan
*Corresponding author, e-mail: iwasa.masahiro@nihon-u.ac.jp

Abstract. We characterized and categorized the C-band patterns of the house mouse *Mus musculus* from four areas in Hokkaido and Honshu of the Japanese Islands as a biparental marker. The C-band patterns are categorized as polymorphic, monomorphic, or intermediate, corresponding to those of the Korean mice, C57BL/6, and F1 hybrid mice bred from the Japanese mice and a laboratory mouse, respectively. The C-band patterns mainly differ between mice from Hokkaido and Honshu. The polymorphic patterns are shown in mice in Honshu, while the intermediate patterns are shown in mice in Hokkaido, with an exceptional case of a monomorphic pattern found in one locality. In the other localities of Hokkaido and northeastern Honshu, the C-band patterns are not congruent with an estimation by maternal element in our previous study, whereas the congruence is observed in other localities. It is suggested that the characteristics of the Japanese house mice have been formed through complicated processes by different expansions between biparental and maternal elements.

Keywords. C-band pattern, *Mus musculus*, the Japanese house mouse, hybridization, replacement.

INTRODUCTION

The Japanese house mouse, *Mus musculus* (Mammalia, Rodentia), has been colonized in the Japanese Islands through artificially complicated processes by overseas mice based on the genetic and morphological analyses (Myoshu and Iwasa 2018). According to previous studies of intraspecific variations of mitochondrial DNA (mtDNA) haplotypes, the Japanese house mice have been derived from two lineages as the MUS and CAS types, corresponding to the subspecific *musculus* and *castaneus*, respectively, that currently occur in the Korean Peninsula and southern China (MUS-1c and CAS-1a groups in Suzuki et al. 2013). In addition, the colonization history of the Japanese house mice is estimated as following scenario: mice migrated primarily from southern China or southeastern Asia; secondarily, mice migrated from the Korean Peninsula and replaced the distributions of the former mice, considering the distribution patterns of mtDNA haplotypes

(Yonekawa et al. 1988; Terashima et al. 2006; Nunome et al. 2010, 2013; Suzuki et al. 2013; Kuwayama et al. 2017; Myoshu and Iwasa 2018). Nuclear genome analysis has shown evidence of the introgression and replacement (Kuwayama et al. 2017). Additionally, many studies suggest recent migrations by stowaway introduction in several areas, including non-port areas (Miyashita et al. 1985; Yonekawa et al. 2000; Tsuda et al. 2001, 2002; Terashima et al. 2006; Nunome et al. 2010; Kodama et al. 2015; Kuwayama et al. 2017; Myoshu and Iwasa 2018).

On the other hand, the distribution of nuclear DNA types is not always congruent with that of mtDNA haplotypes in the Japanese house mice. The sequence of the *musculus* lineage is observed in all targeted regions of the nuclear genome, or relatively short segments of the *castaneus* lineage are observed in some targeted regions, although its samples were obtained from a locality where the CAS type is exclusively observed (Kuwayama et al. 2017). In addition, our previous study (Myoshu and Iwasa 2018) shows that observed external characteristics sometimes do not coincide with the subspecific characteristics estimated by the mitochondrial haplotypes. Thus, these incongruences between nuclear traits and mtDNA traits suggest complicated hybridization and/or replacement process, regarding different progress between biparental and maternal elements. To elucidate the process of replacement by the Korean mice, it is necessary to comprehensively investigate the biparental element by a marker distinguishing the Korean mice.

Cytogenetically, variations in the C-band patterns have been well studied in wild house mice (Dev et al. 1973, 1975; Miller et al. 1976; Moriwaki and Minezawa 1976; Ikeuchi 1978; Moriwaki et al. 1985, 1986; Moriwaki 2010; Yonekawa et al. 2012; Myoshu and Iwasa 2016). By evaluating the C-band patterns, we can confirm whether the Japanese house mice have experienced hybridization and/or replacement with the mice that introduced from northern China and the Korean Peninsula, or not. According to these previous studies, the C-banding patterns of house mice can be roughly categorized into two patterns. The European, central and southern Asiatic, and laboratory mice show a monomorphism of C-band sizes in a homologue; almost all chromosomes carry smaller centromeric C-bands (hereinafter called a "monomorphic pattern"). On the other hand, northern Chinese and/or Korean mice show a polymorphism of C-band sizes in a homologue; a few chromosomes carry larger centromeric C-bands, and most of the residual chromosomes carry no C-band (hereinafter called a "polymorphic pattern"). The C-banding patterns of the Japanese house mice are visually categorized as the latter (Dev et al. 1973, 1975; Moriwaki and Minezawa 1976; Ikeuchi 1978; Moriwaki et al. 1985, 1986, 2009; Moriwaki 2010; Yonekawa et al. 2012), polymorphic states of C-bands (Myoshu and Iwasa 2016). The mice in southern China and/or southeastern Asia, which primarily migrated to the Japanese Islands (Suzuki et al. 2013; Kuwayama et al. 2017), shows the former type of C-band pattern (Moriwaki et al. 1986; Yonekawa et al. 2012). In addition, the C-band patterns of F1 offspring reveal the inheritance states of the C-band size, because the C-band size does not vary over a generation (Dev et al. 1973, 1975; Miller et al. 1976). Thus, the C-band pattern is a useful marker to comprehensively investigate the biparental element.

In this study, we statistically characterized the C-band patterns of house mice from four areas in Hokkaido and Honshu of the Japanese Islands that we previously analysed for mtDNA haplotypes and morphological characteristics (Myoshu and Iwasa 2018). According to results of previous mtDNA analysis and the present analysis, we elucidated the migration, hybridization, and replacement processes of maternal and biparental elements in the four areas.

MATERIALS AND METHODS

Mouse samples

Wild-caught mice of the Japanese Islands (*Mus musculus*) were collected (n = 31; Table 1 and Figure 1) in the Sorachi and Iburi areas of Hokkaido (n = 3; HKD1, including BBI and HYK; Table 1, 1 and 2 in Figure 1(a)), the Hidaka area of Hokkaido (n = 8; HKD2, including MID, KB1, KB2, and NK2; Table 1, 3 to 6 in Figure 1(a)), Iwate and Miyagi Prefectures in Honshu (n = 3; HON1, including SYG, TNS, and FTK; Table 1, 7 to 9 in Figure 1(b)) and Kanagawa and Chiba Prefectures in Honshu (n = 11; HON2, including KZK, KMN, OHB, and CGS; Table 1, 10 to 12 in Figure 1(c)) using Sherman traps baited with oatmeal. We used the same division names and abbreviations of areas and localities in this study as in Myoshu and Iwasa (2018). In addition, a wild-caught mouse (*M. musculus*) collected in Seongmodo Island, neighboring the Korean Peninsula, was used (n = 1; SMD in Table 1; 14 in Figure 1(d)). A laboratory mouse (C57BL/6, Japan SLC Inc.) was also used for the analysis as a standard. Moreover, hybrid mice from a cross experiment using a female wild-caught mouse from Kanagawa Prefecture (specimen nos.: MAI-1239, 1306 and 1308) and a male C57BL/6N were analyzed (n = 3; Table 1) to confirm intermediate C-banding patterns from their parents.

Table 1. House mouse samples examined in this study.

Collecting locality (code*)	Specimen No. (sex)
Wild caught mice	
Sorachi and Iburi areas, Hokkaido, Japan (HKD1)	
Koshunai-cho, Bibai, Hokkaido (BBI, 1)	MAI-1919 (f)
Hayakita-tomioka, Abira-cho, Yufursu-gun, Hokkaido (HYK, 2)	MAI-1895 (f), 1915 (m)
Hidaka area, Hokkaido Japan (HKD2)	
Midorimachi, Hidaka-cho, Saru-gun, Hokkaido (MID,3)	MAI-1837 (m), 1840 (f)
Kabari, Hidaka-cho, Saru-gun, Hokkaido (KB1, 4)	MAI-1916 (m), 1917 (m)
Kabari, Hidaka-cho, Saru-gun, Hokkaido (KB2, 5)	MAI-1913 (m), 1918 (f)
Bansei, Niikappu-cho, Niikappu-gun, Hokaido (NK2, 6)	MAI-2004 (f), 2016 (m)
Northeastern Honshu area, Japan (HON1)	
Shimoyahagi, Rikuzentakata, Iwate Pref., Honshu (SYG, 7)	MAI-1289 (m)
Takinosato, Rikuzentakata, Iwate Pref., Honshu (TNS, 8)	MAI-1293 (m)
Futaki, Sendai, Miyagi Pref., Honshu (FTK, 9)	MAI-1843 (m)
Central Honshu area, Japan (HON2)	
Kohzaki, Katori-gun, Chiba Pref., Honshu (KZK, 10)	MAI-1991 (m), 1992 (f)
Kameino, Fujisawa, Kanagawa Pref., Honshu (KMN, 11)	MAI-1114 (f), 1120 (f), 1443 (m), 1444 (f)
Ohba, Fujisawa, Kanagawa Pref., Honshu (OHB, 12)	MAI-1239 (f), 1306 (f), 1308 (f), 1309 (m)
Akabane, Chigasaki, Kanagawa Pref., Honshu (CGS, 13)	MAI-1548 (f)
Korea	
Seongmodo Is., Ganghwa-gun, Incheon-gwangyeoksi, Korea (SMD, 14)	HEG007-97 (m)
Laboratory mouse C57BL/6N	MAI-1301 (m)
Hybrid mice (wild caught mice x Laboratory mouse)	
MAI-1239 x 1301	MAI-1450 (f), MAI-1452 (f)
MAI-1306 x 1301	MAI-1379 (f)
MAI-1308 x 1301	MAI-1563 (m)

*Code numbers are corresponding to those in Figure 1.

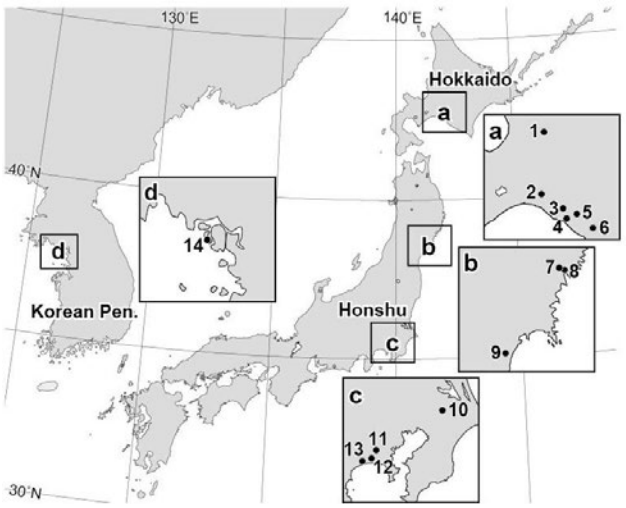

Fig. 1. Collection localities of the house mice examined in this study. Locality code numbers correspond to those in Table 1.

C-banding for somatic cells

Chromosome preparations were performed from bone marrow cells. Bone marrow cells were cultured in MEM including 15% calf serum containing colchicine (final concentration: 0.025 μg/ml) at 37 ˚C for 40 min. These cells were treated in 0.075 M KCl at 37 ˚C for 20 min as a hypotonic treatment. Subsequently, the cells were fixed with modified Carnoy's fixative (methanol : acetic acid = 3 : 1) three times. Then air-dried cells were primarily G-banded using the ASG technique (Sumner et al. 1971) to identify each chromosome by Committee of Standardized Genetic Nomenclature for Mice (1972) and Cowell (1984). After destaining using Carnoy's fixative, the cells were subsequently C-banded using the BSG technique by Summer (1972).

Quantification of the C-band pattern

Photographs of somatic metaphases were obtained using a digital camera under a microscope (Olym-

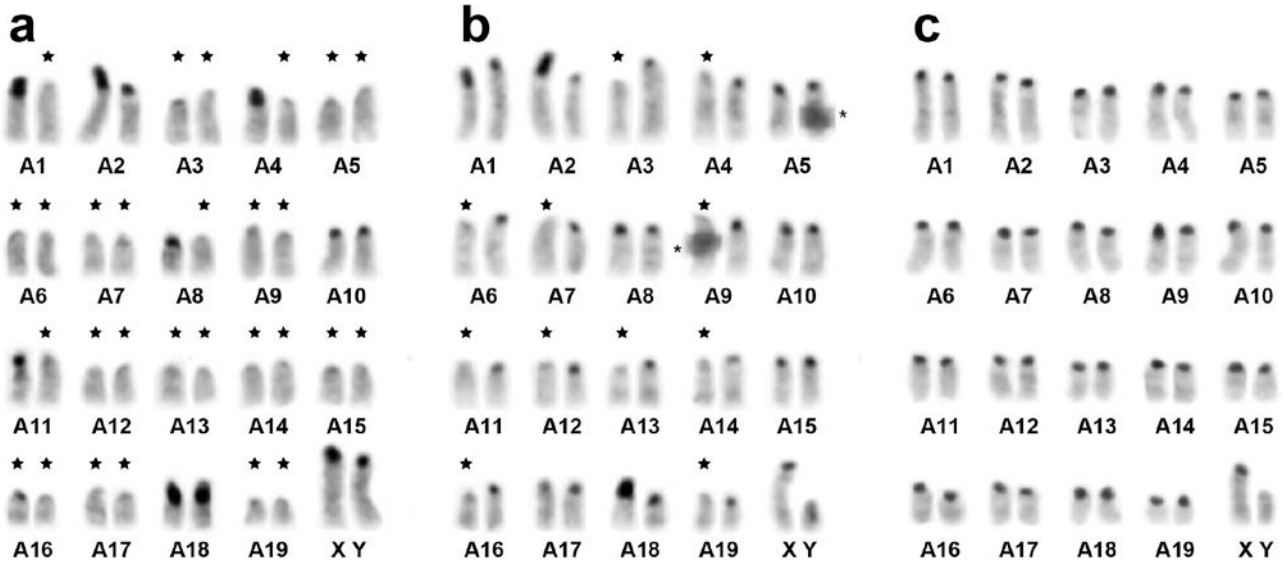

Fig. 2. Typical C-banded karyotypes of a wild-caught mouse (a, MAI-1239), a hybrid mouse (b, MAI-1452), and a C57BL/6N mouse (c, MAI-1301). Stars indicate chromosomes with null C-bands. Asterisks indicate crossing of chromosomes.

pus BX41). To correct errors caused by variations in the extension condition of chromosomes among metaphase plates, we calculated the relative lengths of the C-bands. Primarily, the boundary between negatively and positively stained regions was identified at the proximal region of the long arm in the No. 2 chromosomes according to Myoshu and Iwasa (2016). Subsequently, the distance from the distal end of the long arm to the proximal boundary of the negatively stained region was measured in one of the No. 2 chromosomes as a control length for all relative lengths on its metaphase using Adobe Illustrator CC. In addition, the lengths of all of positively C-banded regions on all chromosomes were measured by the same method. Finally, the relative lengths of the C-bands on each chromosome were calculated using following formula: the length of the positively stained C-band region of each chromosome / the control length of the No. 2 chromosome in its metaphase plate. When a positively stained C-band region was not observed in a chromosome or when the entire chromosome was stained lightly, as seen in the Y chromosome (Figure 2), we considered relative length of the chromosome to be zero. The relative lengths of C-bands for all chromosomes were calculated in five or more metaphase plates per individual.

All of the relative lengths of C-bands were categorized as classes by 0.1. The mean number of chromosomes of each class in an individual was calculated using following formula: the observed number of chromosomes included in each class in an individual / the number of observed metaphase plates in an individual. Regarding the set of all mean numbers in each class for an individual as the C-band pattern of the individual, we performed a clustering analysis for the C-band patterns of all individuals to estimate analogies among them. We first calculated Euclidian distances using all sets of the mean numbers for each class from all mouse samples. Then we performed a clustering analysis using the ward method based on these distances.

RESULTS

In the karyotypes of wild-caught mice, the hybrid individuals and C57BL/6, typical examples of the C-banded metaphases (samples prepared from wild-caught mice in SMD, HON1, HON2, NK2, and HKD1, and from C57BL/6N and the hybrid mice) were shown in Figure 3. These C-banding patterns showed the presence of chromosomes with null C-bands in the mouse samples without C57BL/6N carrying the Y chromosome negatively stained by C-banding (Figures 2 and 3). The C-band patterns of the hybrid individual seemed to be inherited from those of the parents (a wild-caught mouse and C57BL/6N) as their intermediate type (Figure 2). In addition, size variations of C-bands seemed to be confirmed in all of the mice excluding C57BL/6 (Figures 2 and 3).

The mean numbers of chromosomes with a C-band and with a null C-band were classified into classes based on the relative length; 0.01–0.10, 0.11–0.20, 0.21–0.30, 0.31–0.40, 0.41–0.50, and >0.51 as in Table 2, and the

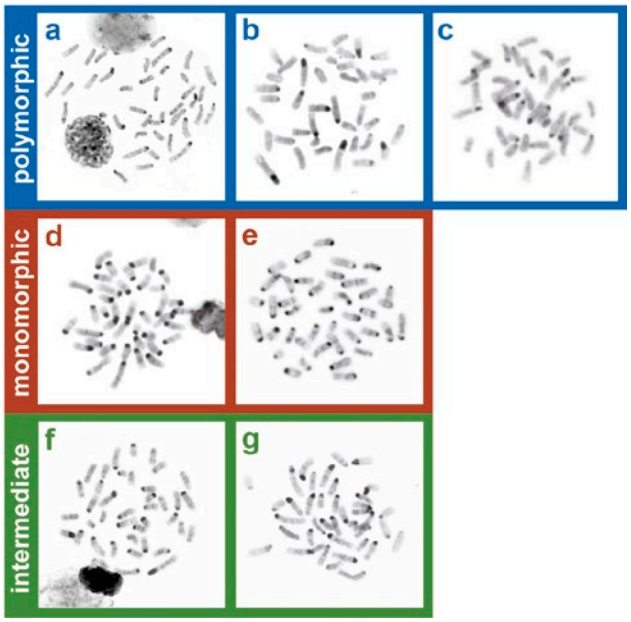

Fig. 3. Typical examples of C-banded metaphase plates of polymorphic patterns: Seongmodo Is. (a, HEG007-97), Ohba (b, MAI-1306), and Takinosato (c, MAI-1293); monomorphic patterns: C57BL/6N (d, MAI-1301) and Niikappu-2 (e, MAI-2004); and intermediate patterns: a hybrid mouse (f, MAI-1379) and Hayakita (g, MAI-1839).

histograms of these mean numbers were indicated in Figure 4. On the basis of our observation and calculation of C-bands on a metaphase plate of C57BL/6 (Table 2 and Figure 3(d), upper histogram in Figure 4), we defined the C-bands (0.01–0.30 in relative length) as "smaller C-bands". In contrast, we defined the C-bands that is never observed in C57BL/6 (> 0.31 in relative length) as 'larger C-bands'. Furthermore, the result of clustering analysis showed clear discriminations with three major clades consisting of the HON1/HON2 mice and the SMD mouse, HKD1/HKD2 (without NK2) mice and the hybrid mice, and HKD2 (NK2) mice and C57BL/6 (Figure 5).

The HON1/HON2 mice and the SMD mouse in a major clade (Figure 5) showed high frequencies of null C-band chromosomes (the mean numbers ranged from 23.6 to 29.5 per metaphase plate, Table 2). In addition, there were residual chromosomes carrying positively stained C-bands showing variable sizes, including larger C-bands with relative lengths of not only 0.31–0.50 but also > 0.51 (sums of the mean numbers of chromosomes with relative lengths of > 0.31 ranged from 1.4 to 7.0 per metaphase). On the other hand, the mean numbers of smaller C-bands were lower (sums of the mean numbers of chromosomes with relative lengths of 0.01–0.30 ranged from 5.2 to 14.4 per metaphase). Of these, smaller C-bands with relative lengths of 0.21–0.30 were observed much more than those with relative lengths of 0.11–0.20 in HON2; however, individuals from HON1 showed the highest number of C-bands with relative lengths of 0.11–0.20 (Table 2 and Figure 4). Moreover, the larger C-bands on the No.2 chromosomes, which were usually observed in the HON1/HON2 mice (Figure 3(b) and 3(c), respectively) were not observed in the SMD mouse (Figure 3(a)).

Furthermore, hybrid mice and the HKD1/HKD2 (without NK2) mice belonged to the other major clade (Figure 5). The mean numbers of null C-bands were apparently lower (the mean numbers ranged from 14.2 to 19.4 per metaphase, Table 2) than those from HON1/HON2 and SMD (the mean numbers ranged from 23.6 to 29.5 per metaphase, Table 2) and higher than those of C57BL/6N and NK2 of HKD2 (the mean numbers ranged from 1.2 to 9.0 per metaphase, Table 2). Additionally, the mean numbers of the smaller C-bands (sums of the mean numbers with relative lengths of 0.01–0.30 ranged from 17.8 to 23.8 per metaphase, Table 2) was also intermediate between those from HON1/HON2 and SMD (5.2~14.4) and that from C57BL/6N (38.8). Moreover, there was lower number of larger C-bands, at least one chromosome per metaphase (sums of the mean numbers with relative lengths of > 0.31 ranged from 0.4 to 1.0 per metaphase, Table 2).

The third major clade consisted of C57BL/6 and mice from NK2 of HKD2 (Figure 5). C57BL/6 showed smaller C-bands in all of the chromosomes (sum of the mean numbers of chromosomes with relative lengths of 0.01–0.30 was 38.8 per metaphase, Table 2). In addition, C57BL/6 showed no larger C-band with relative lengths of > 0.31 and lower numbers of null C-bands (the mean number was 1.2 per metaphase, Table 2). Meanwhile, individuals from NK2 of HKD2 (specimen nos. MAI-2004 and MAI-2016) carried a pattern similar to that of C57BL/6, especially in terms of the higher number of appearances of smaller C-bands (sums of the mean numbers of chromosomes with relative lengths of 0.01–0.30 were 36.2 and 30.0 per metaphase in MAI-2004 and MAI-2016, respectively, Table 2). Moreover, they carried no more than a chromosome with a larger C-band (sums of the mean numbers of chromosomes with relative lengths of > 0.31 were 0.2 and 1.0 per metaphase in MAI-2004 and MAI-2016, respectively, Table 2) and several chromosomes with null C-bands (the mean numbers were 3.6 and 9.0 per cell in MAI-2004 and MAI-2016, respectively).

Table 2. Mean numbers of chromosomes with null C-band and C-band classified into each class of relative length.

Specimen	Null C-band	Classification							
		Smaller C-band Relative length of C-band				Larger C-band Relative length of C-band			
		0.01~0.10	0.11~0.20	0.21~0.30	Total	0.31~0.40	0.41~0.50	>0.51	Total
HKD1									
MAI-1919	19,0	0	10,4	7,6	**18,0**	2,8	0,2	0	**3,0**
MAI-1895	18,2	1,4	11,2	7,6	**20,2**	1,6	0	0	**1,6**
MAI-1915	18,2	0,2	10,6	7,8	**18,6**	3,0	0,2	0	**3,2**
HKD2									
MAI-1837	15,8	1,2	13,4	5,6	**20,2**	2,4	1,4	0	**3,8**
MAI-1840	17,4	0	9,0	8,8	**17,8**	2,6	1,4	0	**4,0**
MAI-1916	19,4	0,8	13,0	5,6	**19,4**	1,2	0	0	**1,2**
MAI-1917	18,2	0,4	10,4	8,2	**19,0**	2,6	0,2	0	**2,8**
MAI-1913	16,6	0	13,3	7,9	**21,2**	1,9	0,3	0	**2,2**
MAI-1918	18,4	0,8	15,6	4,8	**21,2**	0,2	0,2	0	**0,4**
MAI-2004	3,6	1,2	31,4	3,6	**36,2**	0,2	0	0	**0,2**
MAI-2016	9,0	3,2	23,4	3,4	**30,0**	0,6	0,4	0	**1,0**
HON1									
MAI-1289	25,0	0	7,4	5,2	**12,6**	2,0	0,4	0	**2,4**
MAI-1293	23,6	0,4	10,4	3,6	**14,4**	1,2	0,6	0,2	**2,0**
MAI-1843	27,6	0,6	2,8	4,4	**7,8**	2,6	2,0	0,0	**4,6**
HON2									
MAI-1991	28,0	0	1,0	4,6	**5,6**	3,4	2,6	0,4	**6,4**
MAI-1992	27,3	0	3,0	5,0	**8,0**	3,3	0,9	0,6	**4,7**
MAI-1114	29,5	0	1,2	4,0	**5,2**	2,0	1,8	1,5	**5,3**
MAI-1120	29,2	0,2	0,8	4,2	**5,2**	3,2	1,5	1,0	**5,7**
MAI-1443	27,8	0	5,2	5,6	**10,8**	0,8	0,6	0	**1,4**
MAI-1444	29,2	0	0	3,8	**3,8**	2,8	2,6	1,6	**7,0**
MAI-1239	28,2	0,2	1,8	5,4	**7,4**	3,0	1,0	0,4	**4,4**
MAI-1306	24,8	1,3	6,2	3,1	**10,7**	2,4	1,9	0,2	**4,6**
MAI-1308	28,0	0,2	3,8	4,2	**8,2**	2,7	1,0	0,2	**3,8**
MAI-1309	28,0	0	2,4	3,6	**6,0**	2,5	2,2	1,3	**6,0**
MAI-1548	29,2	0	3,6	3,8	**7,4**	2,8	0,6	0	**3,4**
Korea									
HEG007-97	25,2	0,2	9,6	3,4	**13,2**	1,0	0,6	0	**1,6**
Labolatory mouse									
MAI-1301	1,2	0,2	34,8	3,8	**38,8**	0	0	0	**0**
Hybrid mice									
MAI-1450	14,4	0	16,6	7,2	**23,8**	0,8	0,6	0,4	**1,8**
MAI-1452	14,4	0,2	13,2	9,0	**22,4**	1,4	1,0	0,8	**3,2**
MAI-1379	15,8	1,4	16,2	4,0	**21,6**	0,8	1,6	0,2	**2,6**
MAI-1563	14,2	1,6	16,2	4,4	**22,2**	2,8	0,6	0,2	**3,6**

DISCUSSION

The polymorphic pattern in two areas geographically isolated in the Japanese Islands, HKD1/HKD2 (without NK2) and HON1/HON2, are categorized into two groups (Figure 5), which include the SMD and hybrid mice, respectively. On the other hand, the monomorphic pattern consists of many smaller C-bands without a null C-band and a larger C-band (Table 2 and Figure 4) and belongs to the cluster including C57BL/6N (Fig-

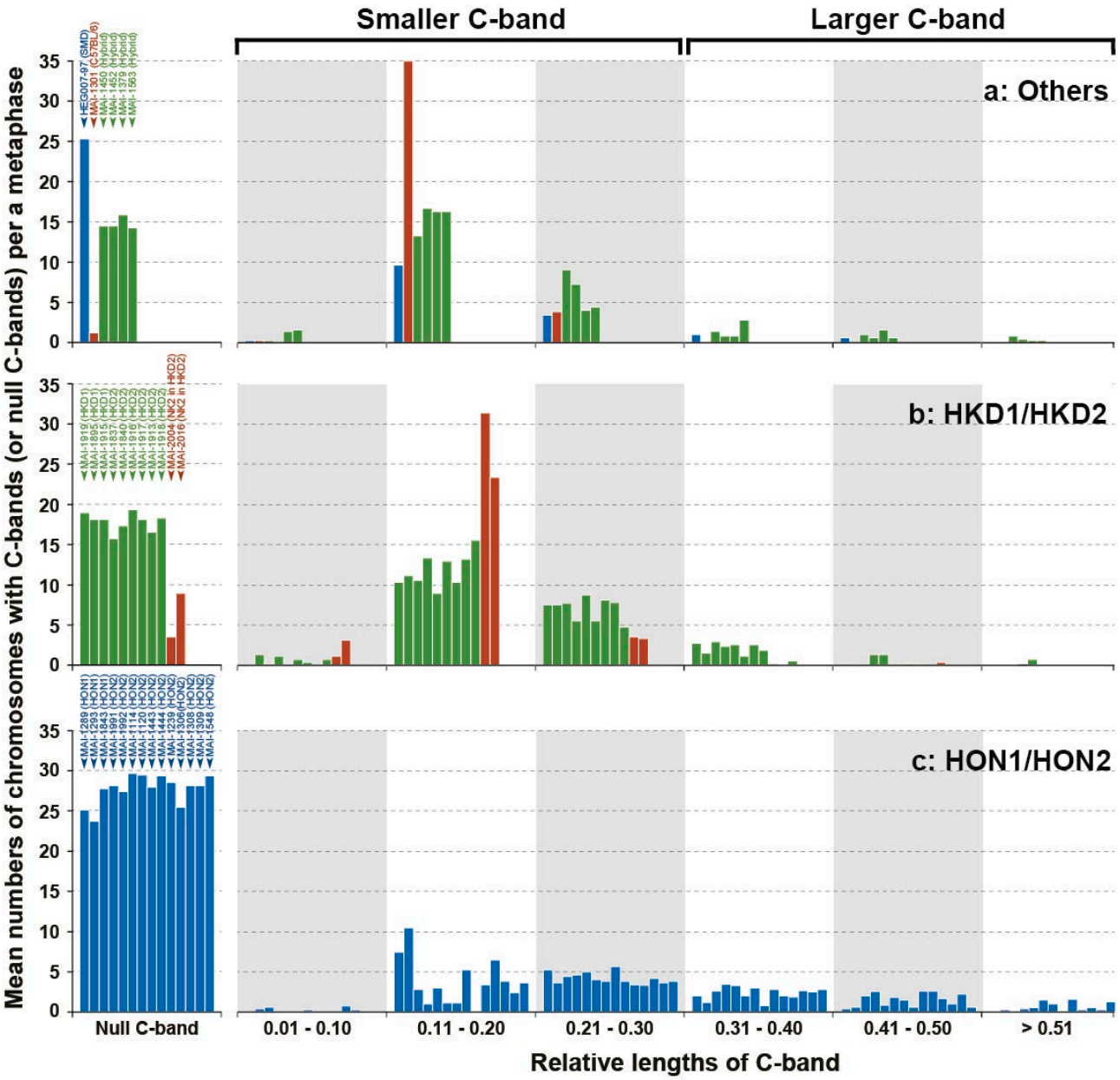

Fig. 4. Histograms showing mean numbers of chromosomes without C-bands or with C-bands per metaphase, classified into each class of relative length with 0.01–0.10, 0.11–0.20, 0.21–0.30, 0.31–0.40, 0.41–0.50, and >0.51.

ure 5). Our previous study (Myoshu and Iwasa 2018) indicates the occurrences of three *Cytb* haplotypes that are confirmed in the same areas of the Japanese Islands, as shown in Table 1. In the areas showing the polymorphic pattern similar to SMD, only the subspecific *castaneus* (CAS) type and only the subspecific *musculus* (MUS) type occur in HON1 and HON2, respectively. Additionally, only the CAS type and multiple haplotypes including the CAS, MUS, and the subspecific *domesticus* (DOM) types occur in the area showing the polymorphic pattern similar to that of hybrid mice, HKD1, and HKD2 without NK2, respectively. On the other hand, not the MUS type but rather the CAS and DOM types occur in NK2 showing the monomorphic pattern. According to these results, a concordant combination between biparental C-band pattern and maternal *Cytb* haplotype is shown in HON2 and HKD2 but is not shown in HON1 and HKD1.

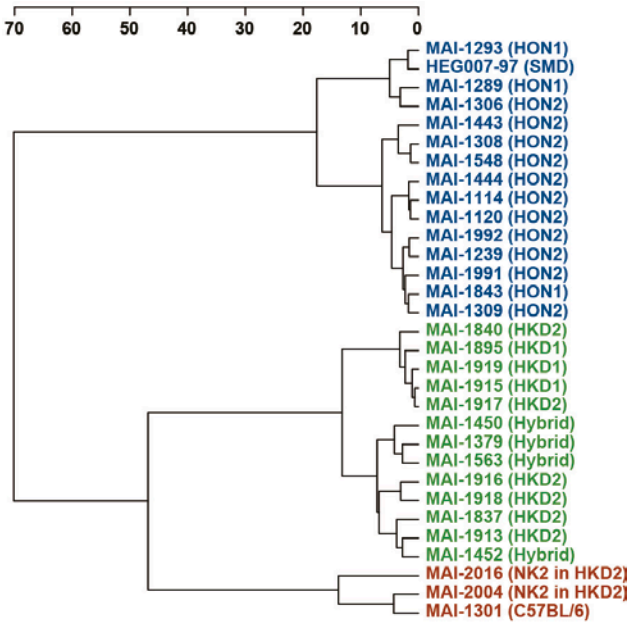

Fig. 5. Cluster analysis considering the mean numbers of chromosomes without C-bands or with C-bands in each class. Top values indicate Euclidian distances.

The present C-band results can agree with the finding of *Cytb* properties in HON2/HKD2 and the potential founders, mice in northern China and/or the Korean peninsula (Yonekawa et al. 1988; Terashima et al. 2006; Nunome et al. 2010, 2013; Suzuki et al. 2013), carry the polymorphic C-bands and the MUS type as in the HON2 mice (Myoshu and Iwasa 2018; Figures 3, 4, 5). On the basis of these results, it is a feasible explanation from both viewpoints by chromosome and mtDNA traits (Myoshu and Iwasa 2018; Figures 3, 4, 5) that the HON2 mice have maintained the traits of potential founders. In HKD2, on the basis of a simple inheritance of the C-band size (Dev et al. 1975; Figure 2), the hybridization between mice carrying a combination of the monomorphic pattern and the CAS or DOM type, and mice carrying a combination of the polymorphic pattern and the MUS type from northern China and/or the Korean peninsula is concordantly estimated by both viewpoints from these analyses (Myoshu and Iwasa 2018; Figures 3, 4, 5). The monomorphic pattern of NK2 is in accordance with our previous results showing not only the occurrence of *Cytb* haplotypes (the CAS and DOM types) but also their morphological characteristics (external body dimensions and coat coloration) (Myoshu and Iwasa 2018). There is a possibility that the distribution in the Japanese Islands of the predominant mice which were introduced from northern China and/or the Korean Peninsula (Yonekawa et al. 1988; Terashima et al. 2006; Nunome et al. 2010, 2013; Suzuki et al. 2013) has not yet expanded into NK2. However, putting emphasis on their larger head and body length as the subspecies *M. musculus domesticus* (Myoshu and Iwasa 2018) and the occurrence of the "intact" stowaway haplotype of nuclear DNA (Nunome et al. 2010; Kodama et al. 2015) and mtDNA (Yonekawa et al. 2000; Tsuda et al. 2001, 2002) in the Japan Islands, a more feasible explanation is that a relatively recent introduction(s) has led stowaway mice to this locality.

In the areas with exclusive occurrence of the CAS type from southern China and/or southeastern Asia (Suzuki et al. 2013; Kuwayama et al. 2017), HKD1 and HON1, there are discordances between the both viewpoints mentioned above (Myoshu and Iwasa 2018; Table 2; Figures 3, 4, 5). In contrast to the *Cytb* finding, the C-band patterns of the HKD1 mice and the HON1 mice are estimated to have been affected by the introgression from northern Chinese and/or Korean mice carrying the polymorphic patterns (Yoshida and Kodama 1983; Moriwaki et al. 1985, 1986; Moriwaki 2010; Yonekawa et al. 2012). In addition, although the CAS type occurs exclusively in both areas, the C-band patterns are not categorized into the same groups (Figure 5). Specifically, the numbers of null C-bands (23.6–27.6) and smaller C-bands (7.8-14.4) of the HON1 mice are especially more similar to those in the HON2 mice (24.8-29.5 null C-bands; 3.8-10.8 smaller C-bands) than those in the HKD1 mice (18.0-20.2 null C-bands; 18.6-20.2 smaller C-bands). Moreover, the sizes of the smaller C-bands differ between HON1 (more frequent relative length: 0.11-0.20, Table 2 and Figure 4) and HON2 (more frequent relative length: 0.21-0.30, Table 2 and Figure 4). These results suggest that the C-band patterns of HON1 and HKD1 are not genetically identical.

Several studies using biparental markers, which are the haplotypes on the haemoglobin bate chain (*Hbb*) locus (Minezawa et al. 1979; Miyashita et al. 1985; Kawashima et al. 1991, 1995; Ueda et al. 1999; Sato et al. 2006, 2008; Yonekawa et al. 2012), eight (Nunome et al. 2010) and seven (Kodama et al. 2015) linked nuclear genes, would provide a suggestion for why the difference in the C-band pattern has been caused in the same mtDNA occurrence areas. According to these previous studies, the distributions of the polymorphic C-band patterns (Moriwaki and Minezawa 1976; Moriwaki et al. 1985, 1986; Yonekawa et al. 2012; Myoshu and Iwasa 2016; Table 1 and Figures 4, 5) overlap the distributions of the *p* (Minezawa et al. 1979; Miyashita et al. 1985; Kawashima et al. 1995; Ueda et al. 1999; Yonekawa et al. 2012) and the MUS-II haplotype groups (Nunome et al. 2010; Kodama et al. 2015) which are derived from the

musculus lineage. The other hapolotype groups, which are recognized as the *d* (Minezawa et al. 1979; Miyashita et al. 1985; Kawashima et al. 1995; Yonekawa et al. 2012) and the recombinant haplotype groups (Nunome et al. 2010; Kodama et al. 2015) mainly derived from the *castaneus* lineage, have been observed in northern Honshu and Hokkaido localities. However, a survey of the *Hbb* allele reveals the difference in *p* frequency between the northeastern area of Honshu (37.0% in Minezawa et al. 1979) and Hokkaido (7.9% in Minezawa et al. 1979). Thus, the introgression of the lineage with MUS-II and *p* haplotypes, which has been derived from Eurasian mice carrying the polymorphic C-band patterns, has strongly affected the HON1 mice more than the HKD1 mice. In addition, since male mice have larger dispersal areas than female mice (Pocock et al. 2005), expansions of maternal genetic traits would be later than those of the paternal and biparental genetic traits. On the basis of this dispersal pattern, it is estimated that the polymorphic patterns as a biparental trait primarily expand into populations including both male and female mice with monomorphic patterns and the CAS type, by male mice considering the larger dispersal potential. Therefore, the polymorphic patterns from male mice have less affected mice in HKD1 than in HON1, based on the sign of hybridization in its C-band patterns is significantly observed in HKD1. In HON1, where the C-band patterns are similar to those in HON2 and SMD, the mice may have been replaced completely by the male mice carrying the polymorphic patterns. Otherwise, the HON1 mice have hybridized and/or maintained the traits of mice carrying a discordant combination, for example the polymorphic pattern and the CAS type, which may have been caused in other places as suggested in Searle et al. (2009), Nunome et al. (2010), Kodama et al. (2015) and Kuwayama et al. (2017).

ACKNOWLEDGEMENTS

We thank Dr. Keisuke Nakata for cooperation in current sampling of wild mice.

REFERENCES

Committee of Standardized Genetic Nomenclature for Mice. 1972. Standard karyotype of the mouse, Mus musculus. J Hered. 63: 69–72.

Cowell JK. 1984. A photographic representation of the variability in the G-banded structure of the chromosomes in the mouse karyotype: A guide to the identification of the individual chromosomes. Chromosoma. 89: 294–320.

Dev VG, Miller DA, Miller OJ. 1973. Chromosome Markers in *Mus musculus*: Strain Differences in C-banding. Genetics. 75: 663–670.

Dev VG, Miller DA, Tantravahi R, Sehreck RR, Roderiek TK, Erlanger BF, Miller OJ. 1975. Chromosome markers in *Mus musculus*: Differences in C-banding between the subspecies *M. m. musculus* and *M. m. molossinus*. Chromosoma. 53: 335–344.

Ikeuchi T. 1978. Notes on the centromeric heterochromatin of the Japanese wild mouse (*Mus musculus molossinus*). Chrom Inf Serv. 25: 24–26.

Kawashima R, Miyashita N, Wang C, He X, Jin M, Wu Z, Moriwaki K. 1991. A new haplotype of β-globin gene complex, Hbb^{w1}, in Chinese wild mouse. Jpn J Genet. 66: 491–500.

Kawashima T, Miyashita N, Tsuchiya K, Li H, Wang F, Wang CH, Wu XL, Wang C, Jin ML, He XQ, et al. 1995. Geographical distribution of the *Hbb* haplotypes in the *Mus musculus* subspecies in Eastern Asia. Jpn J Genet. 70: 17–23.

Kodama S, Nunome M, Moriwaki K, Suzuki H. 2015. Ancient onset of geographical divergence, interpopulation genetic exchange, and natural selection on the *Mc1r* coat-colour gene in the house mouse (*Mus musculus*). Biol J Linn Soc. 114: 778–794.

Kuwayama T, Nunome M, Kinoshita G, Abe K, Suzuki H. 2017. Heterogeneous genetic make-up of Japanese house mice (*Mus musculus*) created by multiple independent introductions and spatio-temporally diverse hybridization processes. Biol J Linn Soc. 122: 661–674.

Miller DA, Tantravahi R, Dev VG, Miller OJ. 1976. Q-and C-band chromosome markers in inbred strains of *Mus musculus*. Genetics. 84: 67–75.

Minezawa M, Moriwaki K, Kondo K. 1979. Geographical distribution of Hbb^{p} allele in the Japanese wild mouse, *Mus musculus molossinus*. Jpn J Genet. 54: 165–173.

Miyashita N, Moriwaki K, Minezawa M, Yonekawa H, Bonhomme F, Migita S, Yu ZC, Lu DY, Cho WS, Thohari M. 1985. Allelic constitution of the hemoglobin beta chain in wild populations of the house mouse, *Mus musculus*. Biochem Genet. 23: 975–986.

Moriwaki K. 2010. Award Recipient (Evolutionary history of muroid rodents inscribed in the genome). Mamm Sci. 50: 67–80. Japanese.

Moriwaki K, Minezawa M. 1976. Geographical distribution of No. 18 chromosome polymorphism. Ann Rep Natl Inst Genet. 27: 46–47.

Moriwaki K, Miyashita N, Yonekawa H. 1985. Genetic survey of the origin of laboratory mice and its implica-

tion in genetic monitoring. In: Archibald J, Ditchfield J, Rowsell HC, editors. The Contribution of Laboratory Animal Science to the Welfare of Man and Animals. Stuttgart (BW): Gustav Fischer Verlag; p. 237–247.

Moriwaki K, Miyashita N, Suzuki H, Kurihara Y, Yonekawa H. 1986. Genetic features of major geographical isolates of *Mus musculus*. Curr Top Microbiol Immunol 127: 55–61.

Moriwaki K, Myashita N, Mita A, Gotoh H, Tsuchiya K, Kato H, Mekada K, Noro C, Oota S, Yoshiki A, et al. 2009. Unique inbred strain MSM/Ms established from the Japanese wild mouse. Exp Anim. 58: 123–134.

Myoshu H, Iwasa MA. 2016. Polymorphic state of C-bands in the Japanese house mice, *Mus musculus*. Cytologia. 81: 459–463.

Myoshu H, Iwasa MA. 2018. Colonization and differentiation traits of the Japanese house mouse, *Mus musculus* (Rodentia, Muridae), inferred from mitochondrial haplotypes and external body characteristics. Zool Sci. 35: 222–232.

Nunome M, Ishimori C, Aplin KP, Tsuchiya K, Yonekawa H, Moriwaki K, Suzuki H. 2010. Detection of recombinant haplotypes in wild mice (*Mus musculus*) provides new insights into the origin of Japanese mice. Mol Ecol. 19: 2474–2489.

Nunome M, Suzuki H, Moriwaki K. 2013. Historical introduction of Japanese wild mice, *Mus musculus*, from South China and the Korean Peninsula. Anim Syst Evol Divers. 29: 267–271.

Pocock MJO, Hauffe HC, Searle JB. 2005. Dispersal in house mice. Biol J Linn Soc. 84: 565–583.

Sato JJ, Tsuru Y, Hirai K, Yamaguchi Y, Mekada K, Takahata N, Moriwaki K. 2006. Further evidence for recombination between mouse hemoglobin beta b1 and b2 genes based on the nucleotide sequences of intron, UTR, and intergenic spacer regions. Genes Genet Syst. 81: 201–209.

Sato JJ, Shinohara A, Miyashita N, Koshimoto C, Tsuchiya K, Nakahara I, Morita T, Yonekawa H, Moriwaki K, Yamaguchi Y. 2008. Discovery of a new HBB haplotype w2 wild-derived house mouse, *Mus musculus*. Mamm Genome. 19: 155–162.

Searle JB, Jamieson PM, Gündüz İ, Stevens MI, Jones EP, Gemmill CE, King CM. 2009. The diverse origins of New Zealand house mice. Proc R Soc Lond B Biol Sci. 276: 209–217.

Sumner AT. 1972. A simple technique for demonstrating centromeric heterochromatin. Exp Cell Res. 75: 304–306.

Sumner AT, Evans HJ, Buckland RA. 1971. New technique for distinguishing between human chromosomes. Nat New Biol. 232: 31–32.

Suzuki H, Nunome M, Kinoshita G, Aplin KP, Vogel P, Kryukov AP, Jin ML, Han SH, Maryanto I, Tsuchiya K, et al. 2013. Evolutionary and dispersal history of Eurasian house mice *Mus musculus* clarified by more extensive geographic sampling of mitochondrial DNA. Heredity. 111: 375–390.

Terashima M, Furusawa S, Hanazawa N, Tsuchiya K, Suyanto A, Moriwaki K, Yonekawa H, Suzuki H. 2006. Phylogeographic origin of Hokkaido house mice (*Mus musculus*) as indicated by genetic marker with maternal, parental and bilateral inheritance. Heredity. 96: 128–138.

Tsuda K, Tsuchiya K, Aoki E, Iizuka S, Suzuki S, Uchida Y, Yonekawa H. 2001. Distributions of *Mus musculus* subspecies at coastal areas in Japan (2). J Jpn Quarant Med Assoc. 3: 150–160. Japanese with English abstract.

Tsuda K, Tsuchiya K, Aoki E, Iizuka S, Suzuki S, Uchida Y, Yonekawa H. 2002. Distributions of *Mus musculus* subspecies at coastal areas in Japan (3). J Jpn Quarant Med Assoc. 4: 136–147. Japanese with English abstract.

Ueda Y, Miyashita N, Imai K, Yamaguchi Y, Takamura K, Notohara M, Shiroishi T, Kawashima T, Ning L, Wang C, et al. 1999. Nucleotide sequences of the mouse globin beta gene cDNAs in a wild derived new haplotype Hbbw1. Mamm Genome. 10: 879–882.

Yonekawa H, Moriwaki K, Gotoh O, Miyashita N, Matsushima Y, Shi LI, Cho WS, Zhen XL, Tagashira Y. 1988. A hybrid origin of Japanese mice '*Mus musculus molossinus*': evidence from restriction analysis of mitochondrial DNA. Mol Biol Evol. 5: 63–78.

Yonekawa H, Tsuda K, Tsuchiya K, Aoki E, Iizuka S, Suzuki S, Uchida Y. 2000. Distributions of *Mus musculus* subspecies at coastal areas in Japan. J Jpn Quarant Med Assoc. 2: 51–58. Japanese with English abstract.

Yonekawa H, Sato JJ, Suzuki H, Moriwaki K. 2012. Origin and genetic status of *Mus musculus molossinus*: a typical example of reticulate evolution in the genus Mus. In: Macholán M, Baird SJE, Munclinger P, Piálek J, editors. Evolution of the House Mouse. Cambridge (UK): Cambridge University Press; p. 94–113.

Yoshida MC, Kodama Y. 1983. C-band patterns of chromosomes in 17 strains of mice. Cytogenet Cell Genet. 35: 51–56.

Caryologia
International Journal of Cytology, Cytosystematics and Cytogenetics

Firenze University Press
www.fupress.com/caryologia

Citation: N.M. Travenzoli, I.C. de Oliveira Barbosa, G.A. Carvalho-Zilse, T.M.F. Salomão, D.M. Lopes (2019) Karyotypic description and repetitive DNA chromosome mapping of *Melipona interrupta* Latreille, 1811 (Hymenoptera: Meliponini). *Caryologia* 72(2): 91-95. doi: 10.13128/cayologia-239

Published: December 5, 2019

Data Availability Statement: All relevant data are within the paper and its Supporting Information files.

Competing Interests: The Author(s) declare(s) no conflict of interest.

Karyotypic description and repetitive DNA chromosome mapping of *Melipona interrupta* Latreille, 1811 (Hymenoptera: Meliponini)

Natália Martins Travenzoli[1], Ingrid Cândido de Oliveira Barbosa[2], Gislene Almeida Carvalho-Zilse[2], Tânia Maria Fernandes Salomão[3], Denilce Meneses Lopes[1,*]

[1] *Laboratório de Citogenética de Insetos, Departamento de Biologia Geral, Universidade Federal de Viçosa, CEP 36570-900, Viçosa, Minas Gerais, Brazil*
[2] *Grupo de Pesquisas em Abelhas, Coordenação de Biodiversidade, Instituto Nacional de Pesquisas da Amazônia (INPA), CEP 69067-375, Manaus, Amazonas, Brazil*
[3] *Laboratório de Biologia Molecular de Insetos, Departamento de Biologia Geral, Universidade Federal de Viçosa, CEP 36570-900, Viçosa, Minas Gerais, Brazil*
*Corresponding author: denilce.lopes@ufv.br

Abstract. Heterochromatic patterns in the genus *Melipona* vary among subgenera species. *Melikerria* is the only subgenus that presents species with different content of heterochromatin. Thus, the cytogenetic knowledge of other species of this subgenus is important for the understanding of karyotype evolution in *Melipona*. Here, we describe the karyotype of *Melipona* (*Melikerria*) *interrupta* based on the chromosomal heterochromatic patterns, AT and GC richness, mapping sequences of rDNA, microsatellites and telomeric regions. We observed 2*n*=18 chromosomes, with a high heterochromatin content rich in AT and euchromatic regions rich in GC base pairs. The high GC content was observed at interstitial region near the junction of the stained euchromatin and heterochromatin of the first chromosomal pair, the same region marked for the rDNA 18S locus. Microsatellites hybridized only on euchromatin regions and the telomeric probe on terminal regions of all chromosomes. *Melipona* (*Melikerria*) *interrupta* belongs to previous described heterochromatic Group II, suggesting there has been an increase in heterochromatin content in *Melikerria*. The *M. quinquefasciata*, belonging to the same subgenus as *Melipona* (*Melikerria*) *interrupta*, has low content of heterochromatin and appears to be evolving independently. So, the differences in the content heterochromatin, in the marker regions of CMA_3 and the rDNA 18S locus in species of *Melikerria* is an important feature to be investigated further.

Keywords. Cytogenetics, Fluorescence *in situ* Hybridization (FISH), Heterochromatin, *Melikerria*, Stingless bee.

1. INTRODUCTION

Bees of the genus *Melipona* Illiger, 1806, are eusocial insects belonging to the Meliponini tribe and occur throughout the Neotropical region (Michener 2007; Camargo and Pedro 2013). This genus is represented by 73 species, 43

of which can be found in Brazil (Camargo and Pedro 2013; Pedro 2014). Morphologically, the genus *Melipona* is grouped into four subgenera: *Eomelipona*, *Melikerria*, *Melipona stricto sensu*, and *Michmelia* (Camargo and Pedro 2013). The *Melikerria*, *Melipona stricto sensu,* and *Michmelia* subgenera are considered monophyletic, whereas *Eomelipona* is polyphyletic according to molecular phylogenies (Rasmussen and Cameron 2010; Ramírez et al. 2010).

Cytogenetically, only 28 of all the *Melipona* species have had their karyotypes described. These species are characterized by a conserved diploid number of $2n = 18$ chromosomes in females and $n = 9$ in males, except for *M. seminigra merrilae* and *M. seminigra pernigra*, with $2n = 22$ (Francini et al. 2011). In addition, the pattern of heterochromatin distribution in some *Melipona* species differs from that observed in the majority of species in the Meliponini tribe (reviewed in Tavares et al. 2017; Cunha et al. 2018; Silva et al. 2018). The genus can be divided into two groups based on the pattern of distribution and content of heterochromatin: Group I is composed of species with low heterochromatin content present only in the pericentromeric regions, similar to that in the other Meliponini; and Group II comprised by species with a high heterochromatin content that covers large extensions of their chromosomes (Rocha and Pompolo 1998; Rocha et al. 2002).

From all the analyzed species, those belonging to the *Eomelipona* and *Melipona stricto sensu* subgenera present low levels of heterochromatin, whereas all those of the subgenus *Michmelia* have high levels of heterochromatin (Rocha and Pompolo 1998; Rocha et al. 2002; Rocha et al. 2003; Lopes et al. 2011; Cunha et al. 2018). However, *Melikerria* has only three species described cytogenetically that present the two patterns: *Melipona fasciculata* Smith, 1854 and *Melipona grandis* Guérin, 1844, with high content of heterochromatin and *Melipona quinquefasciata* Lepeletier, 1836 with a low content (Rocha et al. 2002; Rocha 2002; Lopes et al. 2011), making heterochromatic evolution in this group difficult to elucidate. Thus, cytogenetic studies with other species of the subgenus *Melikerria* are needed since they may help to elucidate the processes leading to the chromosomal alterations in the genus.

The aim of this study was to characterize the karyotype of *Melipona* (*Melikerria*) *interrupta* based on the heterochromatin distribution pattern and chromosomal regions rich in Guanine-Cytosine (GC) and Adenine-Thymine (AT) base pairs, as well as mapping the ribosomal 18S DNA sites, the microsatellites $GA_{(15)}$, $GAG_{(10)}$, $CAA_{(10)}$, and $CGG_{(10),}$ and the regions containing telomeric $TTAGG_{(6)}$ sequences.

2. MATERIAL AND METHODS

Larvae of *Melipona* (*Melikerria*) *interrupta* were collected from three colonies in Itacoatiara, Amazonas, Brazil and kept in the Meliponary of the Instituto Nacional de Pesquisas da Amazônia (INPA), Manaus, Amazônia, Brazil. Mitotic chromosomes were obtained from the larval brain ganglia at the last larval instar as described by Imai et al. (1988), and stained with Giemsa. The heterochromatin regions were visualized by the C-band technique (Sumner 1972) and the DAPI and CMA_3 fluorochromes were used according to Schweizer (1980). Fifteen individuals were used, with 10 metaphases being analyzed on average for each slide. The images were obtained with an Olympus BX60 epifluorescence microscope, using Olympus Q-Color3™ software Olympus® images.

Fluorescent *in situ* Hybridization (FISH) was performed according to Pinkel et al. (1986), with modifications: (metaphase chromosomes were denatured in 70%/2xSSC formamide at 75 °C for 5 min; the probes were hybridized with chromosomes in 20 μL of hybridization mix and heated for 10 min at 85 ° C). The 18S ribosomal DNA probe was labeled with digoxigenin-11-dUTP (Roche Applied Science) and the signal was detected with anti-digoxigenin-rhodamine (Roche Applied Science). This probe was obtained by Polymerase Chain Reaction (PCR) amplification, using the primers F1(5′-GTCATATGTTGTCTCAAAGA-3′) and 18SR1.1 (3′-TCTAATTTTTTCAAAGTAAACGC-5′) designed for the species *Melipona quinquefasciata* (Pereira 2006). The microsatellites $GA_{(15)}$, $GAG_{(10)}$, $CAA_{(10)}$, $CGG_{(10)}$, and $TTAGG_{(6)}$ were labeled directly with Cy3 in the 5′ regions (Sigma, St. Louis, MO, USA). The metaphase images were obtained with an Olympus BX53 microscope fitted with an Olympus DP73F camera, using the CellSens Imaging software.

3. RESULTS AND DISCUSSION

The chromosome number observed in *M.* (*Melikerria*) *interrupta* was $2n = 18$ (Fig. 1a) similar the number finding by Barbosa (2018), which does not differ from that reported by Kerr (1969, 1972). The C-band revealed a karyotype with high heterochromatin content (Fig. 1b), making visualization of the centromere difficult. Thus, we could not identify chromosome morphology to determine the karyotype of this species. Based on the heterochromatic patterns, *M.* (*Melikerria*) *interrupta* can be classified as belonging to the group composed of species with more than 50% of heterochromatin in their chro-

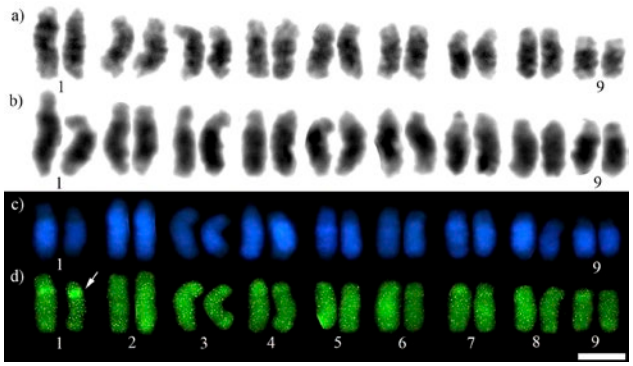

Fig. 1. Mitotic metaphase chromosomes of *Melipona* (*Melikerria*) *interrupta* stained with Giemsa (a), C- banding (b), DAPI (c), and CMA_3 (d). Scale bar = 5 µm.

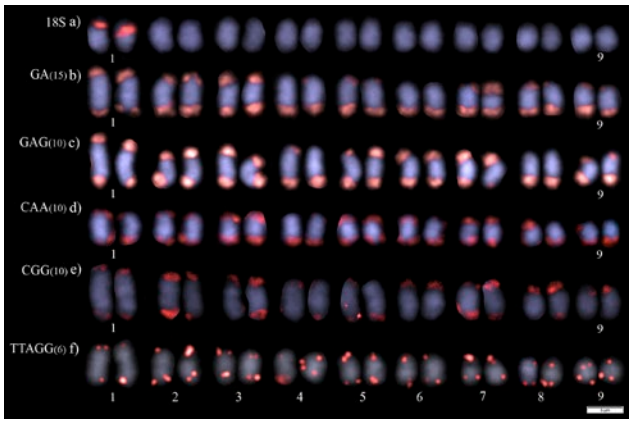

Fig. 2. Patterns obtained in metaphase chromosomes of *Melipona* (*Melikerria*) *interrupta* with FISH using the following repetitive DNA probes: 18S (a), $GA_{(15)}$ (b), $GAG_{(15)}$ (c), $CAA_{(10)}$ (d), $CGG_{(10)}$ (e), and $TTAGG_{(6)}$ (f). In blue: chromosomes stained with DAPI. In red: regions hybridized with probes. Scale bar = 5 µm.

mosomes, designated as Group II by Rocha and Pompolo et al. (1998). The species *M.* (*Melikerria*) *fasciculata* and *M.* (*Melikerria*) *grandis* were classified as belonging to this group (Lopes et al. 2011; Andrade-Souza et al. 2018) as well as *M.* (*Melikerria*) *interrupta*. Unlike, *M.* (*Melikerria*) *quinquefasciata* has a low heterochromatin content (Rocha et al. 2007), indicating that the karyotype of *M. quinquefasciata* may be evolving independently or have been the karyotype plesiomorphic within the *Melikerria*. So, in this subgenus may have been an increase in the levels of heterochromatin in the karyotype of the species. In fact, it has been, suggested that independent amplification of heterochromatin or differentiation in distinct *Melipona* subgenus (Piccoli et al. 2018).

Staining with the base-specific fluorophores, DAPI and CMA_3, indicated that the heterochromatic regions were $DAPI^+$ (Fig. 1c) and the euchromatic regions were CMA_3^+. Stronger labeling with CMA_3 was seen in the interstitial region near the euchromatin and heterochromatin junction of the first chromosomal pair (Fig. 1d), coincident with the hybridization site of the 18S rDNA probe (Fig. 2a). Staining with DAPI has shown that heterochromatin in eusocial bees is generally AT-rich (Brito et al. 2003; Rocha et al. 2003; Lopes et al. 2011; Godoy et al. 2013). This characteristic seems to be shared by *Melipona* species that contain either high or low levels of heterochromatin.

Although the numbers of CMA_3^+ and rDNA markers on a single pair of chromosomes are conserved traits in the genus (Cunha et al. 2018; Andrade-Souza et al. 2018), the chromosomal positions differ among species, even in those with a high heterochromatin content. According to the results of CMA_3^+ and rDNA probe, species with a low heterochromatin content exhibited pericentromeric markings in the first chromosome pair, while Group II species showed terminal markings (reviewed in Cunha et al. 2018). Although *M.* (*Melikerria*) *interrupta* is classified as belonging to Group II, CMA_3^+ and rDNA markings were observed in the interstitial region of the first chromosomal pair. *Melipona* (*Melikerria*) *fasciculata* and *M.* (*Melikerria*) *grandis*, which belongs to the same subgenus, also showed CMA_3^+ markings in this region (Lopes et al. 2011; Andrade-Souza et al. 2018), different to that observed in the other species with high heterochromatin content (reviewed in Cunha et al. 2018). These results suggest that variation in the positions of GC rich regions and 18S rDNA sites may be results of divergent heterochromatin evolutionary pathways in the *Melipona* as suggested by Cunha et al. (2018) and Picolli et al (2018). As the markings in other species of Group II is at the chromosome end, the occurrence of rearrangements, such as inversion, would result in a portion of heterochromatin at the ends of the chromosome. However, we did not find heterochromatin in these regions suggesting that the position of CMA_3 and rDNA no result of chromosome inversion events.

The microsatellite probes $GA_{(15)}$, $GAG_{(10)}$, $CAA_{(10)}$, and $CGG_{(10)}$ labeled only euchromatin regions (Fig. 2b-e), while the telomeric probe $TTAGG_{(6)}$ showed staining in the terminal regions of the chromosomes of *M.* (*Melikerria*) *interrupta* (Fig. 2f). This staining pattern in regions of euchromatin was also observed in the chromosomal mapping of *Melipona scutellaris* Latreille, 1811 using different repetitive DNA sequences ($CA_{(15)}$, $GAC_{(10)}$, and $TAA_{(10)}$) (Piccoli et al. 2018). The $TTAGG_{(6)}$ labeling on the terminal regions of the chromosomes indicated the presence of the TTAGG sequence in the

telomeric sites in the karyotype of *M.* (*Melikerria*) *interrupta*. Studies have shown that TTAGG (Sahara et al. 1999) and TCAGG (Mravinac et al. 2011) were observed in telomeres of several Hymenoptera species, including Apidae (*Apis mellifera*) (Meyne et al. 1995; Sahara et al. 1999) and Formicidae (*Tapinoma nigerrimum*, *Myrmecia* spp. and *Acromyrmex striatus*) (Meyne et al. 1995; Lorite et al. 2002; Frydrychová et al. 2004; Pereira et al. 2018). However, in many other Hymenoptera the TTAGG sequence was not observed in the telomeres of the chromosomes, suggesting that it has been lost and recovered in Apidae and Formicidae or that multiple losses of this region have occurred throughout the evolutionary history of the groups (Menezes et al. 2017). In this study, we report for the first time the telomeric sequence based on the FISH technique on a bee species of Meliponini tribe. This information added to the cytogenetic characteristics of *Melipona* already described in the literature may contribute to the understanding of karyotype evolution in these bees.

We conclude that *M.* (*Melikerria*) *interrupta* is classified as belonging to Group II based on heterochromatic patterns, which suggests an increase in the amount of heterochromatin in the subgenus *Melikerria*. It further suggests that karyotype the *M. quinquefasciata* be plesiomorphic or this may be evolving independently in the group, and that the differences in the CMA_3 and 18S marker regions interstitial, reported in the two species of *Melikerria* subgenus with high heterochromatin content, are an important feature to be further investigated.

5. ACKNOWLEDGMENT

The "Coordenação de Aperfeiçoamento de Pessoal de Nível Superior (CAPES)", "Fundação de Amparo à Pesquisa do Estado de Minas Gerais (FAPEMIG)" and the "Fundação de Amparo à Pesquisa do Estado do Amazonas (FAPEAM)".

6. BIBLIOGRAPHIC REFERENCES

Andrade-Souza V, Duarte OMP, Martins CCC, Santos IS, Costa MGC, Costa MA. 2018. Comparative molecular cytogenetics in *Melipona* Illiger species (Hymenoptera, Apidae). Sociobiology. 65 (4): 696-705.

Barbosa ICO. 2018. Caracterização citogenética e análise do perfil de metilação em *Melipona seminigra* e *Melipona interrupta* (Hymenoptera, Apidae). Dissertation, Instituto Nacional de Pesquisas da Amazônia. 42pp.

Brito RM, Caixeiro APA, Pompolo SG, Azevedo GG. 2003. Cytogenetic data of *Partamona peckolti* (Hymenoptera, Apidae, Meliponini) by C banding and fluorochrome staining with DA/ CMA_3 and DA/DAPI. Genet. Mol. Biol. 26 (1): 53-57.

Camargo JMF, Pedro SRM. 2013. Meliponini Lepeletier, 1836. In Moure, JS, Urban, D. and Melo, GA R (Orgs). Catalogue of Bees (Hymenoptera, Apoidea) in the Neotropical Region - online version. Available at http://www.moure.cria.org.br/catalogue. Accessed 18 january 2019.

Cunha MS, Travenzoli NM, Ferreira RP, Cassinela EK, Silva H, Salomão TMF, Lopes DM. (2018). Comparative cytogenetics in three *Melipona* species (Hymenoptera: Apidae) with two divergent heterochromatic patterns. Genet. Mol. Biol. 41 (4): 806-813.

Francini IB, Gross MC, Nunes-Silva CG, Carvalho-Zilse GA. 2011. Cytogenetic analysis of the Amazon stingless bee *Melipona seminigra merrillae* reveals different chromosome number for the genus. Sci. Agric. 68 (5): 592-593.

Frydrychová R, Grossmann P, Trubac P, Vítková M, Marec FE. 2004. Phylogenetic distribution of TTAGG telomeric repeats in insects. Genome. 47: 163-178.

Godoy DC, Ferreira RP, Lopes DM. 2013. Chromosomal Variation and Cytogenetics of *Plebeia lucii* and *P. phrynostoma* (Hymenoptera: Apidae). Fla. Entomol. 96 (4): 1559-1566.

Imai HT, Taylor RW, Crosland MW, Crozier RH. 1988. Modes of spontaneous chromosomal mutation and karyotype evolution in ants with reference to the minimum interaction hypothesis. JPN J. Genet. 63 (2): 159-185.

Kerr WE. 1969. Some aspects of the Evolution of social bees. Evol. Biol. 3, 119-175.

Kerr WE. 1972. Number of chromosomes in some species of bees. J. Kansas Entomol. Soc. 45: 111-122.

Lopes DM, Fernandes A, Praça-Fontes MM, Werneck HA, Resende HC, Campos LAO. 2011. Cytogenetics of three *Melipona* species (Hymenoptera, Apidae, Meliponini). Sociobiology. 57 (2): 185-194.

Lorite P, Carrillo JA, Palomeque T. 2002. Conservation of (TTAGG) n telomeric sequences among ants (Hymenoptera, Formicidae). J. Hered. 93: 282-285.

Menezes RS, Bardella, VB, Cabral-de-Mello DC, Lucena DA, Almeida EA. 2017. Are the TTAGG and TTAGGG telomeric repeats phylogenetically conserved in aculeate Hymenoptera?. Sci. Nat. 104 (9-10): 85.

Meyne J, Hirai H, Imai HT. 1995. FISH analysis of the telomere sequences of bulldog ants (Myrmecia: Formicidae). Chromosoma. 104 (1): 14-18

Michener CD. 2007. The bees of the world. The John Hopkins University Press, Baltimore, Maryland.

Mravinac B, Meštrović N, Čavrak VV, Plohl M. 2011. TCAGG, an alternative telomeric sequence in insects. Chromosoma. 120 (4): 367-376.

Pedro SRM. 2014. The stingless bee fauna in Brazil (Hymenoptera: Apidae). Sociobiology. 61 (4): 348-354.

Pereira JOP. 2006. Diversidade genética da abelha sem ferrão *Melipona quinquefasciata* baseada no sequenciamento das regiões ITS1 parcial e 18S do DNA ribossômico nuclear. Thesis, Universidade Federal do Ceará, Fortaleza, Ceará.

Pereira TTP, dos Reis ACCC, Cardoso DC, Cristiano MP. 2018. Molecular phylogenetic reconstruction and localization of the (TTAGG)n telomeric repeats in the chromosomes of *Acromyrmex striatus* (Roger, 1863) suggests a lower ancestral karyotype for leafcutter ants (Hymenoptera). Comp. Cytogenet. 12 (1): 13.

Piccoli MCA, Bardella VB, Cabral-de-Mello DC. 2018. Repetitive DNAs in *Melipona scutellaris* (Hymenoptera: Apidae: Meliponidae): chromosomal distribution and test of multiple heterochromatin amplification in the genus. Apidologie. 49 (4): 497-504.

Pinkel D, Straume T, Gray JW. 1986. Cytogenetic analysis using quantitative, high sensitivity, fluorescence hybridization. Proc. Natl. Acad. Sci. USA 83 (9): 2934-2938.

Ramírez SR, Nieh JC, Quental TB, Roubik DW, Imperatriz-Fonseca VL, Pierce NE. 2010. A molecular phylogeny of the stingless bee genus *Melipona* (Hymenoptera: Apidae). Mol. Phylogenet. Evol. 56 (2): 519-525.

Rasmussen C, Cameron AS. 2010. Global stingless bee phylogeny supports ancient divergence, vicariance, and long distance dispersal. Biol. J. Linn. Soc. 99 (1): 206-232.

Rocha MP. 2002. Análises citogenéticas em abelhas do gênero *Melipona* Hymenoptera, Meliponini). Dissertation, Universidade Federal de Viçosa.

Rocha MP, Cruz MP, Fernandes A, Waldschmidt AM, Silva-Júnior JC, Pompolo SG. 2003. Longitudinal differentiation in *Melipona mandacaia* (Hymenoptera, Meliponini) chromossomes. Hereditas. 138 (2): 133-137.

Rocha MP, Pompolo SG. 1998. Karyotypes and heterochromatin variation (C-bands) in *Melipona* species (Hymenoptera, Apidae, Meliponinae). Genet. Mol. Biol. 21 (1): 41-45.

Rocha MP, Pompolo SG, Dergam JA, Fernandes A, Campos LAO. 2002. DNA characterization and karyotypic evolution in the bee genus *Melipona* (Hymenoptera, Meliponini). Hereditas. 136 (1): 19-27.

Rocha MP, Pompolo SG, Fernandes A, Campos LAO. 2007. *Melipona*: Six decade of cytogenetic. Biosc. J. 1: 111-117.

Sahara K, Marec F, Traut W. 1999. TTAGG telomeric repeats in chromosomes of some insects and other arthropods. Chromosome Res. **7** (6): 449-460.

Schweizer D. 1980. Simultaneous fluorescent staining of R bands and specific heterochromatic regions (DA-DAPI bands) in human chromosomes. Cytogen. Cell. Genet. 27 (6): 190-193.

Silva AA, Rocha MP, Pompolo SG, Campos LAO, Tavares MG. 2018. Karyotypic description of the stingless bee *Melipona quinquefasciata* Lepeletier, 1836 (Hymenoptera, Meliponini) with emphasis on the presence of B chromosomes. Comp. Cytogenet. 12 (4): 471.

Sumner AT. 1972. A simple technique for demonstrating centromeric heterochromatin. Exp. Cell. Res. 75 (1): 304-306.

Tavares MG, Lopes DM, Campos LAO. 2017. An overview of cytogenetics of the tribe Meliponine (Hymenoptera: Apidae). Genetica 145 (6): 1-18.

Finito di stampare da
Logo s.r.l. – Borgoricco (PD) – Italia

OPEN ACCESS POLICY

Caryologia provides immediate open access to its content. Our publisher, Firenze University Press at the University of Florence, complies with the Budapest Open Access Initiative definition of Open Access: By "open access" , we mean the free availability on the public internet, the permission for all users to read, download, copy, distribute, print, search, or link to the full text of the articles, crawl them for indexing, pass them as data to software, or use them for any other lawful purpose, without financial, legal, or technical barriers other than those inseparable from gaining access to the internet itself. The only constraint on reproduction and distribution, and the only role for copyright in this domain is to guarantee the original authors with control over the integrity of their work and the right to be properly acknowledged and cited. We support a greater global exchange of knowledge by making the research published in our journal open to the public and reusable under the terms of a Creative Commons Attribution 4.0 International Public License (CC-BY-4.0). Furthermore, we encourage authors to post their pre-publication manuscript in institutional repositories or on their websites prior to and during the submission process and to post the Publisher's final formatted PDF version after publication without embargo. These practices benefit authors with productive exchanges as well as earlier and greater citation of published work.

PUBLICATION FREQUENCY

Papers will be published online as soon as they are accepted, and tagged with a DOI code. The final full bibliographic record for each article (initial-final page) will be released with the hard copies of *Caryologia*. Manuscripts are accepted at any time through the online submission system.

COPYRIGHT NOTICE

Authors who publish with *Caryologia* agree to the following terms:

- Authors retain the copyright and grant the journal right of first publication with the work simultaneously licensed under a Creative Commons Attribution 4.0 International Public License (CC-BY-4.0) that allows others to share the work with an acknowledgment of the work's authorship and initial publication in Caryologia.
- Authors are able to enter into separate, additional contractual arrangements for the non-exclusive distribution of the journal's published version of the work (e.g., post it to an institutional repository or publish it in a book), with an acknowledgment of its initial publication in this journal.
- Authors are permitted and encouraged to post their work online (e.g., in institutional repositories or on their website) prior to and during the submission process, as it can lead to productive exchanges, as well as earlier and greater citation of published work (See The Effect of Open Access).

PUBLICATION FEES

Open access publishing is not without costs. *Caryologia* therefore levies an article-processing charge of € 150.00 for each article accepted for publication, plus VAT or local taxes where applicable.

We routinely waive charges for authors from low-income countries. For other countries, article-processing charge waivers or discounts are granted on a case-by-case basis to authors with insufficient funds. Authors can request a waiver or discount during the submission process.

PUBLICATION ETHICS

Responsibilities of *Caryologia*'s editors, reviewers, and authors concerning publication ethics and publication malpractice are described in *Caryologia*'s Guidelines on Publication Ethics.

CORRECTIONS AND RETRACTIONS

In accordance with the generally accepted standards of scholarly publishing, *Caryologia* does not alter articles after publication: "Articles that have been published should remain extant, exact and unaltered to the maximum extent possible".

In cases of serious errors or (suspected) misconduct *Caryologia* publishes corrections and retractions (expressions of concern).

Corrections

In cases of serious errors that affect or significantly impair the reader's understanding or evaluation of the article, *Caryologia* publishes a correction note that is linked to the published article. The published article will be left unchanged.

Retractions

In accordance with the "Retraction Guidelines" by the Committee on Publication Ethics (COPE) *Caryologia* will retract a published article if:

- there is clear evidence that the findings are unreliable, either as a result of misconduct (e.g. data fabrication) or honest error (e.g. miscalculation)
- the findings have previously been published elsewhere without proper crossreferencing, permission or justification (i.e. cases of redundant publication)
- it turns out to be an act of plagiarism
- it reports unethical research.

An article is retracted by publishing a retraction notice that is linked to or replaces the retracted article. *Caryologia* will make any effort to clearly identify a retracted article as such.

If an investigation is underway that might result in the retraction of an article *Caryologia* may choose to alert readers by publishing an expression of concern.

COMPLYNG WITH ETHICS OF EXPERIMENTATION

Please ensure that all research reported in submitted papers has been conducted in an ethical and responsible manner, and is in full compliance with all relevant codes of experimentation and legislation. All papers which report in vivo experiments or clinical trials on humans or animals must include a written statement in the Methods section. This should explain that all work was conducted with the formal approval of the local human subject or animal care committees (institutional and national), and that clinical trials have been registered as legislation requires. Authors who do not have formal ethics review committees should include a statement that their study follows the principles of the Declaration of Helsinki

ARCHIVING

Caryologia and Firenze University Press are experimenting a National legal deposition and long-term digital preservation service.

ARTICLE PROCESSING CHARGES

All articles published in *Caryologia* are open access and freely available online, immediately upon publication. This is made possible by an article-processing charge (APC) that covers the range of publishing services we provide. This includes provision of online tools for editors and authors, article production and hosting, liaison with abstracting and indexing services, and customer services. The APC, payable when your manuscript is editorially accepted and before publication, is charged to either you, or your funder, institution or employer.

Open access publishing is not without costs. *Caryologia* therefore levies an article-processing charge of € 150.00 for each article accepted for publication, plus VAT or local taxes where applicable.

FREQUENTLY-ASKED QUESTIONS (FAQ)

Who is responsible for making or arranging the payment?

As the corresponding author of the manuscript you are responsible for making or arranging the payment (for instance, via your institution) upon editorial acceptance of the manuscript.

At which stage is the amount I will need to pay fixed?

The APC payable for an article is agreed as part of the manuscript submission process. The agreed charge will not change, regardless of any change to the journal's APC.

When and how do I pay?

Upon editorial acceptance of an article, the corresponding author (you) will be notified that payment is due.

We advise prompt payment as we are unable to publish accepted articles until payment has been received. Payment can be made by Invoice. Payment is due within 30 days of the manuscript receiving editorial acceptance. Receipts are available on request.

No taxes are included in this charge. If you are resident in any European Union country you have to add Value-Added Tax (VAT) at the rate applicable in the respective country. Institutions that are not based in the EU and are paying your fee on your behalf can have the VAT charge recorded under the EU reverse charge method, this means VAT does not need to be added to the invoice. Such institutions are required to supply us with their VAT registration number. If you are resident in Japan you have to add Japanese Consumption Tax (JCT) at the rate set by the Japanese government.

Can charges be waived if I lack funds?

We consider individual waiver requests for articles in Caryologia on a case-by-case basis and they may be granted in cases of lack of funds. To apply for a waiver please request one during the submission process. A decision on the waiver will normally be made within two working days. Requests made during the review process or after acceptance will not be considered.

I am from a low-income country, do I have to pay an APC?

We will provide a waiver or discount if you are based in a country which is classified by the World Bank as a low-income or a lower-middle-income economy with a gross domestic product (GDP) of less than $200bn. Please request this waiver of discount during submission.

What funding sources are available?

Many funding agencies allow the use of grants to cover APCs. An increasing number of funders and agencies strongly encourage open access publication. For more detailed information and to learn about our support service for authors.

APC waivers for substantial critiques of articles published in OA journals

Where authors are submitting a manuscript that represents a substantial critique of an article previously published in the same fully open access journal, they may apply for a waiver of the article processing charge (APC).

In order to apply for an APC waiver on these grounds, please contact the journal editorial team at the point of submission. Requests will not be considered until a manuscript has been submitted, and will be awarded at the discretion of the editor. Contact details for the journal editorial offices may be found on the journal website.

What is your APC refund policy?

Firenze University Press will refund an article processing charge (APC) if an error on our part has resulted in a failure to publish an article under the open access terms selected by the authors. This may include the failure to make an article openly available on the journal platform, or publication of an article under a different Creative Commons licence from that selected by the author(s). A refund will only be offered if these errors have not been corrected within 30 days of publication.

2019
Vol. 72 – n. 2

Caryologia

International Journal of Cytology, Cytosystematics and Cytogenetics

Table of contents

€ 25,00